2011-07-10

Investigation of the C-Terminal Helix of HIV-1 Matrix: A Region Essential for Multiple Functions in the Viral Life Cycle: A Dissertation

Laura A. Brandano
University of Massachusetts Medical School

INVESTIGATION OF THE C-TERMINAL HELIX OF HIV-1 MATRIX: A REGION ESSENTIAL FOR MULTIPLE FUNCTIONS IN THE VIRAL LIFE CYCLE

A Dissertation Presented

by

Laura A. Brandano

Submitted to the Faculty of the

University of Massachusetts Graduate School of Biomedical Sciences, Worcester

in partial fulfillment of the requirements for the degree of

DOCTOR OF PHILOSOPHY

July 10th, 2011

Interdisciplinary Graduate Program

INVESTIGATION OF THE C-TERMINAL HYDROPHOBIC POCKET OF HIV-1 MATRIX: A REGION ESSENTIAL FOR MULTIPLE FUNCTIONS IN THE VIRAL LIFE CYCLE

A Dissertation Presented By

Laura Ann Brandano

The signatures of the Dissertation Defense Committee signifies completion and approval as to style and content of the Dissertation

Mario Stevenson, Ph.D., Thesis Advisor

Paul Clapham, Ph.D., Member of Committee

Heinrich Gottlinger, Ph.D., Member of Committee

Gregory Melikyan, Ph.D., Member of Committee

The signature of the Chair of the Committee signifies that the written dissertation meets the requirements of the Dissertation Committee

Maria Zapp, Ph.D. Chair of Committee

The signature of the Dean of the Graduate School of Biomedical Sciences signifies that the student has met all graduation requirements of the School

Anthony Carruthers, Ph.D.
Dean of the Graduate School of Biomedical Sciences

Interdisciplinary Graduate Program
July 29, 2011

ACKNOWLEDGEMENTS

There are many people that have contributed to my personal and professional growth during my graduate work at UMass. First, I would like to thank my thesis advisor, Dr. Mario Stevenson, who gave me the opportunity to work in his lab and provided me with the resources I needed to carry out these studies. Mario, while working in your lab, I have grown into an independent thinker and scientist, and I have learned a great deal about myself in this process.

I am also grateful to other members of the Stevenson lab who kept me grounded during some tough times, especially Dunja Babic, Patrick Younan, Ruza Stranska, Ann Dauphin and Simon Swingler. In addition, I gratefully thank Drs. Mohan Somasandran, Heather Friberg-Robertson, Mike Krashes, and Mike Vaine who were extremely helpful in reading and providing constructive criticisms of this written thesis.

This thesis would not have been possible without the guidance and encouragement of my Thesis Committee: Drs. Paul Clapham, Heinrich Gottlinger and Maria Zapp. Our detailed discussions were invaluable, especially in the early stages of this project. Your sage advice was essential for directing these studies and pushed the work to its completion. I must also express sincere gratitude to Dr. Greg Melikyan, who was of great assistance to me in performing the Beta-Lactamase Fusion assay. It is an honor to have you as the external examiner for my Defense Committee.

It is difficult to overstate my gratitude to Dr. Maria Zapp, who far exceeded any expectation one should have of their committee chair. Maria, your passion for mentorship was inspiring to witness, and I hope to honor you by paying it forward in the future

during my career. Your eye for detail rivals that of any great scientist I have met. UMass is lucky to have you, and I am indebted to you for supporting me and believing in my abilities from the beginning.

Finally, this thesis would never have been completed without the encouragement and devotion of my family. Mom and Dad, you have shown me unwavering love. Your persistent confidence in me, throughout my entire life, continues to drive me to this day. I love you both more than you will ever know. And to my wonderful husband Pete, thank you for pushing me to do my best. I would not have accomplished this feat without your incredible patience- I love you with all my heart. I am grateful for all the sacrifices you have made for me especially during these last few months, and for giving me my most precious gift, Lillian Joyce. You have been learning with me every step of the way during my time at UMass, and this degree belongs to both of us.

ABSTRACT

Since the first cases were reported over thirty years ago, great strides have been made to control disease progression in people living with HIV/AIDS. However, current estimates report that there are about 34 million individuals infected with HIV worldwide. Critical in the ongoing fight against this pandemic is the continuing development of highly active anti-retroviral therapies, ideally those with novel mechanisms of action. Currently, there are no medications approved for use that exploit the HIV-1 MA protein, despite its central role in multiple stages of the virus life cycle.

This thesis sought to examine whether a highly conserved glutamate residue at position 99 in the understudied C-terminal helix of MA is required for HIV-1 replication. I characterized a panel of mutant viruses that contain different amino acid substitutions at this position using viral infectivity studies, virus-cell fusion assays, and immunoblotting. In doing so, I found that substitution of this glutamate with either a valine (E99V) or lysine (E99K) residue disrupted Env incorporation into nascent HIV particles, and abrogated their ability to fuse with target-cell membranes. In determining that the strain of HIV could affect the magnitude of E99V-associated defects, I identified a compensatory substitution at MA residue 84 that rescued both E99V- and E99K-associated impairments.

I further characterized the MA E99V and E99K mutations by truncating HIV Env and pseudotyping with heterologous envelope proteins in an attempt to overcome the Env incorporation defect. Unexpectedly, I found that facilitating fusion at the plasma membrane was not sufficient to reverse the severe impairments in virus infectivity. Using

quantitative PCR, I determined that an early post-entry step is disrupted in these particles that contain the E99V or E99K MA substitutions. However, allowing entry of mutant virus particles into cells through an endosomal route conferred a partial rescue in infectivity. As the characterization of this post-entry defect was limited by established virological methods, I designed a novel technique to analyze post-fusion events in retroviral infection. Thus, I present preliminary data regarding the development of a novel PCR-based assay that monitors trafficking of the viral reverse transcription complex (RTC) in an infected cell.

The data presented in this thesis indicate that a single residue in MA, E99, has a previously unsuspected and key role in multiple facets of HIV-1 MA function. The pleiotropic defects that arise from specific substitutions of this amino acid implicate a hydrophobic pocket in MA in Env incorporation and an early post-entry function of the protein. These findings suggest that this understudied region of MA could be an important target in the development of a novel antiretroviral therapy.

TABLE OF CONTENTS

ACKNOWLEDGEMENTS ..... **iii**

ABSTRACT ..... **v**

LIST OF TABLES ..... **xi**

LIST OF FIGURES ..... **xii**

LIST OF THIRD PARTY COPYRIGHTED MATERIAL ..... **xv**

ABBREVIATIONS ..... **xvi**

CHAPTER I: INTRODUCTION **1**

1.1 The Identification of HIV and the Development of Therapeutics 1

1.2 HIV Infection and Disease Progression 5

1.3 Overview of HIV-1 Replication 8

1.4 Overview of HIV-1 Genes 12

1.4.1 The Structural Proteins 12

1.4.2 The Enzymatic Proteins 15

1.4.3 The Regulatory Proteins 16

1.4.4 The Accessory Proteins 17

1.5 MA in the HIV-1 Life Cycle 21

1.5.1 HIV-1 MA in Late Events 25

1.5.2 HIV-1 MA in Early Events 30

1.5.3 HIV-1 MA is a Potential Virokine 35

1.6 Scope of Thesis 36

CHAPTER II: MATERIALS AND METHODS 38

2.1 Tissue Culture Cell-Lines 38
2.2 DNA Constructions 38
2.3 Expression Vectors 42
2.4 Virus Production 42
2.5 Reverse Transcriptase (RT) Activity Assays 43
2.6 p24 ELISA 43
2.7 Immunoblot Analyses 43
2.8 Virus-Cell Fusion Assays 44
2.9 Beta Glo® Assays of Viral Infectivity 48
2.10 Quantification of HIV-1 Reverse Transcription Products 49
2.11 RTC Trafficking Assay 50
2.11.1 Infection Protocol 50
2.11.2 Cell Harvesting and NP-40 Fractionation 51
2.11.3 RNA Extraction and RT-PCR 51
2.11.4 Quantitative PCR to Analyze cDNA Copy Number 52

CHAPTER III: CHARACTERIZATION OF HIV-1 VIRUSES ENCODING SUBSTITUTIONS AT MA RESIDUE 99 53

3.1 Introduction 53
3.2 Results 54
3.2.1 Virus production and Gag processing is normal in LAI-derived particles bearing the E99V MA mutation 54
3.2.2 LAI-derived particles bearing the E99V or E99K MA mutations have severe infectivity defects 58
3.2.3 LAI-derived particles bearing the E99V or E99K MA mutations have a severe defect in Env incorporation 66

3.2.4 LAI-derived particles bearing the E99V or E99K MA mutations are markedly impaired for fusion with target cells.....69

3.2.5 Defects associated with the E99V MA mutation are mitigated when expressed in the NL4.3 strain.....73

3.3 Discussion.....81

CHAPTER IV: IDENTIFICATION OF A COMPENSATORY MUTATION AT MA RESIDUE 84.....86

4.1 Introduction 86

4.2 Results 87

4.2.1 Identification of MA residue 84 in potentially modulating E99V-associated defects 87

4.2.2 MA V84 modulates the E99V-associated defects 91

4.2.3 MA V84 modulation is specific for MA E99 mutations 95

4.3 Discussion.....106

CHAPTER V: IDENTIFICATION OF AN ADDITIONAL DEFECT IMPOSED BY E99 MA MUTATIONS AT AN EARLY, POST-FUSION STEP 111

5.1 Introduction 111

5.2 Results 113

5.2.1 HIV-1 Env truncation restores fusion but not infectivity of viruses with mutations at MA E99.....113

5.2.2 VSV-G pseudotyping can partially rescue the post-entry block .124

5.3 Discussion.....136

CHAPTER VI: DEVELOPMENT OF AN ASSAY TO MONITOR RTC TRAFFICKING IN INFECTED CELLS.....142

6.1 Introduction 142
6.2 Results 143
6.2.1 Experimental rationale and overview of the methods 143
6.2.2 Optimization of fractionation techniques 144
6.2.3 Characterization of positive and negative controls.....152
6.2.4 Effectiveness of endocytosis inhibition.....157
6.2.5 RTC trafficking in the absence of reverse transcription.....161
6.3 Discussion.....163
CHAPTER VII: DISCUSSION.....165
7.1 Summary of results.....165
7.2 Potential mechanism for E99 in Env incorporation.....166
7.3 Potential mechanisms for E99 in membrane dissociation of MA 168
7.4 Future Studies.....171
7.5 Implications for the development of a novel anti-HIV therapeutic.....173
7.6 Conclusions 174
CHAPTER VIII: References.....176
APPENDIX A: a-MLV Pseudotyping Studies.....206
APPENDIX B: Single-Cycle Infectivity Data 217

LIST OF TABLES

Table 3.1 Summary of Results from Chapter 3 **……..……. 82**

Table 4.1 Fold enhancement in relative infectivity of LAI-derived viruses bearing the T84V MA substitution **……..…… 99**

Table 4.2 Summary of Results from Chapter 4 **……..…….…. 107**

Table 5.1 Relative infectivities of LAI-derived viruses bearing single amino substitutions in MA **……..……. 115**

Table 5.2 Relative infectivities of LAI-derived mutants encoding a gp41 CT truncation and individual substitutions in MA **……..……. 116**

Table 5.3 Relative infectivities of LAI-derived MA mutants pseudotyped with VSV-G Env**…….…..…..……. 128**

Table 5.4 Summary of Results from Chapter 5 **…….…….140**

Table A.1 Relative infectivities of LAI-derived MA mutants pseudotyped with a-MLV env **…….…..…….. 209**

Table B.1 RLUs from TZM-bl cell infections with LAI-derived viruses bearing single amino substitutions in MA **……. 217**

Table B.2 RLUs from TZM-bl cell infections with LAI-derived double mutants bearing gp41 cytoplasmic domain truncation and individual substitutions in MA **……..……. 218**

Table B.3 RLUs from TZM-bl cell infections with LAI-derived MA mutants pseudotyped with VSV-G **……..…….……..……..…. 219**

Table B.4 RLUs from TZM-bl cell infections with LAI-derived MA mutants pseudotyped with a-MLV env **……..……..…. 220**

LIST OF FIGURES

Figure 1.1 Kinetics of immunologic and virologic events associated with HIV infection during the acute, chronic and AIDS phases …… **7**

Figure 1.2 The HIV-1 replication cycle ……..…….…… **11**

Figure 1.3 Genomic map of HIV-1 …….……..… **20**

Figure 1.4 Ribbon diagrams of HIV-1 MA …….……..… **23**

Figure 2.1 Relative locations of changes made to LAI proviral clones …… **41**

Figure 2.2 Virus-cell membrane fusion assay ……..…..… **46**

Figure 3.1 Functional domains and amino acid substitutions in HIV-1 MA …… **56**

Figure 3.2 Effect of the MA E99V mutation on LAI particle production ……..… **57**

Figure 3.3 Western blot analysis of Gag processing in LAI-derived virus..……..… **59**

Figure 3.4 Single-cycle infectivities of LAI-derived MA mutants …….…..…… **62**

Figure 3.5 Replication kinetics of LAI-derived virus in human T-cell lines ….....… **64**

Figure 3.6 Effects of MA mutations on HIV-1 Env incorporation in LAI-derived virus ……..… **68**

Figure 3.7 Effects of MA mutations on virus-cell membrane fusion capacity in LAI-derived virus ……...…..… **71**

Figure 3.8 Effect of the MA E99V mutation on NL4.3 particle production ….....… **75**

Figure 3.9 Western blot analysis of Gag processing in NL4.3- and LAI-derived viruses ……...…**76**

Figure 3.10 Effects of MA E99V in LAI- and NL4.3-derived particles ……. **78**

Figure 4.1 Amino acid differences between the LAI and NL4.3 MA proteins and their locations relative to E99 …….……..… **89**

Figure 4.2 Single-cycle infectivities of LAI- or NL4.3-derived viruses bearing single or double mutations at MA positions 84 and 99 **……...… 93**

Figure 4.3 Effects of mutations at MA position 84 on Env incorporation in LAI- and NL4.3-derived particles bearing the E99V MA substitution **……...… 94**

Figure 4.4 Effects of single and double MA substitutions on virus-cell membrane fusion capacity in LAI- and NL4.3-derived viruses **……..……..…… 96**

Figure 4.5 Effects on infectivity by the T84V MA mutation on LAI- derived particles bearing primary MA mutations **…… 98**

Figure 4.6 Effects of the T84V MA substitution on Env incorporation in LAI-derived particles containing WT MA or other MA mutations **…… 103**

Figure 4.7 Effects of single and double MA substitutions on virus-cell membrane fusion capacity in LAI-derived viruses **……..…… 105**

Figure 5.1 Effects on infectivity by Env truncation in LAI-derived particles bearing individual MA mutations **……...… 119**

Figure 5.2 Effects of Env truncation on virus-cell membrane fusion capacity in LAI-derived viruses bearing MA substitutions **……..…… 123**

Figure 5.3 Early reverse transcription products in cells infected with LAI-derived virus containing truncated HIV-1 Env with and without the E99V MA substitution **……..… 125**

Figure 5.4 Single-cycle infectivities of LAI-derived MA mutants, containing either WT HIV-1 Env, or pseudotyped with VSV-G **……...…… 131**

Figure 5.5 Effects of VSV-G pseudotyping on virus-cell membrane fusion capacity in LAI-derived viruses bearing MA substitutions **……..…… 132**

Figure 5.6 Analysis of reverse transcription products in cells infected with VSV-G pseudotyped MA mutants **……...… 134**

Figure 6.1 Schematic representation of the proposed RTC migration assay **…..… 145**

Figure 6.2 A comparison of the efficiencies of fractionation procedures designed for separating cytoplasm from intact nuclei **…… 148**

Figure 6.3 Optimization of the NP-40 fractionation method **……..…… 151**

Figure 6.4 A schematic representation of the locations in the HIV-1 genome targeted by the RT-PCR and qPCR steps **…… 154**

Figure 6.5 Analysis of potential positive and negative controls in the RTC migration assay **……...… 156**

Figure 6.6 The effect of sucrose exposure on blocking virus endocytosis **……..… 158**

Figure 6.7 Comparison of two methods for inhibiting endocytosis **…… 160**

Figure 6.8 Analysis of RTC migration in the absence of reverse transcription **..… 162**

Figure A.1 Single-cycle infectivities of LAI-derived MA mutants containing WT HIV-1 Env or pseudotyped with a-MLV env **…….…... 210**

Figure A.2 Effects of a-MLV pseudotyping on virus-cell membrane fusion capacity in LAI-derived viruses bearing MA substitutions **……..... 213**

Figure A.3 Analysis of early products in cells infected with pseudotyped HIV-1 MA mutants **……... 216**

LIST OF THIRD PARTY COPYRIGHTED MATERIAL

The figures listed below were reproduced with publisher's permission

Figure Number	Publisher	License Number
Figure 1.1	Nature Medicine	2703130508936
Figure 1.2	Nature Reviews	2703130996770
Figure 1.3	Virology J.	open access
Figure 1.4	Proc. Nat. Acad. Sci.	perm. granted 8/19/11
Figure 2.1A	Virology J.	open access
Figure 2.1B	J. Biol. Chem.	open access
Figure 2.2A	Nature Biotech.	2703130716541

ABBREVIATIONS

2LTR	2LTR circles
AIDS	Acquired Immune Deficiency Syndrome
a-MLV	amphotropic Murine Leukemia Virus
BLaM	Beta Lactamase
CA	HIV-1 capsid
CDC	Centers for Disease Control
cPPT-CTS	central DNA flap
CT	cytoplasmic tail
CTD	C-terminal domain
ELISA	enzyme linked immuno sorbant assay
Env	HIV-1 envelope
EP	early reverse transcription products
ER	endoplasmic reticulum
ESCRT	endosomal sorting complex required for transport
Gag	HIV-1 $Pr55^{gag}$ polyprotein
gRNA	genomic RNA
HAART	highly active antiretroviral therapy
HIV	human immunodeficiency virus
IFN-γ	interferon gamma
IN	integrase
Kb	kilobases

kDa	kilodalton
LTR	long terminal repeat
MA	HIV-1 matrix
MHC-I	major histocompatibility complex class I
MOI	multiplicity of infection
MVB	multivesicular bodies
NC	HIV-1 nucleocapsid
NIH	National Institute of Health
Nef	negative factor
NES	nuclear export signal
NLS	nuclear localization signal
NMR	nuclear magnetic resonance
ORF	open reading frame
PBMC	peripheral blood mononuclear cells
PCR	polymerase chain reaction
PIC	pre-integration complex
$PI(4,5)P_2$	phosphatidylinositol 4,5-bisphosphate
PM	plasma membrane
PR	HIV-1 protease
qPCR	quantitative polymerase chain reaction
RLU	relative luciferase units
RRE	Rev-responsive element

RT	reverse transcriptase
RT-PCR	reverse transcription PCR
RTC	reverse transcription complex
RTU	reverse transcriptase unit
sCD4	soluble CD4
SDS-PAGE	sodium dodecyl sulfate polyacrylamide gel electrophoresis
siRNA	small interfering RNA
SU	surface unit
TIP47	tail interacting protein 47 kDa
TAR	transactivation response
TGN	trans-golgi network
TM	transmembrane
Vif	viral infectivity factor
Vpr	viral protein r
Vpu	viral protein u
VSV-G	Vesicular Stomatitis Virus glycoprotein
WCE	whole cell extract
WT	wild-type

CHAPTER I: INTRODUCTION

1.1 The Identification of HIV and the Development of Therapeutics

In the spring of 1981, physicians in New York and California identified rare illnesses in previously healthy gay men (33, 83, 125). It was determined that the immune deficiencies exhibited in these patients correlated with a severe depletion of CD4+ T lymphocytes and was given the title Gay-Related Immune Deficiency, or GRID, by the Centers for Disease Control (CDC) (11, 33). However, this term quickly stigmatized the gay community as carriers of the disease even as it became apparent that individuals beyond the male homosexual population were also at a heightened risk, such as intravenous drug users, hemophiliacs and heterosexuals. The following year, the disease was linked to blood, and was renamed Acquired Immune Deficiency Syndrome, or AIDS, by the CDC.

In 1983, Luc Montagnier's team from the Pasteur Institute in France identified a retrovirus as the causative agent of AIDS (9). Soon after, Robert Gallo's group at the National Institute of Health (NIH) published more evidence confirming the link between this novel human retrovirus and AIDS (78). The virus was given the name Human Immunodeficiency Virus (HIV). The first diagnostic blood test was developed and approved in 1985, enabling hospitals to screen the blood supply for HIV (132). As the disease- now an epidemic- continued to spread, a glimmer of hope finally appeared in 1987 when the first anti-HIV therapeutic, a nucleoside analog called AZT, was developed and approved for use. Unfortunately, optimism faded when doctors quickly recognized

that AZT monotherapy was futile, as AZT-resistant strains emerged soon after patients took the drug (156).

Things began to improve again in 1995, when Saquinavir- the first of a new antiretroviral drug class, the Protease Inhibitors, was developed. The following year, the first non-nucleoside reverse transcriptase inhibitor, Nevirapine, was approved for use in the US. Physicians soon recognized that the prognosis of HIV-infected patients rapidly improved when the new classes of drugs were used in combination. Thus, a new era in HIV treatment began when doctors recommended that patients receive a cocktail of three antiretroviral drugs, in a regimen referred to as Highly Active Antiretroviral Therapy (HAART) (156). This new approach proved to be very efficacious, and its significance became evident in 1997 when the CDC reported that for the first time since the early 1980's, the incidence of HIV and annual AIDS deaths had declined in the US (156). Globally, however, the pandemic was still on the rise, as 22 million people around the world were living with HIV and 3.2 million individuals were newly infected in that year alone (196).

By 2001, AIDS was determined to be the leading cause of death in sub-Saharan Africa (135, 196). Of the 21 million deaths that were attributed to AIDS around the globe, 17 million were from this region of Africa (196). In an effort to bring some relief to this area of the world, European drug companies began to manufacture and distribute less expensive, generic versions of HIV medications. Despite the impact made through this relief effort, scientists recognized that the real breakthrough in combating the AIDS pandemic would be in the development of an anti-HIV vaccine. Efforts to develop an

effective vaccine were underway, but unfortunately the first large-scale clinical trial of an AIDS vaccine, AIDSVAX, failed in 2003. Studies revealed that it did not reduce the incidence of HIV infection in more than 2,000 intravenous drug users who volunteered for the trial (112, 187).

The next big advancement in HIV therapy came in 2006 with the approval of Atripla, the first once-a-day HIV treatment option. Atripla consisted of three medications from two different classes of anti-retrovirals in a single pill, and its use eased the burden of complicated drug regimens that many patients previously had to endure. However, progress in HIV vaccine development continued to stall when testing for another major HIV vaccine candidate, the STEP trial, was abruptly terminated (199). The data revealed that administration of the vaccine conferred no benefit, and that unfortunately the adenovirus vector used to deliver the HIV antigens might have even enhanced susceptibility to HIV infection in some of the trial participants (185). Nonetheless, promising findings regarding an HIV vaccine candidate finally came in 2009 with the RV114 trial conducted in Thailand. This vaccine utilized a canary pox vector expressing HIV genes in conjunction with a recombinant HIV envelope glycoprotein. Modest efficacy was observed after three years, as participants receiving the vaccine were found to have a lowered rate of HIV infection by 31.2% compared to unvaccinated control subjects (112, 169).

Amazingly, recent reports suggest that a blood stem cell transplant may have cured the first person ever of AIDS (121). This approach utilizes a rare mutation (CCR5Δ32) in the human gene that encodes a co-receptor required by HIV for entry into

host cells. This mutation, present in only 1% of Caucasians, is believed to provide a natural resistance to HIV infection (96). San Francisco native Timothy Ray Brown lived for 11 years with HIV before he was diagnosed with Leukemia in 2006. The following year, doctors located an individual who was not only a tissue match for Brown, but who also had this rare CCR5 mutation. Brown underwent a risky blood stem cell transplant, and although his cancer came back a year later, his HIV did not. Today, Brown no longer receives any antiretroviral treatment and HIV has not been detected in any of his tissues. While this method would be impractical in widespread use, it is a remarkable proof of concept that may be used to manage disease in those living with HIV, or possibly even lead to a cure (121).

This past June marked the 30th anniversary of the first reported cases of AIDS. Considerable progress has been made, as the use of HAART has enabled HIV patients to live for decades before developing AIDS, and mother to child transmission has been reduced from 25% thirty years ago, to less than 3% today (196). However, the HIV/AIDS pandemic has taken the lives of nearly 30 million people worldwide, and there are about 34 million individuals that currently live with the disease (196). Patients continue to endure devastating side effects that are associated with existing medications and drug-resistant strains often emerge in those unable to tolerate the strict drug adherence protocols. Thus, without an effective vaccine in sight, the development of new anti-HIV drugs remains critical.

1.2 HIV Infection and Disease Progression

Two types of HIV exist in the world, HIV-1 and HIV-2. HIV-2 is concentrated in West Africa, and appears to be less easily transmitted than HIV-1 (37). HIV-1, on the other hand, is the predominant strain and associated with a shorter time between initial infection and illness. Despite these differences, the overall pattern of virus replication kinetics and CD4+ T-cell depletion is similar in infected individuals, and both types cause clinically indistinguishable AIDS (85). The immunologic and virologic events that are associated with the acute, chronic and AIDS phases of an average HIV infection is illustrated in Figure 1.1.

The acute phase of an HIV infection refers to the period between primary exposure to the virus and completion of the initial immune responses. Upon entry into a host, the virus is quickly disseminated throughout the body and seeds the lymphoid tissues. The number of virus particles circulating in the bloodstream is usually highest between 2 and 4 weeks post-exposure, and patients are highly infectious during this phase (85). This massive viremia induces a rapid CD4+ T lymphocyte depletion, with immune cells of the mucosa being the most affected target (130). While approximately 70% of patients develop a flu-like illness, routine tests for HIV antibodies often fail during this time (85). Consequently, most cases are either undiagnosed or misdiagnosed in the acute phase. The length of this phase varies, depending on the individual and HIV strain. Normally, symptoms resolve between a week and a few months (85).

Once an immune response is generated, the infection enters the clinical latency period. During this time, CD4+ T cell counts increase and although they may rebound to

80-90% of its original level, gut-associated CD4+ T-cell depletion never fully recovers (85, 130). Still, patients may be asymptomatic during the latency phase since the overall immune system remains sufficiently intact to prevent most other infections. The viremia is also resolved to some extent, as plasma levels can drop below the limit of detection. However, immune responses do not suppress viral replication completely; HIV continues to persist in the lymphoid organs and other reservoirs even in the presence of high antibody titers (3, 85). The extent of viremia associated with this asymptomatic phase is referred to as the viral set point, and oftentimes disease progression parallels that of the viral load after the immune response (85).

The ability of the virus to evade host immune responses is in part a consequence of its high mutation rate. Indeed, recombination events and mistakes made by the reverse transcriptase enzyme cause many different variants, or quasi-species, of HIV to develop in an individual. Since long-lived cells are infected, these variants persist throughout the course of infection. It has been estimated that billions of new HIV virions are produced and destroyed daily (85). In an attempt to keep virus replication at bay, the immune system produces CD4+ cells at 10 to 100 times the normal rate (85). Such chronic immune activation imposes a significant strain on the maintenance of new CD4+ cells. In many patients, this latent phase lasts for 7 to 11 years (37).

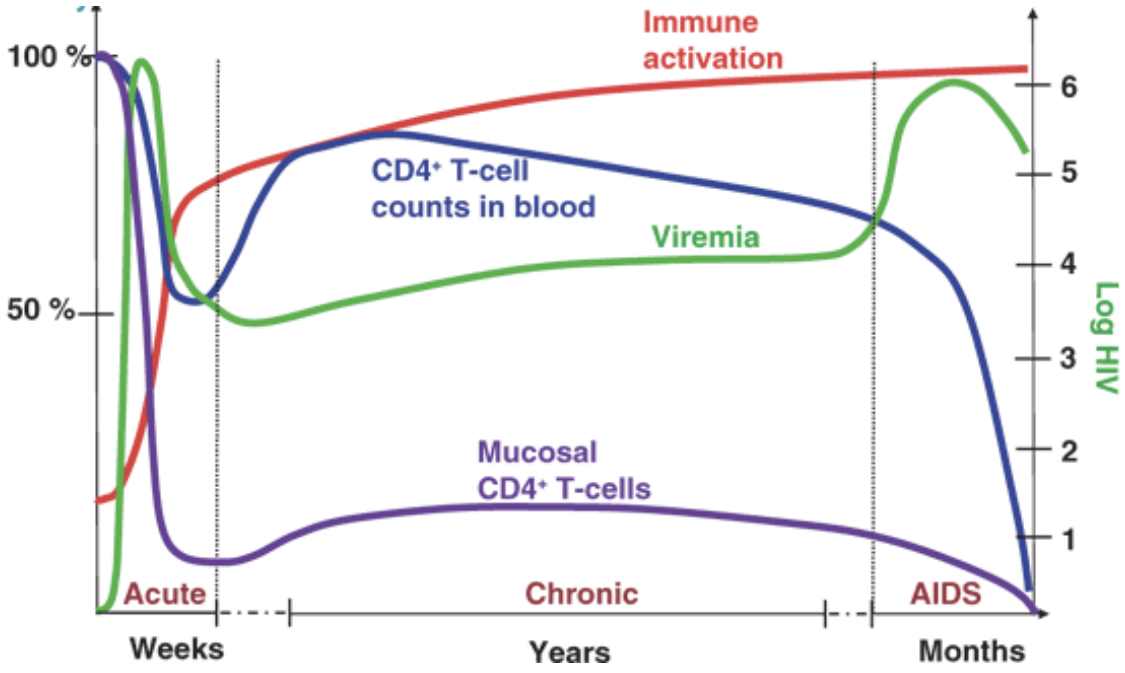

Figure 1.1 Kinetics of immunologic and virologic events associated with HIV infection during the acute, chronic and AIDS phases. (85) A schematic representation of changes in mucosal (purple) and blood (blue) CD4+ T-cells, virus levels in the blood (green), and immune activation (red) over the course of an average HIV infection. During the acute phase, mucosal CD4+ T-cells are rapidly lost and virus titers rise sharply. The immune system becomes activated and controls viremia to some extent to mark entry into the chronic phase. Blood-associated CD4+ T-cell counts recover moderately during the chronic phase. The immune system remains in a highly active state throughout the course of infection. As viremia continues to rise, the regenerative capacity of CD4+ T-cells declines and clinical AIDS develops.

Eventually, the immune system becomes overwhelmed by the high levels of viral replication. The collapse of the immune system leads to the development of clinical AIDS, the most advanced stage of disease. AIDS is diagnosed once CD4+ T-cell counts have fallen substantially, and is associated with opportunistic infections or cancers that do not usually affect healthy individuals (37). Patients can also display a range of neurological problems depending on the extent of infection in the brain. Most patients diagnosed with clinical AIDS ultimately succumb to the disease within months if not treated (3).

1.3 Overview of HIV-1 Replication

The replication cycle of HIV-1 is a complex multi-step process, regulated by both viral and cellular proteins. Events in the viral life cycle can be divided into early and late stages, based on when they occur in relation to viral DNA integration. The HIV replication cycle is depicted in Figure 1.2.

Early events begin with an interaction between the viral surface envelope glycoprotein gp120 and the cellular receptor CD4. This CD4 binding induces a subsequent interaction with the host CCR5 or CXCR4 co-receptor. A membrane fusion reaction is triggered by co-receptor binding, whereby conformational changes in both gp120 and the transmembrane glycoprotein gp41 promote fusion of the viral lipid envelope and the host plasma membrane (PM) (36, 70). This fusion event delivers the viral core into the cytoplasm of the target cell. The HIV core is composed of a capsid protein shell that encases the single-stranded, dimeric viral RNA genome and several

viral and host proteins (8, 129, 131). The core then associates with cortical actin microfilaments of the host cell cytoskeleton, which then promotes core migration through the cytoplasm (21). It is believed that further advancement of the complex toward the cell's nucleus occurs through subsequent transfer to the microtubule network (7, 129). Dissociation of the capsid shell takes place during an uncoating step and exposes a reverse transcription complex (RTC) made up of the genomic RNA, and the viral proteins nucleocapsid (NC), reverse transcriptase (RT), integrase (IN), viral protein R (Vpr) and matrix (MA) (19, 25, 59). Inside the RTC, genomic RNA is reverse transcribed by RT into a double-stranded proviral DNA. The resulting high-molecular weight complex, now referred to as the preintegration complex (PIC), is transported across the nuclear envelope using the components of the cellular nuclear transport machinery (24, 113). Once in the nucleus, IN catalyzes integration of the viral DNA into the host cell genome (57). This integration step assures that the proviral HIV-1 endures for the lifetime of the infected host cell.

After the integration step are late events, which begin with transcription of integrated proviral DNA. Cellular RNA Polymerase II synthesizes HIV transcripts expressed from the promoter located in the 5′ long terminal repeat (LTR) of the proviral template. The rate and processivity of transcription is greatly enhanced by the viral regulatory protein, Tat (144). There are three classes of viral RNAs- fully spliced, partially spliced or unspliced. The latter two forms of mRNAs contain the cis-acting Rev Response Element (RRE) that is recognized and bound by the viral Rev protein. By shuttling between the nucleus and cytoplasm, Rev mediates the nuclear export of partially

spliced or unspliced mRNAs through the cellular nuclear export machinery to the cytoplasm (144). HIV-1 particle formation is directed by the expression of viral Gag proteins, and requires components of host adaptor protein complexes that control endocytic trafficking (12, 51). It has been proposed that full-length viral genomic RNA may act as a scaffold along which Gag molecules align and pack (103, 176). Gag coordinates the incorporation of each of the viral protein components and viral genomic RNA dimers into the assembling particle (64). In most cell types, the components are transported to the PM for assembly. However, in macrophages and dendritic cells, viral assembly is thought to take place within membranes of an intracellular compartment (13, 98, 160). Nascent virions are then thought to engage with lipid raft-rich regions of the PM before budding into the extracellular environment (15, 29, 95). Release is facilitated by a sequence in the p6 domain of Gag, which interacts with host machinery that normally functions in membrane fission events (65, 66, 80, 99, 123, 186). During or shortly after virus release, the immature spherical virus particle undergoes a morphologic change known as maturation. This final step involves proteolytic processing of the Gag and Gag-Pol polyproteins by the viral protease to form the condensed, conical core that is characteristic of mature infectious HIV-1 virions (39, 166).

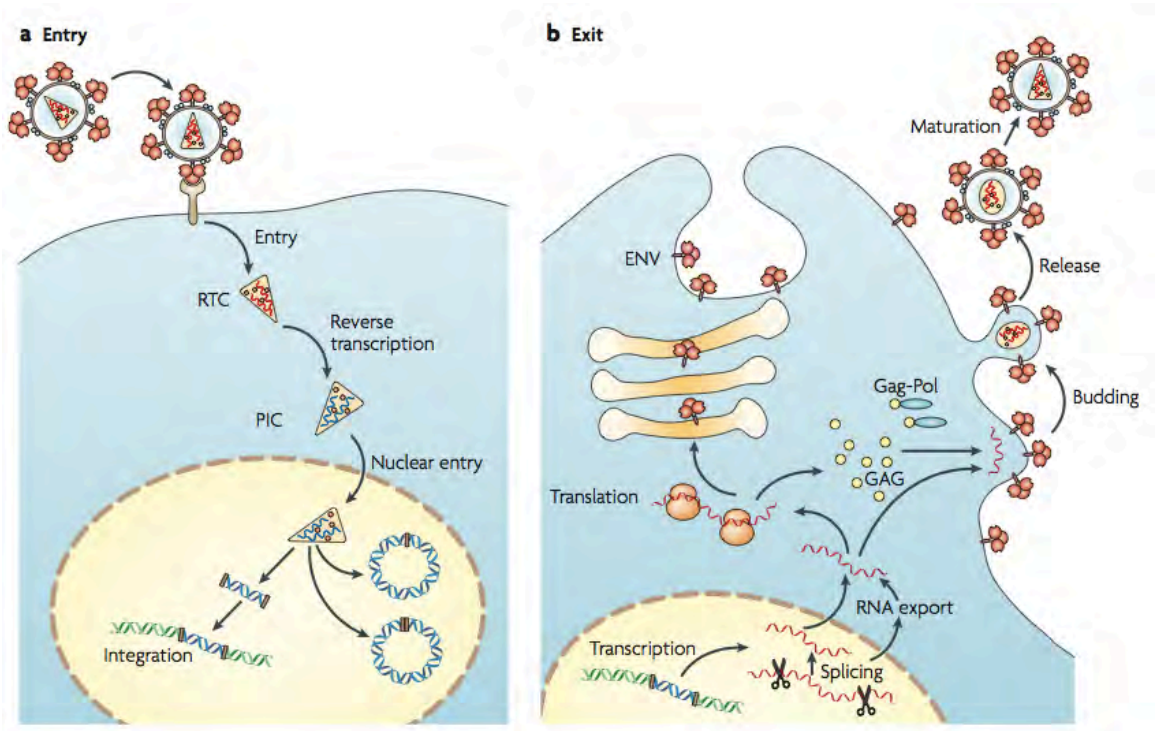

<u>Figure 1.2</u> The HIV-1 replication cycle. (81) Events of the HIV-1 life cycle are described as early or late, depending on when they occur in relation to the integration step. The early steps are depicted in the left panel and include virus attachment and entry into a host cell, uncoating of the capsid core, reverse transcription of the viral genomic RNA into DNA, its nuclear import, and then integration of the viral DNA into the host's genome. Late events, shown in the panel on the right, consist of viral gene transcription, export of fully spliced, partially spliced and unspliced mRNA into the cytoplasm, translation, nascent particle assembly, budding and release into the extracellular environment and finally, particle maturation. A more detailed description of each of these events in HIV replication is included in the text.

1.4 Overview of HIV-1 Genes

The genome of HIV-1 is about 9.7 kilobases (Kb) in length and exists as two copies of positive, single-stranded RNAs in a typical virus particle. Downstream from a 5' long terminal repeat (LTR) are nine open reading frames (ORFs), which encode fifteen distinct proteins. A schematic representation of the DNA form of the HIV-1 genome is depicted in Figure 1.3. Exhibiting a multitude of activities, these proteins can be categorized into four groups based on their individual functions: structural, enzymatic, regulatory, and accessory proteins.

1.4.1 The Structural Proteins

Gag and Envelope (Env) are the HIV-1 structural proteins and are initially expressed as polyproteins in an infected cell. Proteolytic cleavage of these precursors occurs through different mechanisms, and are necessary events in the production of infectious particles. The $Pr55^{gag}$ polyprotein (Gag) is comprised of distinct structural and functional domains that are essential in the virus life cycle (reviewed in ref. 64). During late events, Gag exists in the 55 kilodalton (kDa) precursor form and is cleaved by the viral protease upon particle maturation. This processing step yields the matrix (MA/p17), capsid (CA/p24), and nucleocapsid (NC/p7) proteins, as well as p6 and two additional spacer peptides, p1 and p2.

My thesis research focuses on MA, which is encoded by the N-terminal 132 residues of Gag, and later processed into a mature 17 kDa form. MA is best characterized by its roles in assembly, where it directs Gag to the cellular membrane and facilitates the incorporation of envelope glycoproteins into nascent virions. Upon cleavage, a small

subset of MA molecules is selectively phosphorylated, and is though to participate in early events. A more in depth analysis of MA structure and functions is included in section 1.5.

Downstream of MA is the CA domain of Gag. CA is critical in virus assembly by its contribution to Gag-Gag interactions, and packaging of Gag-Pol precursors and host cyclophilin A (CypA) proteins into nascent particles. By forming a protective shell around the viral RNA genome (gRNA) and core-associated proteins, CA molecules facilitate optimal delivery of the HIV-1 genome into target cells and promote efficient reverse transcription.

The next Gag domain is the NC sequence, which has several important functions in virus assembly. By associating with gRNA, NC directs its dimerization and incorporation into particles. As part of Gag, it also promotes the tight packing of Gag molecules, membrane binding, and virus release. Following cleavage from the Gag precursor, NC is released from the other structural proteins and participates in early events by stimulating reverse transcription and stabilizing the PIC (64).

P6 makes up the C-terminal portion of Gag and participates in assembly by incorporating the accessory protein Vpr into virus particles. A Pro-Thr-Ala-Pro-Pro (PTAP) sequence near the N-terminus of the domain promotes virus release into the extracellular environment by engaging with Tsg101 and other host proteins (65).

Env is the other main structural gene of HIV-1, and it is synthesized as a 160 kDa precursor (gp160) on ribosomes associated with the endoplasmic reticulum (ER) (reviewed in ref. 70). The envelope polyproteins are co-translationally glycosylated, and

then oligomerized into trimers before transport from the ER to the Golgi complex. Once in the Golgi, gp160 is proteolytically cleaved by a cellular enzyme, which generates the mature glycoproteins gp120 and gp41. This processing step is essential for transport to the PM, however little is known about how Env is transported from the Golgi network to the cell surface (15). Both gp120 and gp41 are maintained in the assembled Env trimers through non-covalent interactions.

The surface glycoprotein gp120 is responsible for receptor and co-receptor binding onto the target cell. The protein has five variable regions (V1 through V5) that are well exposed on the surface of the molecule (70, 162). Interspersed between these variable loops are five conserved regions that fold into the gp120 core. While elements from both the core and surface domains contribute to CD4 binding, the attachment to chemokine receptors is mainly governed by sequences in the gp120 V3 region.

The gp41 glycoprotein catalyzes virus-cell membrane fusion events. It is made up of an ectodomain that is largely responsible for trimerization and fusion, a membrane-spanning anchor (TM), and a cytoplasmic tail domain (CT). A striking feature of lentiviruses is the extended length of the gp41 CT, which is generally about five times longer than those of avian and murine retroviruses (64, 90). The CT of HIV-1 gp41 is necessary for recruitment by the MA region of Gag during particle assembly (40, 53, 71, 115, 153). Some evidence also suggests that the CT is important in virus infectivity, however, this function appears to be cell-type dependent (70, 162.)

1.4.2 The Enzymatic Proteins

The *pol* gene resides downstream of the *gag* gene, and a negative ribosomal frameshift error which occurs during 5% of all Gag translation events, leads to its synthesis as part of a Gag-Pol precursor protein (Pr160). Encoded in the *pol* gene are three viral enzymes: protease (PR), reverse transcriptase (RT) and integrase (IN). All of these proteins provide essential enzymatic functions, and therefore, each of their activities has been used as targets for anti-HIV therapies (reviewed in ref. 94).

Structural studies of PR reveal that it must dimerize to form the protein's active site (143). Dimerization of the identical PR subunits is concentration dependent and favored during virion assembly. The first substrate of PR is likely to be itself so that it can be released and continue cleaving the Gag and Gag-Pol precursors. Processing of these polyproteins by PR is the main event in virion maturation, and precipitates a morphological change in the particle that is required for virus infectivity.

The RT gene comes after the protease domain in *pol*, and encodes an RNA-dependent DNA polymerase (reviewed in ref. 82). During the early stages of the viral life cycle, RT generates double-stranded proviral DNAs from the single-stranded viral RNA genomes. The active form of HIV-1 RT is made up of two chains, referred to as p51 and p66. While p51 has a mainly structural function, p66 contains the catalytic site for DNA polymerization. For reverse transcription to occur, the RNA template, primer, two divalent cations, and dNTPs must localize to a cavity within p66, formed by the protein's fingers, palm, and thumb subdomains (82). The p66 chain also has an RNase H activity that cleaves the genomic RNA template while it is still hybridized to DNA during double-

stranded DNA synthesis. HIV-1 RT is regarded as an error prone polymerase, as it exhibits no exonucleolytic proofreading activity.

Integrase (IN) makes up the C-terminal region of the Gag-Pol proteins (reviewed in ref. 57). During maturation, IN is cleaved into its 32 kDa mature form and associates with the viral core. Following nuclear import, IN carries out the first two steps required for integration of the double-stranded viral DNA into the host genome. First, IN cleaves the blunt ends of the viral DNA to form an active intermediate. Next is the strand-transfer step, where the processed ends of the viral DNA are inserted into one of the cell's chromosomes. This step is also carried out by IN, and assisted by LEDGF/p75, which tethers IN to chromatin, and several other host cofactors (182). Finally, host machinery fills the gaps at the 5'-ends of the viral DNA to complete the integration process.

1.4.3 The Regulatory Proteins

Two regulatory proteins, Tat and Rev, make up the next class of HIV-1 gene products. The efficient expression of most viral proteins is dependent on these two proteins, and therefore both factors are indispensable in HIV-1 replication.

The transcriptional transactivator (Tat) is one of the earliest viral proteins expressed in an infected cell, and is essential for synthesis of full-length transcripts from the HIV-1 provirus (reviewed in ref. 144). By binding to the transactivation response (TAR) element at the 5′ end of nascent HIV-1 mRNAs, Tat recruits a host factor called P-TEFb. This interaction then signals a cyclin T1/CDK9 complex to hypo-phosphorylate the C-terminal domain of RNA polymerase II (Pol II), stimulating LTR-directed transcriptional elongation.

The regulatory Rev protein encodes two functional domains, an arginine-rich nuclear localization signal (NLS) and a leucine-rich nuclear exporting signal (NES) (144). These regions are essential for the protein's nucleocytoplasmic shuttling activity. Rev binds to the Rev responsive element (RRE) present in unspliced and partially spliced viral transcripts through its arginine rich motif. Using an interaction with Ran GTP, Rev directs the export of *gag-pol* and *env* mRNAs from the nucleus to the cytoplasm.

1.4.4 The Accessory Proteins

The final category of HIV-1 gene products include the "accessory" proteins, a term given because their absence in proviral clones has little bearing on viral replication in cell cultures. However, recent studies have uncovered that, *in vivo*, they are key determinants for HIV virulence (194). These proteins are called viral infectivity factor (Vif), viral protein u (Vpu), viral protein r (Vpr) and negative factor (Nef).

Vif is a late gene product present in most lentiviruses that counteracts the antiviral effects of the human restriction factor, apolipoprotein B mRNA-editing enzyme catalytic polypeptide-like 3G (APOBEC3G) (178). APOBEC3G is a cytosine deanimase that, in the absence of Vif, is incorporated into nascent virus particles. If packaged, this host protein converts cytosine (C) residues in minus-strand reverse transcripts of the viral genome into uracil (U) residues. During reverse transcription, RT registers this change as a thymine (T), resulting in guanine (G) to adenine (A) hypermutations in the viral genome. Vif effectively antagonizes the antiviral effects of APOBEC3G in the majority of wild-type viral infections, through the recruitment of a ubiquitin ligase that induces the polyubiquitylation and degradation of both APOBEC3G and Vif.

The Vpu gene product is translated from a bicistronic mRNA that also contains the *env* open reading frame. As an integral membrane phosphoprotein, it associates mainly with the internal membranes of the cell and carries a dual function. First, it down-regulates intracellular CD4 expression, which is thought to increase the infectivity of HIV-1 virions by enhancing the intracellular transport and maturation of Env. Second, Vpu is reported to counteract the antiviral activity of host protein B cell stromal factor 2 (BST-2) or tetherin (54). In the absence of Vpu, tetherin prevents virus egress, and as a result, particles accumulate at the exterior of the cell or are transported to endosomes. The mechanism by which tetherin prevents virion release is not yet clear, but it has been suggested to involve linking cholesterol-rich lipid rafts together on the PM (54). It has been proposed that Vpu counteracts this restriction factor by altering tetherin trafficking between different cytoplasmic sites (54, 117). By interfering with the antiviral activity of tetherin, Vpu enhances the release of budded particles from the surface of HIV-1 infected cells.

Nef is a myristoylated protein that is a critical determinant of pathogenicity and disease progression *in vivo* (reviewed in ref. 117). One of the first viral proteins to be expressed following infection, Nef enhances virus infection with at least three activities. First, it triggers the rapid endocytosis and lysosomal degradation of CD4 and major histocompatibility complex I (MHC-I). Reducing the surface expression of these molecules may diminish Env interference with CD4, and help infected cells evade detection by the host immune system, respectively. Second, Nef alters T-cell activation pathways, possibly to safeguard against host immunity, which could extend virus

production and long-term persistence. Lastly, minimal amounts of Nef are detected in HIV-1 particles, where they are thought to enhance the initial phases of infection. Its precise roles in early events have yet to be defined, but Nef may assist the core penetrating in the cortical actin network, and stimulate proviral DNA synthesis during reverse transcription.

Finally, Vpr is thought to promote virus replication by altering various factors in the cellular environment. Vpr is packaged into HIV-1 particles through an interaction with the p6 region of Gag, potentially facilitating the infection of macrophages (117). This mechanism might involve connecting the PIC with the cell nuclear-import pathway, or by stimulating transcription from some cellular promoters. Also, Vpr arrests cells in the G2 phase of the cell cycle, which may enhance viral transcription by exploiting the phase associated with the most active host machinery (117). However, this activity has been linked to an enhancement of cell death, and could simply be a consequence of the destruction of an unidentified host protein.

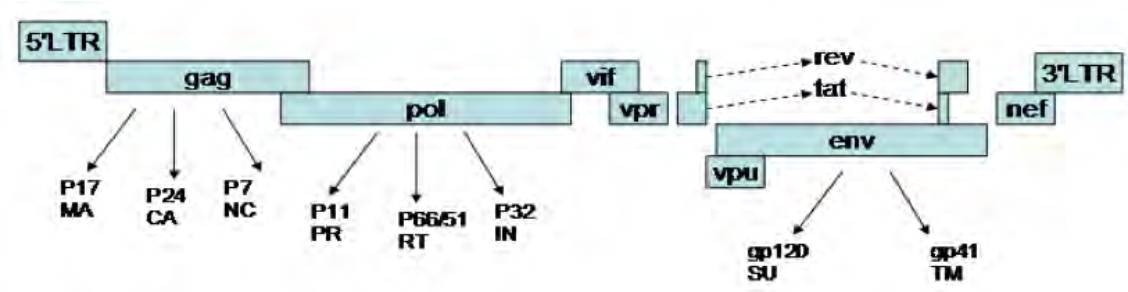

Figure 1.3 Genomic map of HIV-1. (41) The HIV-1 genome comprises nine genes and is flanked by long terminal repeat sequences (LTRs) in its proviral form. Fifteen different proteins are expressed from these nine genes, and each is necessary for HIV disease pathogenesis. *gag* and *env* make up the structural genes. *pol* encodes the enzymatic genes. *tat* and *rev* comprise the regulatory proteins. And the remaining genes *vif, vpr, vpu* and *nef*, encode the HIV-1 accessory proteins. The individual roles of these gene products are described in the text.

1.5 MA in the HIV-1 Life Cycle

Although variable in sequence, Gag proteins of most retroviruses encode a matrix domain that functions to anchor the viral Gag to the PM at a step during particle assembly (reviewed in ref. 90). Certain retroviruses, referred to as type C, form and bud simultaneously at the membrane. Lentiviruses such as HIV, and mammalian and avian retroviruses, are examples of type C viruses. Other retroviruses, referred to as type B and D, fully assemble as a core particle within the cytoplasm before budding from the membrane. Such examples include the mouse mammary tumor virus (MMTV) and the Mason-Pfizer monkey virus (M-PMV), respectively. Interestingly, the sequences within matrix domains that determine assembly localization are very subtle, since a single point mutation is able to change the assembly of a type D virus into that of a type C virus (171).

The structures of retroviral Matrix proteins (MA) are predominantly composed of closely packed α-helices (39). Many retroviral Gag proteins are co-translationally myristoylated at its N-terminal glycine. Myristic acid is a 14-carbon saturated fatty acid that anchor into the PM and plays a key role in Gag trafficking. However, MA regions of some retroviral Gag proteins, such as Rous sarcoma virus (RSV), Visna virus, caprine arthritis-encephalitis virus (CAEV) and equine infectious anemia virus (EIAV), are not myristoylated. Instead, the high membrane affinity of Gag is conferred by an exposed patch of basic amino acids situated within the MA domain that interacts with membrane-associated acidic phospholipids. Nonetheless, the membrane targeting and binding

properties of most retroviral Gag proteins are coordinated by both a myristoyl moiety and polybasic motif in MA.

The HIV-1 MA protein is synthesized as part of a 55 kDa precursor protein encoded by the HIV-1 *gag* gene. As a domain of Gag, MA is critical in coordinating late events in the virus replication cycle. Gag proteins are processed during virus maturation, and MA is released as a mature 17 kDa protein that can interact with the viral core and potentially participate in early events. Both Nuclear Magnetic Resonance (NMR) and X-ray crystallographic approaches have been used to determine the three-dimensional structure of the 17 kDa HIV-1 MA protein (39, 93, 124). These studies have revealed that of the 132 residues in MA, the first 95 make up of four major α-helices and a three-stranded mixed β-sheet that come together, forming a compact globular core domain. Residues 96 through 121 create a fifth, C-terminal helix that projects away from the globular head (93, 124). The remaining C-terminal residues are relatively unstructured and likely serve as a spacer region between the MA and CA domains of Gag (93). Interestingly, the helical topology of HIV-1 MA shares a striking similarity to the immune modulator interferon gamma (IFN-γ), and it has been suggested that MA may act as a viral cytokine *in vivo* (44, 62, 126). A ribbon diagram depicting the structure of HIV-1 MA, is shown in Figure 1.4A. The many roles of HIV-1 MA, during late and early events of the HIV-1 life cycle, and also as a potential virokine, are outlined in the following sections.

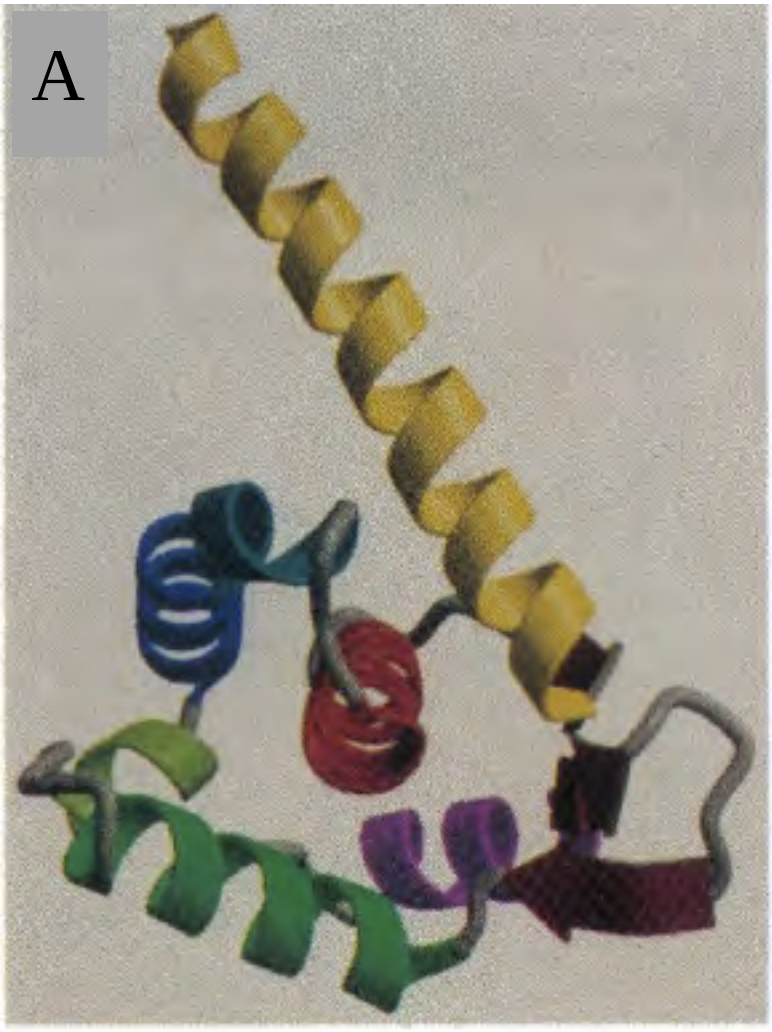
A

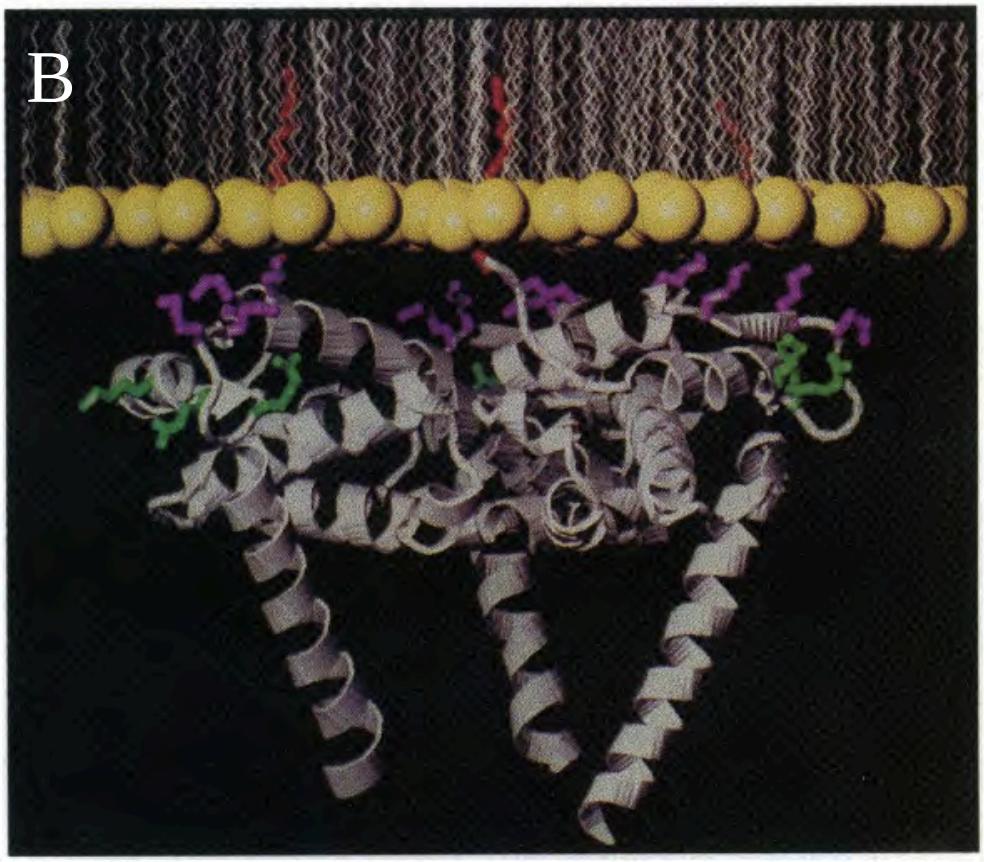

Figure 1.4 Ribbon diagrams of HIV-1 MA. (93) **(A)** A depiction of the MA monomer. The structure of MA consists of five major α-helices and a mixed β-sheet. The first four helices (1-4, shown in magenta, green, blue and red, respectively) come together to form a compact globular core domain that is capped by the mixed β-sheet (maroon). The fourth helix, buried within the hydrophobic core, is important in maintaining the overall structure of the core domain. The C-terminal fifth α-helix (shown in yellow), projects away from the others. **(B)** An HIV-1 MA trimer and its proposed orientation on the plasma membrane. MA favors the trimer formation when expressed in the context of the Gag polyprotein. An N-terminal myristate moiety (shown in red) acts in concert with essential basic residues (magenta) to promote membrane binding of MA trimers. Additional basic residues not required for membrane binding (shown in green) are distributed throughout the protein.

1.5.1 HIV-1 MA in Late Events

As in many other retroviruses, the N-terminal MA domain of HIV-1 Gag provides the membrane-targeting signals that are critical for late events of the virus life cycle. The high membrane affinity of HIV-1 Gag is conferred by a bipartite signal consisting of a myristoyl moiety and a polybasic region located on one side of the MA globular head domain. The myristic acid is covalently attachment to the N-terminal glycine residue of MA during translation. The positively charged motif is formed by a highly basic domain, encoded by MA residues 18 through 32, that comes together with other basic amino acids of MA in the tertiary structure of the protein (93). MA molecules trimerize in solution to form a large membrane-binding surface, whereby the bipartite signals is able to facilitate interactions between Gag and the PM. This association of MA trimers with the PM, as depicted in Figure 1.4B, is necessary for HIV-1 particle production in most cell types (64, 138). The importance of this bipartite signal in HIV-1 has been demonstrated by several mutational studies. For example, substitutions of MA residues required for myristoylation, namely 2G, 3A, 4R, or 5A, (20, 84, 136, 184), as well as mutating the basic amino acids K18, R20, K26, K27 or K30 (69, 72, 150, 177) which are part of the protein's positively charged motif, each cause a marked decrease in HIV-1 particle production. However, it is likely that specific trafficking machineries are also responsible for Gag transport within cellular compartments. This involvement is likely because HIV-1 viral assembly takes place at the limiting membrane of an intracellular compartment in macrophages and dendritic cells, rather than at the PM (13, 51, 146, 147, 160). Thus, the

cooperative membrane targeting by the myristate moiety and basic domain of HIV-1 MA might be cell-type specific.

It has been proposed that some of the basic residues in MA may dictate the specificity of the bound lipid, since particular substitutions have resulted in a re-targeting of Gag to other intracellular membranes (147, 175). Such aberrant Gag trafficking also occurs in HIV-1 infected cells when membrane-bound $PI(4,5)P_2$ is depleted by the over-expression of proteins involved in phospholipid metabolism (4). $PI(4,5)P_2$ is an acidic phospholipid that is predominantly localized on the inner leaflet of the PM and likely associates with MA during HIV assembly. Direct interactions between HIV-1 MA and $PI(4,5)P_2$ have been observed *in vitro* by both NMR spectroscopy (175) and mass spectrometric protein footprinting (181). The MA residues involved in the $PI(4,5)P_2$ interaction have been previously implicated in RNA binding during assembly, however it was also observed that $PI(4,5)P_2$ was the only lipid that could remove nucleic acids bound to basic residues on recombinant HIV-1 MA proteins (5).

Mutations in MA other than basic amino acid substitutions have also been shown to re-target Gag to different membranes in the cell. For example, single amino acid substitutions at positions 85 through 89 have been associated with the re-direction of particle assembly from the PM to intracellular compartments, such as the Golgi or Golgi-derived vesicles (72). Also, deletion of a large region in MA re-targeted virus formation to the ER (58, 77). It is believed that these mutations may act by specifically disrupting a PM targeting signal, or by creating a novel re-targeting signal (90).

In general, any mutation that prevents the correct folding or multimerization of MA is also likely to inhibit particle assembly (30). For example, substitutions of residues at the proposed trimer interface of HIV-1 MA (L64, T70, E74) resulted in inefficient assembly (30, 39, 137). Particle production was also disrupted when MA residues 56 through 60 were mutated, and is likely related to a diminution in the half-life of Gag proteins (72). However, a most intriguing observation was that particles were still generated when the entire MA sequence was replaced with a heterologous membrane-binding domain (168). In this study, assembly was observed at both the plasma and intracellular membranes. One explanation for this phenomenon is that certain MA mutations might exert a dominant-negative effect on the function of Gag that is not seen in the absence of MA (150).

Besides Gag targeting, MA is also involved in the incorporation of particular viral components into nascent virions during assembly. For example, an RNA binding region in the MA basic domain can facilitate packaging of genomic viral RNA into particles in the absence of NC (64). In addition, the incorporation of Env glycoproteins into newly assembled virus is dependent on MA. Results from several different studies have demonstrated that HIV-1 Env packaging is mediated through an interaction between MA and the cytoplasmic tail (CT) of gp41. First, MA mutants that impaired Env incorporation could be rescued by compensatory changes in the gp41 CT (69, 118, 141, 204). Second, the expression of HIV-1 Env *in trans* targeted HIV-1 budding to the basolateral surfaces of polarized epithelial cells. This selective budding site was dependent on the gp41 CT

and could be blocked by mutations in MA (115, 153). Finally, an *in vitro* study detected a direct interaction between HIV-1 MA and gp41 (40).

However, in an apparent contradiction, truncation of the entire gp41 cytoplasmic tail does not block Env incorporation, and heterologous retroviral glycoproteins can be efficiently incorporated into HIV-1 particles (reviewed in ref. 70). This discrepancy has been resolved in part by the observation that single amino substitutions in MA which block the incorporation of full length HIV-1 Env into particles do not inhibit the packaging of truncated HIV-1 Env glycoproteins (69, 118). Thus, it appears that while the inclusion of virus envelopes with short cytoplasmic tails occurs independently of MA, incorporation of full length HIV-1 Env into HIV-1 particles requires a specific interaction with, or at least a modification by MA. It has been suggested that during assembly, MA trimers form a lattice structure containing an arrangement of spaces large enough to accommodate the cytoplasmic tails of gp41 (93, 165). In line with this model, several point mutations within MA that disrupt Env incorporation reside within these putative holes that could potentially interact with the cytoplasmic domains of Env (69, 71).

Most of the single amino acid substitutions that abrogate Env incorporation into particles, namely G11R, L13E, W16A, L30E, V34E or A37P, are located at N-terminal residues of MA (14, 31, 68, 69, 111, 141, 150, 155, 207, 214). However, functional analyses of viruses with in-frame MA deletions suggest that regions throughout the protein are involved in Env incorporation, not just N-terminal sequences. For example, deletion of MA residues 27 through 30, 63 through 65, 77 through 80, or 98 through 100, results in the production of Env-deficient particles (52). Also, in a recent study,

researchers found that the L50D substitution in MA conferred a selective reduction in particle-associated gp120, without diminishing the levels of incorporated gp41 (43). Altogether, these findings suggest that regions throughout the entire globular core of MA are involved in HIV-1 Env incorporation, and that some might be required for stabilizing gp41-gp120 complexes.

Currently, the initial site of this putative MA-Env interaction is unknown. It is widely believed that cellular cofactors help facilitate HIV-1 Env incorporation, and that identification of such cofactors could provide insight into the cellular location hosting the initial MA-Env encounter (51, 90). TIP47 is a cytosolic protein required for the retrograde transport of certain proteins from late endosomes to the *trans*-Golgi network (TGN), and has been shown to form a ternary complex with the MA domain of Gag and the TM of Env (16, 49, 116). The TIP47-MA interaction was abolished by mutations of MA residues W15 and E16, which interestingly, also impaired Env incorporation into HIV-1 particles (116). These particular MA residues are located within a region of MA previously implicated to associate with the AP3 adaptor complex (51). AP3 is host trafficking machinery that localizes to the TGN and peripheral endosomal compartments. Disruption of the MA-AP3 interaction has been shown to drastically diminish particle assembly (47, 51). These results suggest that Gag could associate with Env and TIP47 on endosomal compartments (90).

During assembly, both Gag and Env associate with concentrated microdomains of specific lipids on membranes called lipid rafts (50, 114). Often made up of cholesterol, sphingolipids and membrane proteins, these domains may be platforms for signal

transduction and cell activation (6). HIV-1 particles bud preferentially through these raft microdomains of the PM, and HIV-1 viral membranes have an unusually high cholesterol and sphingomeylin content (6, 29, 89, 146, 148, 149). Other studies have shown that cholesterol depletion from producer cell membranes impairs Gag multimerization, and significantly reduces the production of HIV-1 viral particles (86, 147, 152, 175, 181). It has been proposed that the initial docking of Gag at the PM is followed by lateral transport to lipid rafts, since lipid raft targeting appears to be a slower process than membrane association (149). Although recent findings suggest that Gag might be necessary for Env to associate with lipid rafts, whether MA actively aggregates these membrane microdomains or binds to pre-formed platforms, is not yet known (15, 90).

1.5.2 HIV-1 MA in Early Events

In addition to the key roles of MA as a domain of Gag, several lines of evidence suggest that the mature 17 kDa form of MA functions in early events of the HIV-1 life cycle. During HIV-1 maturation, the viral protease cleaves the 132-residue domain of MA from other Gag structural proteins. The majority of these cleaved MA proteins form a protective shell that is attached to the inner surface of the viral membrane (84, 145). However, a small subset of the 17 kDa MA molecules dissociates from the membrane and interacts with the viral core (28, 76, 131, 189, 203). These MA proteins enter the new host cell as part of the RTC, and several studies have even detected them in the viral PIC (23, 74, 131). These observations suggest a role for MA following membrane fusion, and indeed, MA mutations have been reported that impair virus replication without affecting Env incorporation, assembly or release (31, 104, 166, 167, 213)

For a subset of mature MA molecules to interact with the viral core, the protein must somehow reduce its membrane affinity. Early on, it was proposed that the membrane binding property of MA might be regulated by a "myristoyl switch" mechanism that alters the accessibility of its N-terminal myristoyl group (217). In this model, MA can adopt a "relaxed" or "tense" state that facilitates myristate exposure or sequestration, respectively. Thus, burial of the myristoyl group inside a hydrophobic pocket of the MA globular domain might diminish the membrane affinity of MA, and permit an association with the viral core. The structures of both myristoylated and unmyristoylated HIV-1 MA have been resolved, and findings from the studies suggest that MA does not undergo a dramatic conformational change when switching between states (93, 124, 127, 191). Recent data indicate that conversion between the two conformations is entropically regulated and several factors, such as MA concentration and proximity to RNA or $PI(4,5)P_{2,}$ might influence which of the myristate-exposed or –sequestered states is favored (90, 191, 206). It has also been speculated that Gag processing during particle maturation might promote sequestration of the myristoyl moiety (90, 174). Thus far, only a few MA residues (V7, L8, S9, G10 and G11) have been implicated in regulating the myristoyl switch (174, 191).

It has also been proposed that the membrane affinity of MA might be reduced through specific phosphorylation events inside the virus particle (22, 75, 76, 189). Such modifications might induce structural changes that promote the myristoyl switch. Alternatively, the negative charge conferred by the addition of phosphate groups to a MA protein might counteract electrostatic interactions with acidic phospholipids of the lipid

bilayer (22, 26, 75, 76, 212). Indeed, this post-translational modification has previously been associated with regulating the functions and affinities of other myristoylated proteins. For example, it has been demonstrated that interactions between members of the myristoylated, alanine-rich C kinase substrate (MARCKS) family of proteins and the PM can be reversed through specific phosphorylation events (193).

Although many laboratories have attempted to identify which, if any, phospho-acceptor sites on HIV-1 MA are required for an early post-entry step, they generated conflicting results that suggest a complexity behind MA phosphorylation events (22, 67, 75, 76, 189). For example, studies from one group indicated that a membrane-associated tyrosine kinase is incorporated into budding virions, and phosphorylates the C-terminal tyrosine residue (Y132) of MA (75, 76). This group proposed that this phosphorylation event could promote the membrane dissociation of MA and even facilitate nuclear import through a MA-IN interaction. However, other groups found that phosphorylation of MA Y132 did not prevent infection in primary macrophages, and was therefore dispensable (22, 67). Nonetheless, it was noted that mutation of Y132 resulted in differential phosphorylation of another tyrosine residue in MA (22).

Another group reported that phosphorylation of MA residue S111 was essential for the membrane-binding properties of MA (212). Yet, this requirement could not be subsequently confirmed using site-directed mutagenesis analyses and subcellular fractionation experiments (217). It was later suggested that an additive effect of multiple phosphate acceptor sites in MA, particularly at residues S38, S67, S77, and S111, is required to facilitate MA dissociation from the negatively charged PM (22). In direct

opposition to this hypothesis, however, was the observation by another group that both free and membrane-bound MA molecules are phosphorylated to an equivalent degree (183). In support of single MA residues regulating membrane affinity, yet another study indicates that individual mutations at residues S9, S67, S72 and S77 inhibited a post-entry MA function (101). However, additional findings indicate that these mutations reduced Env incorporation and likely diminish the fusion capacity of virus particles (14). The authors of the latter study proposed that instead of reducing membrane affinity, abrogation of the phosphorylation sites inhibited the ability of MA to recruit Env to the sites of viral assembly. Nevertheless, they speculated that some of these mutant particles might have had an additional post-entry block to replication, since restoring fusion failed to completely rescue infectivity.

Also implicated in early events of the HIV-1 replication cycle is the C-terminal helix of MA. An early study reported that C-terminal deletions in MA reduced particle infectivity without affecting assembly (213). However, recent findings attribute the impaired infectivity of these viruses to reductions in Env incorporation (14). It has been suggested that large deletions in the extended fifth helix could modify the conformation of Gag precursors, disrupting protein-protein interactions necessary for Env incorporation. Nonetheless, the C-terminal helix of MA has been shown to reduce liposome binding *in vitro,* and this behavior was also reflected *in vivo* (217). The authors of this study hypothesized that the fifth helix in MA exerts a negative effect on the membrane binding of MA, and might regulate the exposure of myristate.

Since MA has been detected inside reverse transcription and preintegration complexes, it has been suggested that MA might act as a karyophilic agent, promoting nuclear migration of these viral complexes. Indeed, two short stretches of basic amino acids, encompassing residues 24 through 31 (NLS-1) and 110 through 114 (NLS-2), have been identified in MA that could potentially act as nuclear localization signals (NLS) (24). Initial findings suggested that the NLSs were functional, since disruptions of these sequences in viruses imposed infectivity blocks that correlated to a reduction in nuclear import (24, 23, 35, 38, 88, 92, 124, 127, 198). However, subsequent studies revealed that MA displayed very low kariophilicity (48, 63, 120, 209). It has since been established that the discrepancies concerning the role of MA sequences in nuclear import might be due to redundant nuclear import signals, since IN, Vpr, and the central DNA flap remaining on viral DNA after reverse transcription (cPPT-CTS) also displays kariophilicity (17, 73, 92, 198, 215). In a recent study, HIV-1-based viruses were analyzed in which all but one of the possible kariophilic entities were removed (172). Among the viral elements analyzed, the cPPT-CTS was reported to provide the most significant nuclear import signal. However, the importance of this element varied in different cell types and was independent of the dividing status of the cell. The current consensus appears to be that MA does not function in this regard, or contains a weak signal that acts cooperatively with other elements of the viral core (73, 92, 168).

Lastly, it has been proposed that MA molecules are involved in HIV-1 integration. An early study reported that the EED protein, an IN-binding partner, interacts with HIV-1 MA, and that the IN-EED-MA complex might be critical for directing the

PIC to host chromatin inside the nucleus (161). EED is normally involved in reducing the accessibility of DNA to maintain the silent state of chromatin, and it was later suggested that this putative MA-EED interaction could trigger transcriptional activation (197). A subsequent study indicates that although substitutions in the putative MA NLS-1 (K27I, K28I) did not significantly alter the nuclear import of the viral PIC, they could reduce viral infectivity by affecting late post-chromatin binding events (120). The authors proposed that MA might have a crucial function in mediating interactions between chromatin-bound PICs and host machinery involved in HIV-1 DNA integration and circularization. Taken together, these findings suggest a potential function of the MA protein in virus integration.

1.5.3 HIV-1 MA is a Potential Virokine

It has been previously demonstrated that viruses may encode virokines, which are cytokine homologues capable of acting as agonists or antagonists that can trigger or prevent specific biological responses, respectively (reviewed in ref. 109). A 1994 study revealed that the helical topology of the HIV-1 MA protein shares a striking similarity with the immune modulator interferon gamma (IFN-γ) (126). Although mature MA did not seem to oligomerize with, or mimic the biological properties of IFN-γ (3), it binds to a cell surface receptor constitutively expressed on peripheral B cells (44, 45). This receptor, termed p17R, is also expressed on T-cells in PBMC cultures at the very early stages of T-cell activation (45). The authors of this study reported that while exogenous MA did not induce any biologically relevant effect on resting T-cells, it increased the T-cell proliferative response even at very weak doses of IL-2. These results suggested that

at least in culture, exogenous MA might have immunomodulatory activities that could promote target cell proliferation, and possibly enhance viral replication. Consistent with this hypothesis, HIV-1 infected PBMCs cultured in the presence of IL-2 and exogenous MA together released higher amounts of virus than infected cells that were cultured in the presence of IL-2 alone (45).

Recent evidence has indicated that *in vitro,* HIV-1 infected cells are able to release a significant amount of MA (51). A later study demonstrated that extracellular MA is abundant in the lymph nodes of HIV-1 infected patients, and even accumulates in the lymph nodes of patients on HAART with undetectable viral loads (164). Multiple groups have reported that MA-specific neutralizing antibodies are produced *in vivo* (44, 157). In cell culture, these anti-MA antibodies inhibited the interaction between MA and its putative p17R receptor, and abolished the exogenous MA cytokine-like activity (44). The p17R receptor-binding region of MA was mapped to the protein's N-terminus, however the authors noted that other sites might contribute to the MA-p17R interaction (44). Collectively, these findings suggest that exogenous MA might exert biological activities *in vivo* and possibly act as a virokine in infected individuals (164).

1.6 Scope of Thesis

The findings presented in this thesis demonstrate that a highly conserved residue within the C-terminal helix of HIV-1 MA has multiple, essential roles in the function of the protein. I determined that substitutions of this residue, a glutamate at position 99 (E99), abolish virus infectivity in multiple cell lines. Further characterization of the defects associated with MA E99 substitutions was achieved using a variety of approaches

designed to analyze individual steps in the virus life cycle. Specifically, I examine Env incorporation, particle production, and Gag processing, and determine that particles bearing specific E99 substitutions are generated at normal levels yet have a reduction in Env packaging. Through virus-cell membrane fusion studies, I functionally link the Env incorporation defect with a diminished capacity to fuse with target cells. A genetic approach was used to identify a compensatory mutation at MA position 84, and although the extent of rescue conferred by this second site change varies in different viral clones, it is specific for rescuing the defects associated with E99 substitutions. Multiple strategies were employed to restore virus-cell fusion in particles bearing the E99 substitutions. Further analyses reveal that these particles remain defective at an early, post-entry step. Finally, preliminary results are presented for the development of a novel method that might be used to identify trafficking defects that are critical for early steps in the HIV-1 life cycle. Such methods could be used to further characterize the post-entry defect exhibited by particles bearing mutations at MA E99. Collectively, the data presented here indicate that the C-terminal hydrophobic pocket of MA, which encompasses both positions 84 and 99, has a previously undiscovered and key role in multiple functions of the protein. These findings may provide new insights that can advance the development of novel anti-HIV therapeutics.

CHAPTER II: MATERIALS AND METHODS

2.1 Tissue Culture Cell-Lines

HeLa, 293-T or TZM-bl were grown in 1X Dulbecco's modified Eagle's medium (DMEM) supplemented with 10% fetal calf serum (FCS) and 1% Penicillin-Streptomycin (Pen-Strep). TZM-bl cells are derived from a HeLa clone that express relatively high surface levels of CD4, CCR5, and CXCR4. They contain stably integrated reporter genes that encode the *Escherichia coli* β-Galactosidase (β-Gal) and *Renilla* Firefly Luciferase. Expressions of both proteins are driven by the HIV-1 LTR, and are thus, Tat-dependent (202). This reporter cell line is susceptible to infection by both R5 and X4 HIV-1 isolates (190). The MAGI cells are also a HeLa-CD4-LTR-β-gal indictor cell line, and were maintained in DMEM with 10% FCS and 1% Pen-Strep that was supplemented with 0.1 mg of hygromycin B and 0.15 mg of G418 per ml (105). MT-4, M8166, and C8166 cells were grown in RPMI 1640 medium supplemented with 10% FCS, and 1% Pen-Strep. All cell lines were grown at 37°C in a 5% CO_2 atmosphere.

2.2 DNA Constructions

HIV-1 MA mutations were created with the Quikchange II Site-Directed Mutagenesis Kit (Stratagene) as previously described (211), using the pLAI or pNL4.3 proviral clones (1, 158). These proviral clones were obtained from the AIDS Reagent Program of NIAID, NIH.

The proviral clone pLAI-Gag(-) encodes a nonfunctional *gag* gene, and was created by introducing two stop codons proximal to the start of the *gag* reading frame, as

previously described (119). The pLAI-ΔEnv proviral clone encodes a nonfunctional *env* gene, due to removal of the 582-nt Bgl2/ Bgl2 fragment (bases 6638-7220) located early in the *env* coding sequence. Truncations of the HIV-1 gp41 CT were made by introducing two consecutive stop codons into the gp41 coding sequences, as described previously (119). The relative locations of each of these changes made in the HIV-1 genome is represented in Figure 2.1A. The gp41 proteins generated from transfection of the LAI-Δ144 proviral clones contain an abbreviated CT that is six residues in length, instead of the normal 150 amino acids. The truncated Env protein is depicted in Figure 2.1B.

Mutagenic primers were designed to introduce changes in pLAI and pNL4.3 proviral clones. The primer sequences are written in the 5' to 3' direction: **L13E/f:** GTA TTA AGC GGG GGA GAA GAA GAT CGA TGG GAA AAA ATT C; **L13E/r:** G AAT TTT TTC CCA TCG ATC TTC TTC TCC CCC GCT TAA TAC; **L21K/f:** GA TGG GAA AAA ATT CGG AAA AGG CCA GGG GGA AAG; **L21K/r:** CTT TCC CCC TGG CCT TTT CCG AAT TTT TTC CCA TC; **K32E/f:** G AAA AAA TAT AAA TTA GAA CAT ATA GTA TGG GCA AGC; **K32E/r:** GCT TGC CCA TAC TAT ATG TTC TAA TTT ATA TTT TTT C; **LAI-E99V/f**: G ATA AAA GAC ACC AAG GTA GCT TTA GAC AAG ATA G; **LAI-E99V/r**: C TAT CTT GTC TAA AGC TAC CTT GGT GTC TTT TAT C; **E99A/f:** G ATA AAA GAC ACC AAG GCA GCT TTA GAC AAG ATA G; **E99A/r:** C TAT CTT GTC TAA AGC TGC CTT GGT GTC TTT TAT C; **E99G/f:** G ATA AAA GAC ACC AAG GGA GCT TTA GAC AAG ATA G; **E99G/r:** C TAT CTT GTC TAA AGC TCC CTT GGT GTC TTT TAT C; **E99D/f:** G ATA AAA GAC ACC AAG GAC GCT TTA GAC AAG ATA G; **E99D/r:** C TAT CTT GTC TAA

AGC GTC CTT GGT GTC TTT TAT C; **E99K/f:** G ATA AAA GAC ACC AAG AAA GCT TTA GAC AAG ATA G; **E99K/r:** C TAT CTT GTC TAA AGC TTT CTT GGT GTC TTT TAT C; **LAIdel84/f:** C ATT ATA TAA TAC AGT AGC AGT CCT CTA TTG TGT GCA TC; **LAIdel84/r:** GA TGC ACA CAA TAG AGG ACT GCT ACT GTA TTA TAT AAT G; **NL43del84/f:** CAT TAT ATA ATA CAA TAG CAA CCC TCT ATT GTG TGC ATC; **NL43del84/r:** GAT GCA CAC AAT AGA GGG TTG CTA TTG TAT TAT ATA AT; **NL-E99V/f:** GTA AAA GAC ACC AAG GTA GCC TTA GAT AAG ATA G; **NL-E99V/r**: C TAT CTT ATC TAA GGC TAC CTT GGT GTC TTT TAC; **LAIdelGAG/f:** G AGA GCG TCA GTA TAA AGC GGG TGA GAA TTA GAT CGA TG; and **LAIdelGAG/r:** CA TCG ATC TAA TTC TCA CCC GCT TTA TAC TGA CGC TCT C.

Sanger sequencing of both DNA strands confirmed nucleotide changes in the HIV-1 mutant proviral clones. All mutations created in the MA domain are named based on their proximity to the initial methionine in the Gag coding sequence.

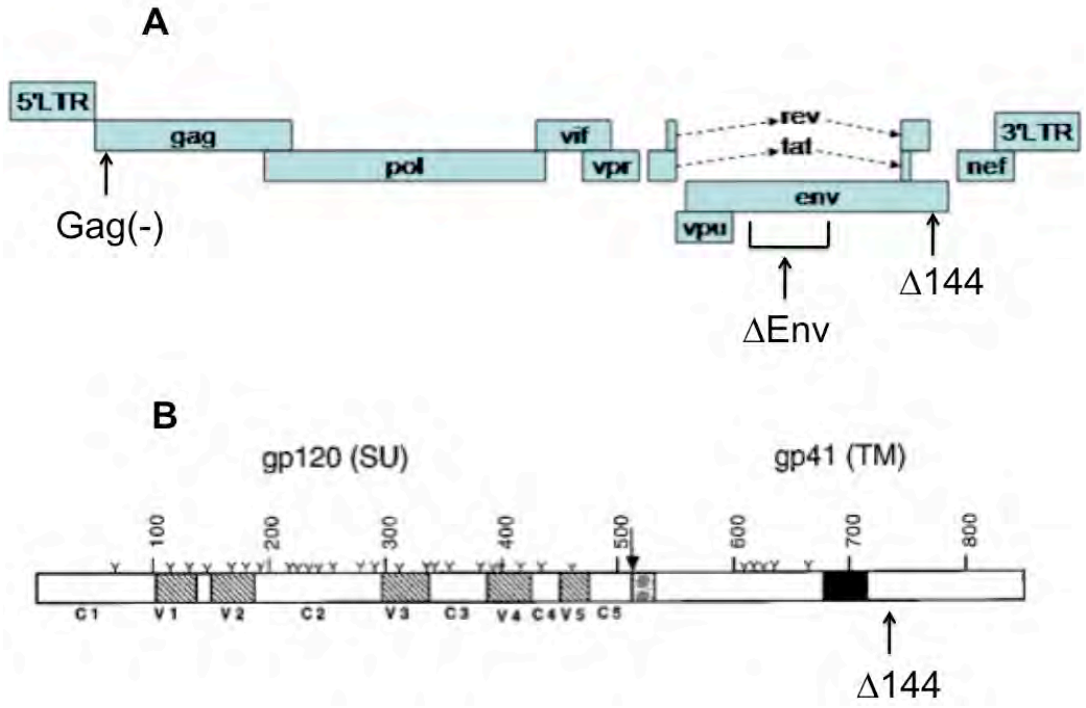

Figure 2.1 Relative locations of changes made to LAI proviral clones. (A) An early stop codon was introduced at the beginning of the *gag* gene to generate the Gag(-) clone. To generate the LAI-ΔEnv clones, a 582 nucleotide fragment (Bgl2-Bgl2 site) within the *env* gene was removed. To generate the LAI-Δ144 proviral clones, two consecutive stop codons were introduced into the *env* gene that removed the C-terminal 144 amino acids from the cytoplasmic tail of gp41. Note: Gag(-), LAI-ΔEnv, and LAI-Δ144 proviral clones had only one of the three changes shown (adapted from 41). **(B)** Truncated Env proteins synthesized from the pLAI-Δ144 proviral clones has a gp41 cytoplasmic tail of six amino acids instead of the normal 150. The site of the last amino acid in the truncated glycoprotein is indicated in the diagram (70).

2.3 Expression Vectors

pHCMV-G expresses the vesicular stomatitis virus envelope glycoprotein G (VSV-G) from a human cytomegalovirus (CMV) promoter (210). pSV-A-MLV expresses the amphotropic Murine Leukemia Virus strain 4070 A *env* (a-MLV-Env) coding sequence expressed from the MLV-LTR promoter (154). The pBLaM-Vpr plasmid expresses β-lactamase (BLaM) fused to the amino terminus of HIV-1 Vpr, under the control of the CMV promoter (32).

2.4 Virus Production

Wild-type (WT) and mutant virus stocks were produced by transient transfection of proviral clones into 293T cells using TransIT-LTI (Mirus Corp.). Fresh media was added six hours post-transfection. HIV-1 particles carrying β-lactamase proteins were produced by co-transfection of an individual proviral clone and pBLaM-Vpr at a ratio of 3:1. VSV-G pseudotyped particles were generated by co-transfection the Env deficient proviral clone and pHCMV-G at a ratio of 6:1. A-MLV-env pseudotyped particles were generated by co-transfection the Env deficient proviral clone and pSV-A-MLV at a ratio of 1:2. Pseudotyped particles were harvested after 24 and 48 hours. Fresh media was added to the cultured cells after the 24-hour harvest. All other viruses were harvested after 48 hours. Viruses were clarified through a 0.45 μm filter (Millipore) immediately after harvesting and aliquotted for storage at -80° C. Stocks were normalized for Reverse Transcriptase (RT) activity using the enzymatic assay described below. For immunoblot

analysis, HeLa cells were transiently transfected with the individual proviral clones and viral lysates prepared as previously described (119).

2.5 Reverse Transcriptase (RT) Activity Assays

HIV-1 RT activity was measured as previously described (163). For each sample, 5 μL of filtered culture supernatant was mixed with 10 μL Solution A (100mM Tris-HCl pH 7.9, 300 mM KCl, 10 mM DTT, 0.1% NP-40) and incubated for 15 minutes at 37° C. Viral lysates were then combined with 25 μL Solution B (50 mM Tris-HCl pH 7.9, 150 mM KCl, 5 mM DTT, 15 mM $MgCl_2$, 0.05% NP-40, 10 μg/ml poly A, 0.250 U/ml oligo dTTP, 10 μCi/ ml ^{3}H-TTP), and incubated overnight at 37°C. Reaction products were precipitated using Stop solution (100% trichloroacetic acid, 0.5M $Na_4P_2O_7$ -$10H_2O$) and RT activity determined as previously described (211).

2.6 p24 ELISA

Equal volumes of supernatants from 293T cells, obtained 48 hours post-transfection of the indicated proviral clones, were diluted in complete media in a 96-well plate and then added to micro-titer plates coated with α-p24 antibody. A 1:10 or 1:20 dilution of supernatants generally resulted in readings within the range of the assay. Viral titers were determined according to the HIV-1 p24 ELISA kit from Perkin Elmer (NEK050B).

2.7 Immunoblot Analyses

Transfected cells were lysed in RIPA buffer with a cocktail tablet of protease inhibitors (Complete, Roche). Cell or viral lysates were resolved on 12% SDS-

polyacrylamide gels and transferred to Hybond-C Extra Nitrocellulose membranes (NC; Amersham Biosciences) using a semi-dry blotter. NC membranes were blocked with 5% dry milk in 1X TBST buffer (25 mM Tris, 150 mM NaCl, 2 mM KCl, pH 7.4, and 0.1% Tween-20) at room temperature for 1 hour, then incubated with primary monoclonal antibodies directed against HIV-1 gp41 (Chessie-8, diluted 1:250), HIV-1 Gag (183-H12-5C, NIH AIDS Reagent Program, diluted 1:500), human β-Actin (AC-15, Sigma, diluted 1:4400) or GAPDH (ab8245, Abcam, diluted 1:5000), or polyclonal antibodies directed against Sam68 (ab26803, Abcam, diluted 1:600), Nup62 (sc-25523, Santa Cruz Biotechnology, diluted 1:200), pyruvate kinase (ab38237, Abcam, diluted 1:200) or HSP90 (sc-7947, Santa Cruz Biotechnology, diluted 1:200). Following three 10-minutes washes in 1X TBST buffer, membranes were incubated with goat α-mouse or mouse α-rabbit secondary antibodies conjugated to horseradish peroxidase (Sigma, diluted 1:10:000). Bands were detected and visualized using enhanced chemiluminescence (SuperSignal West Pico, Thermo Scientific) with Kodak X-Omat Blue film.

2.8 Virus-Cell Fusion Assays

HIV particles are generated through the co-transfection of proviral clones and an expression plasmid encoding a β-lactamase (BLaM)-Vpr chimeric protein. BLaM-Vpr is packaged into particles as a result of the interaction between Vpr and the p6 domain of Gag. Infected cells are loaded with a dye that is a substrate for the BLaM enzyme. BLaM-mediated cleavage of the dye causes cells to turn blue, whereas cells will fluoresce green in the absence of BLaM. Thus, intracellular BLaM activity can be quantified with a

fluorometer to monitor virus-cell fusion events. A schematic overview and images of cells used in this fusion assay are shown in Figure 2.2.

The procedure for the fusion assay is as follows: TZM-bl cells, seeded at 10 x 10^4 cells per well, were inoculated with virus using spinoculation (2100 *x g*) at room temperature for 30 minutes in a total volume of 50 μL. Cells were incubated for up to 3 hours at 37°C. The BLaM substrate, CCF2-AM dye (20 μM, Invitrogen LiveBLAzer™ FRET-B/G Loading Kit), was prepared according to the manufacturer's standard substrate loading protocol, with the exception that Solution C was diluted 1:6 in 1X HBSS++ [Hanks' Balanced Salt Solution, 20 μM Hepes, 2 mM Glutamine]. The CCF2-AM solution was added to cells and the cultures were incubated overnight in the dark at room temperature. Cells were washed in cold 1X PBS (Phosphate Buffered Saline**)** and fluorescence emission was measured at 447 nm or 520 nm following excitation at 409 nm using a fluorometer (BioTek Synergy 2). Intracellular BLaM activity was measured and normalized as previously described (133).

A

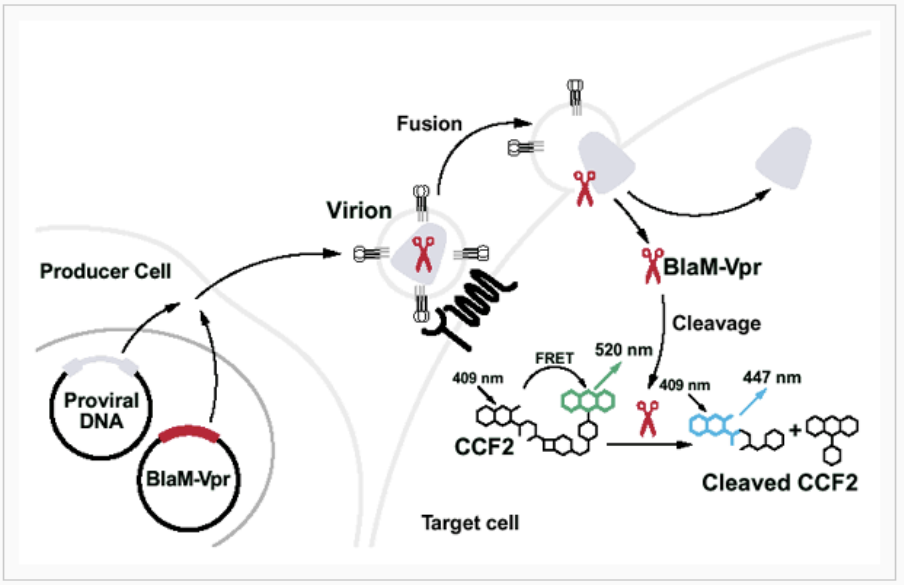

B

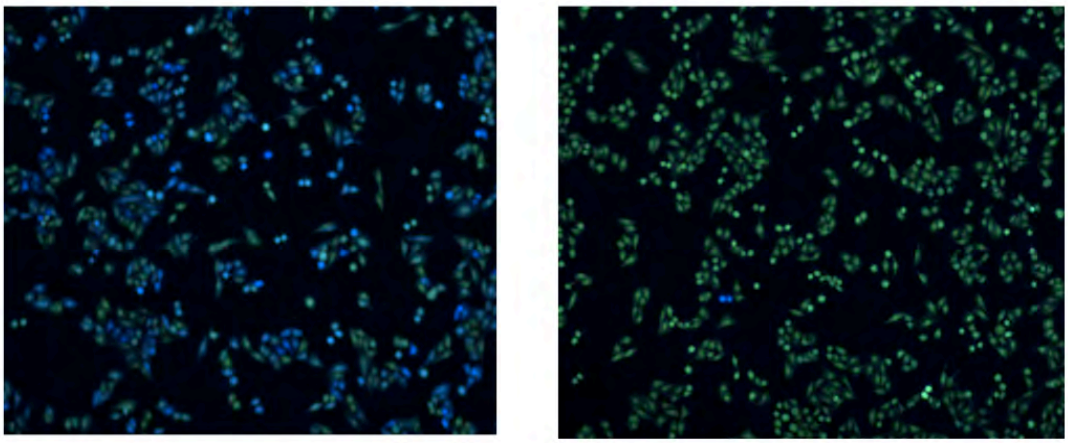

Figure 2.2 Virus-cell membrane fusion assay. (A) Schematic overview of the fusion assay. HIV particles are generated through the co-transfection of proviral clones and an expression plasmid encoding a BLaM-Vpr chimeric protein. The resulting particles are used to infect target cells, which are then incubated with CCF2/AM dye. This dye, a substrate for BLaM, passively diffuses into cells. In the absence of BLaM-Vpr, the cells will fluoresce green. However, if a virus

particle containing BLaM-Vpr chimeras fuses with a cell, then the BLaM enzyme will cleave the dye and the cell will fluoresce blue. The relative quantities of blue or green cells in a given culture can then be quantified using a fluorometer. (32) **(B)** Images from the virus-cell membrane fusion assay. Either LAI-WT **(left panel)** or LAI-ΔEnv **(right panel)** particles, both containing BLaM-Vpr chimeras, were incubated with TZM-bl cells for three hours. Cells were then washed and loaded with CCF2/AM dye. After time was allowed for substrate cleavage, the cells were washed in PBS and pictures were taken under the microscope. LAI-WT particles successfully fused with TZM-bl cells, enabling the BLaM enzyme to cleave the dye inside target cells, resulting in a blue color (**left panel**). However, the LAI-ΔEnv particles could not deliver the BLaM enzyme into target cells, and cells remained green (**right panel**).

2.9 Beta Glo® Assays of Viral Infectivity

The Beta-Glo® assay system (Promega) provides a highly sensitive, quantitative analysis of viral infectivity with a wide range of HIV-1 isolates (91). The TZM-bl cells used in this assay contain separately integrated copies of the β-galactosidase and firefly luciferase reporter genes, whose expressions are driven by the HIV-1 LTR and thus, are Tat-dependent (202). The Beta-Glo® reporter assay utilizes a coupled enzyme reaction system that employs a single reagent, luciferin-galactoside. In living cells, this substrate is cleaved by β-galactosidase to galactose and luciferin, the latter being used by firefly luciferase to generate a luminescent signal that is proportional to the amount of β-galactosidase. Following HIV-1 infection, the enzymatic activity of luciferase in TZM-bl cells can be quantified in terms of relative luminescence units (RLU). The RLU values obtained are directly proportional to the number of infectious virus particles in the viral inoculum. The procedure for this assay was carried out per the manufacturer's instructions. Briefly, TZM-bl cells were seeded at 10×10^4 cells per well of a 96-well plate. Duplicate wells were infected with equal amounts of virus, and incubated for 24 or 48 hours at 37° C. Cells were lysed at room temperature by the addition of Beta Glo® substrate (Promega). Luciferase activity was quantified using a luminometer and normalized as previously described (91).

2.10 Quantification of HIV-1 Reverse Transcription Products

Total cellular DNA was extracted using the DNAeasy kit (Qiagen), as directed by the manufacturer. A single-step, real-time PCR was used to quantify EPs and 2-LTRs from DNA extracts in a 30 µl PCR reaction mix containing 15 µL TaqMan Universal PCR Master Mix (Applied Biosystems) and a fluorescence Taqman probe that targeted the HIV-1 sequence being amplified (2nr4nr: 5′-AGCCTCAATAAAGCTTGCCTTGAGTGC-3′). Amplification reactions were performed using an Applied Biosystems 7000 real-time PCR system with the following program: 95°C for 20 s, then 35-45 cycles of 95°C for 30 s and 60°C for 30 sec. The EP and 2-LTR values were normalized relative to CCR5 gene copy number.

2LTR circles were amplified from 10 µL DNA with 45 cycles using primers C1/f (5′-CTAACTAGGGAACCCACTGCT-3′) and C4/r (5′-GTAGTTCTGCCAATCAGGGAAG-3′). Copy numbers were based on a standard curve generated with a plasmid that harbors the HIV LTR-LTR junction. Early products were amplified from 5 µL DNA with 40 cycles using primers M667/f (5’-GGC TAA CTA GGG AAC CCA CTG C-3’) and AA55/r (5’-CTG CTA GAG ATT TTC CAC ACT GAC-3’). Copy numbers were based on a standard curve generated with a plasmid that harbors the LAI early product sequence between U5 and R. CCR5 gene copies were amplified from 10 µL DNA with 40 cycles using CCR5 specific primers and a CCR5 specific probe. CCR5 copy numbers were based on a standard curve generated with a plasmid that harbors the human CCR5 gene.

2.11 RTC Trafficking Assay

Several variations of this protocol were performed and are described in Chapter 6. A brief overview of the methods is outlined in Figure 6.1. The relative targets of each of the primers used in the PCR steps of this assay are shown in Figure 6.2. Included here is the optimized procedure used to carry out the experiments, and consists of four main steps: virus infection, cell harvesting and fractionation, RT-PCR of viral genomes, and quantification of viral genomes by qPCR.

2.11.1 Infection Protocol

MAGI cells were added to a T-25 flask in MAGI media, and incubated 2-3 days until cells were about 80% confluent. For AZT controls, cells were incubated with 10 μM AZT for two hours at 37° C prior to infection. All viruses were treated with DNase I (Boehringer Mannheim) for 30 minutes at 37° C before added to cells. Media was removed from flasks and 750,000 RT units of virus diluted in cold MAGI media were added. Flasks were incubated at 4° C for one hour, and manually rocked every five minutes to assure that media and virus covered all cells. After an hour, virus was removed from each flask and prewarmed 0.45 M sucrose media was added to cells. Cells were incubated at 37° C for 20 more minutes. Media was again removed from each flask and prewarmed media was added. Infections were incubated further at 37° C until pre-determined time points.

2.11.2 Cell Harvesting and NP-40 Fractionation

Media was removed from each flask and cold 1X PBS was added to wash the cells. PBS was aspirated, and exposed to trypsin-EDTA. Flasks were incubated at 37° C for three minutes, and then gently tapped to detach cells. MAGI media was added to neutralize the trypsin. Cells were transferred to eppendorf tubes and pelleted by centrifugation at 3500 RPM for five minutes at 4° C. Culture supernatants were removed and cells were resuspended in cold PBS. Half of the cell suspensions were transferred to a new tube and frozen at -80° C for subsequent total DNA extraction. The remaining tubes were centrifuged for three minutes at 3500 RPM at 4° C. The PBS was aspirated and cells were resuspended in cold hypotonic Buffer A (0.01 M Hepes pH 7.9, 0.01 M KCl, 0.1 mM EDTA, 1 mM DTT). Cells were left on ice for 15 minutes to swell. NP-40 was added to cells at a final concentration of 0.6% and then vortexed vigorously. The tubes were centrifuged for three minutes at 6500 RPM at 4° C. After the spin, the supernatants (cytoplasmic fractions) were transferred to clean tubes. Nuclei pellets were resuspended in Buffer A and spun for 3 minutes further at 6500 RPM at 4° C. After the spin, the supernatants were aspirated, and the nuclei were resuspended in Buffer B (0.01 M Hepes pH 7.9, 0.05 M NaCl, 0.1 mM EDTA, 25% glycerol) and stored at -80° C.

2.11.3 RNA Extraction and RT-PCR

Each of the tubes were thawed and total RNA was extracted with RNeasy kit (Qiagen), as directed. The Applied Biosystems Reverse Transcription kit (Superscript, Invitrogen) was used to perform reverse transcription, as directed. For this procedure, 8

µL of RNA from each sample was added to 2 µL of a 1:1 dNTP: primer BB (sequence 5'-GGATTAACTGCGAATCGTTC-3') solution and kept on ice. Tubes were incubated in a 65° C water bath for five minutes to denature RNA secondary structure. Tubes were then quickly spun, and placed back on ice for one minute. A mastermix solution was prepared so that each reaction could occur with 2 µL 10X RT buffer, 4 µL of 25 mM MgCl2, 2 µL of 0.1 M DTT and 1 µL of RNase OUT (all components of the kit). 9 µ L of the Mastermix was added to each tube, centrifuged, and added to a 42° C water bath. 1 µL of the Superscript II RT enzyme was added to each tube and reactions were kept in the 42° C water bath for 50 minutes. The tubes were then transferred to a 70° C water bath for 15 minutes to stop the reactions, and then chilled on ice until further analysis.

2.11.4 Quantitative PCR to Analyze cDNA Copy Number

Real-time PCR was used to quantify copy numbers of 1 µL of the HIV-1 cDNA in a 30 µl PCR reaction mix containing 15 µL TaqMan Universal PCR Master Mix (Applied Biosystems), the C1/f primer (5'-GTAGTTCTGCCAATCAGGGAAG -3'), the LA17/r primer (5’-AACTGATCGCCTCCGATCTTCCTCT-3’), and a fluorescence Taqman probe that targeted the HIV-1 sequence being amplified (2nr4nr: 5′-AGCCTCAATAAAGCTTGCCTTGAGTGC-3′). Amplification reactions were performed using an Applied Biosystems 7000 real-time PCR system with the following program: 95°C for 20 sec, then 45 cycles of 95°C for 30 sec and 60°C for 30 sec. Copy numbers were based on a standard curve generated with a plasmid that harbors the LTR-Gag sequence being amplified (the last part of the 2nd strand). cDNA copies were normalized relative to CCR5 gene copy number, quantified from total cellular DNA.

CHAPTER III: CHARACTERIZATION OF HIV-1 VIRUSES ENCODING SUBSTITUTIONS AT MA RESIDUE 99

3.1 Introduction

Previously, several groups have analyzed single amino acid substitutions within MA at highly conserved positions. In doing so, they were able to identify residues involved in a specific MA function. For example, an L13E substitution is one of several individual MA mutations that abrogates incorporation of full length HIV-1 Env into virus particles (72). An L21K substitution in the basic domain of MA enhances membrane binding of Gag and accelerates Gag processing, resulting in a post-entry defect in virus particles (104). Finally, a K32E substitution in MA abolishes viral infectivity in Jurkat cells without significantly affecting virus assembly and release, or Env incorporation (111).

A PCR-based mutagenesis scheme was used in a previous study to generate proviral clones containing different mutations in the MA coding sequence (55). These clones were then screened for defects in nuclear import and export using direct immuno-fluorescence microscopy. Of the MA mutants generated for subsequent study, one such mutant contained a single amino acid substitution, a glutamate to valine change at residue 99 in the LAI background (LAI-E99V). An amino acid sequence alignment of over 1100 HIV-1 isolates in the Los Alamos HIV sequence database (subtypes A through K of group M) reveals a striking degree of conservation at this residue 99 in MA. In fact, 99% of the sequences analyzed had glutamate at residue 99, with aspartate accounting for most other known changes. Figure 3.1 shows a schematic representation of the E99V

substitution relative to MA functional domains and previously characterized MA single amino acid substitutions.

3.2 Results

3.2.1 Virus production and Gag processing is normal in LAI-derived particles bearing the E99V MA mutation

Since assembly is an important function of MA, I determined whether the LAI proviral clone containing the E99V mutation in MA (pLAI-E99V) could produce viral particles. 293T cells were transiently transfected with either a WT proviral clone (pLAI-WT) or pLAI-E99V, using cationic liposomes. After 48 hours, cell supernatants were collected and particle production levels were monitored using an enzymatic assay for HIV-1 p24 ELISA quantification and RT activity (Figure 3.2). Results from these assays indicate that production of LAI-E99V particles (LAI-E99V) was comparable to that of LAI-WT.

Certain mutations in MA have previously been shown to affect the efficiency of Gag processing (84, 100, 104), so next, I decided to examine whether Gag processing is affected in LAI-E99V particles. HeLa cells were transfected with pLAI-WT, pLAI-E99V, an LAI proviral clone encoding either the L21K or K32E mutations in MA (pLAI-L21K or pLAI-K32E), or an LAI proviral clone with a nonfunctional *env* gene (pLAI-ΔEnv). After 48 hours, transfected HeLa cells or virus particles in cell supernatants were harvested and virus was normalized based on RT activity as described above. Equal amounts of virus or cells were resuspended in RIPA buffer, resolved on an SDS-

polyacrylamide gel and analyzed for Gag processing through immunoblotting with an anti-HIV-1 p24 monoclonal antibody (mAb). In both viral (Left Panel) and cellular (Right Panel) lysates, I found that the level of Gag processing was comparable for LAI-WT and LAI-E99V viruses (Figure 3.3). By contrast, and consistent with previous studies, I found that Gag processing was enhanced in the LAI-L21K viral lysates (Left Panel), as evidenced by the appearance of a strong band corresponding to p41, a processing intermediate composed of p17 and p24 (104).

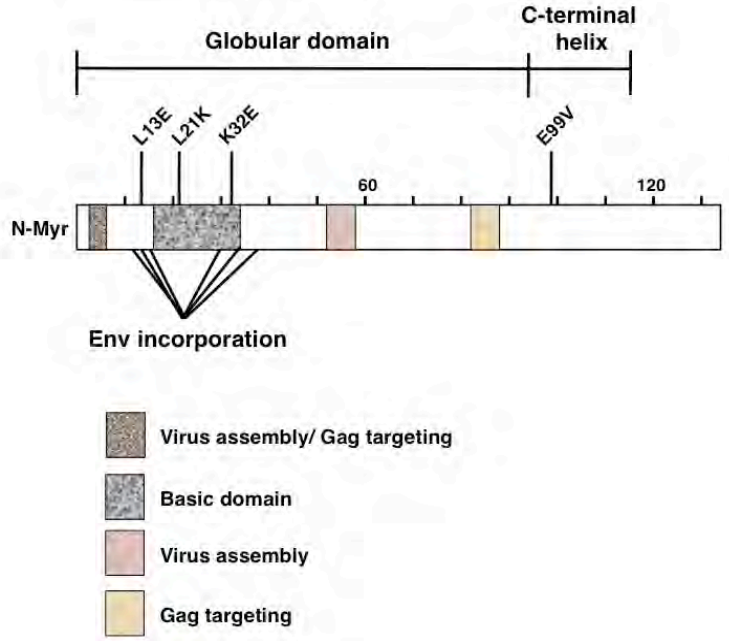

Figure 3.1 Functional domains and single amino acid substitutions in HIV-1 MA. A schematic representation of previously defined functional domains in HIV-1 MA, and the relative locations of single amino acid substitutions, also characterized in earlier studies. The novel E99V MA substitution analyzed in this study is located at the beginning of the C-terminal helix of the protein.

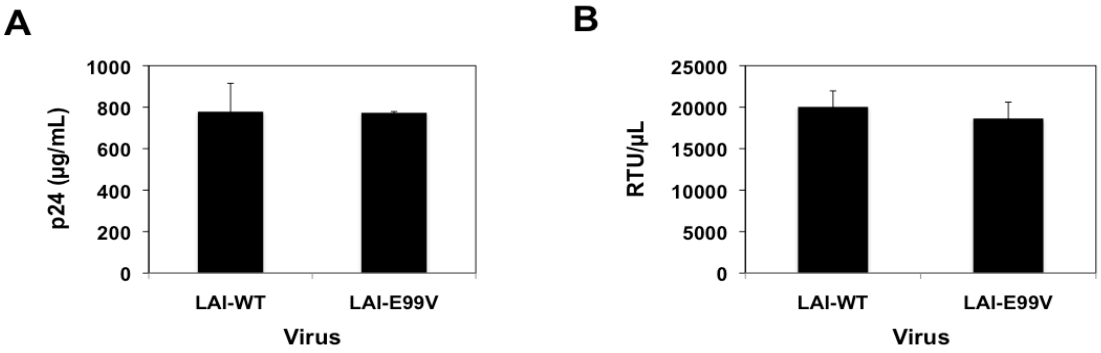

Figure 3.2 Effect of the MA E99V mutation on LAI particle production. Transient transfection of 293T cells with proviral clones pLAI-WT and pLAI-E99V. Particle yield was determined by both p24 ELISA **(A)** and RT analysis **(B)** as described in Methods and Materials**.** The data represent the average of two independent transfections.

3.2.2 LAI-derived particles bearing the E99V or E99K MA mutations have severe infectivity defects

Next, to determine whether an early step in the viral life cycle might be disrupted in LAI-E99V, I analyzed a single-cycle of virus infection in TZM-bl cells using the Beta-Glo® assay system. This reporter system provides a highly sensitive, quantitative analysis of viral infectivity with a wide range of HIV-1 isolates (91). TZM-bl cells have a firefly luciferase gene stably integrated into their genomes, and expression of the reporter gene is driven by the HIV-1 LTR (202). Following HIV-1 infection, the enzymatic activity of luciferase is quantified in cells and is directly proportional to the number of infectious virus particles in the viral inoculum.

Virus particles were produced in 293T cells by transfection with pLAI-WT, pLAI-E99V, pLAI-L21K, pLAI-K32E, pLAI-ΔEnv, or an LAI proviral clone encoding either the L13E mutation in MA (pLAI-L13E). Virus from each culture supernatant was harvested and normalized by RT content. Equal amounts of each virus were then added to TZM-bl cells cultured in 96-well plates.

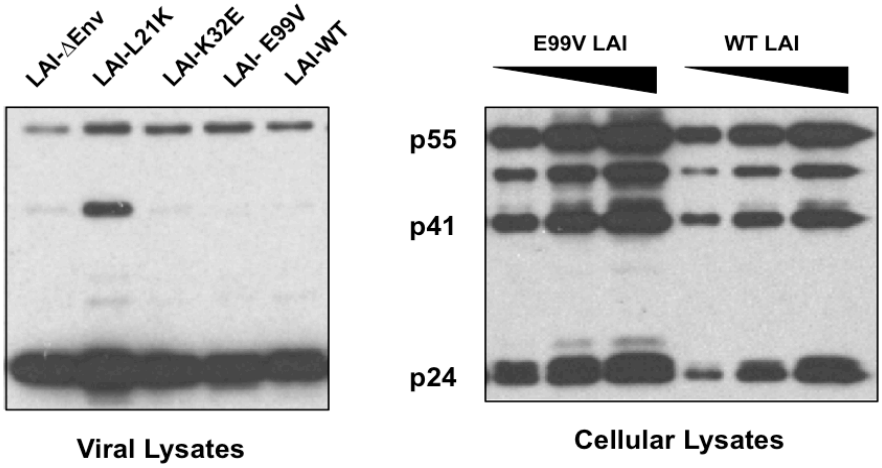

Figure 3.3 Western blot analysis of Gag processing in LAI-derived virus. Equal RT units of virus particles **(Left Panel)** or transfected HeLa cells **(Right Panel)** were harvested, and then resuspended in RIPA buffer, as previously described (119). Gag processing was analyzed by SDS-PAGE and immunoblotting using monoclonal antibodies directed against HIV-1 Gag.

After 24 hours, Beta-Glo® substrate was added to the cells and luciferase activity in each well was quantified using a luminometer. The RLU value from each infection was normalized using the LAI-WT value, which represents 100% infectivity. Figure 3.4 shows that LAI-WT, but not LAI-ΔEnv, was highly competent for viral infection in this assay. Similar to previous reports, I found that the L13E, L21K and K32E mutations in MA reduce viral infectivity by approximately 29-fold, 1.5-fold and 3.5-fold, respectively. Most striking, I observed a 100-fold reduction in infectivity in cells incubated with LAI-E99V. These data suggest that LAI-E99V particles are defective at an early step in the virus life cycle.

Because LAI-E99V was markedly less infectious than the other viruses tested, I analyzed the functional significance of glutamate at residue 99 using specific amino acid substitutions at this position in MA. I selected an alanine or a glycine substitution (E99A, E99G) because of their neutral side chain groups compared to glutamate. An aspartate substitution (E99D) was chosen based on its charge similarity and slightly larger mass. Lastly, a lysine substitution (E99K) was selected because it places a negative, rather than a positive charge at this position. LAI proviral clones encoding these single amino acid substitutions at residue 99 were generated using PCR-based site-directed mutagenesis and individually transfected into 293T cells to produce virus. The levels of viral infectivity were monitored in TZM-bl cells as in the previous section. These results indicate that exchanging glutamate for an alanine, glycine, or aspartate at residue 99 of MA had no discernible effect on viral infectivity (Figure 3.4). By contrast, a lysine substitution at this

position led to a 100-fold decrease in viral infectivity, a level comparable to that observed for the E99V substitution.

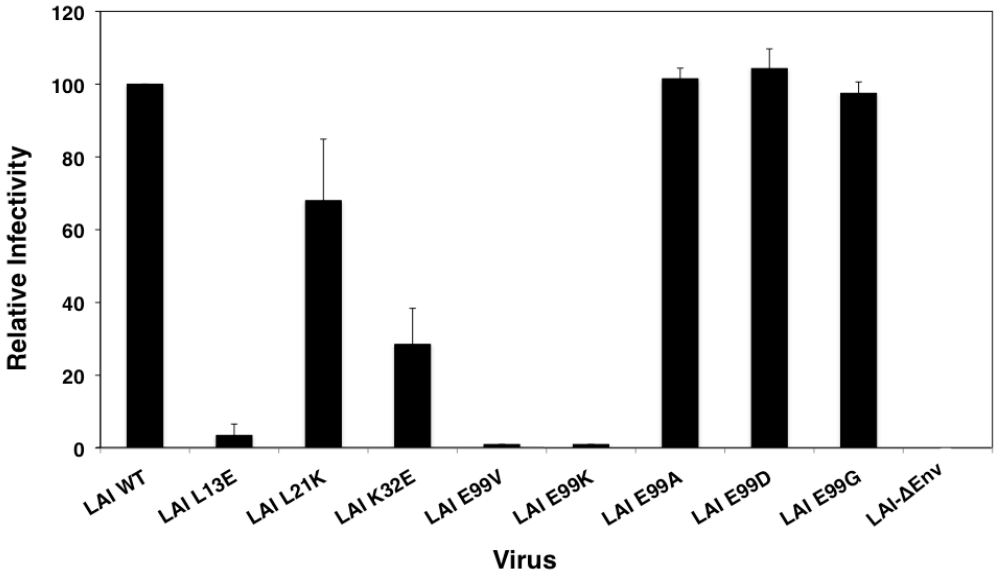

Figure 3.4 Single-cycle infectivities of LAI-derived MA mutants. Virus stocks generated in 293T cells with the indicated pLAI molecular clones were normalized based on RT activity and used to infect TZM-bl cells. Single-cycle infectivity was determined 24 hours post-infection using the Beta-Glo® reporter assay and a luminometer. The assessment of infectivity is based on the level of LAI-WT, which represents 100% infectivity. The data shown is representative of four independent experiments performed in duplicate.

Although I did not detect virus infection in cells inoculated with LAI-E99V using single-cycle reporter assays, it was possible that infection was occurring at a level below the detection limit of the assay. Alternatively, the observed infectivity defect might be an anomaly of TZM-bl cells. As a complementary approach for determining viral infectivity, I examined whether LAI-E99V retained the ability to initiate a spreading infection in a human T-cell line. MT-4 cells were inoculated with LAI-WT, LAI-E99V or LAI-ΔEnv. Four hours post-infection, cells were washed and re-plated in fresh media, and incubated further for fifteen days. An aliquot of each culture supernatant was obtained every other day and stored at -20°C. On day seven, one-half of the culture volume was replaced with an equal volume of fresh cell: media suspension (1:1 ratio). The level of RT activity in each aliquot was measured using a standard enzymatic assay, as described in Materials and Methods. Robust levels of viral replication were detected in the cultures incubated with LAI-WT, but not LAI-ΔEnv. However, LAI-E99V was unable to replicate in these MT-4 cells (Figure 3.5A). I also saw similar results with C8166 and M8166 cell lines (Figures 3.5B and C, respectively). Taken together, these results indicate that LAI-E99V has a marked defect in viral infectivity.

A

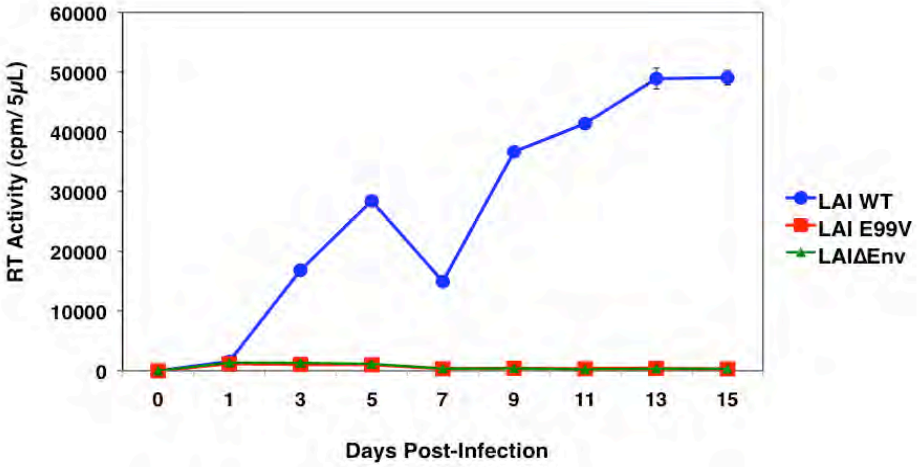
RT Activity (cpm/ 5μL)
60000
50000
40000
30000
20000
10000
0
0 1 3 5 7 9 11 13 15
Days Post-Infection
LAI WT
LAI E99V
LAIΔEnv

B

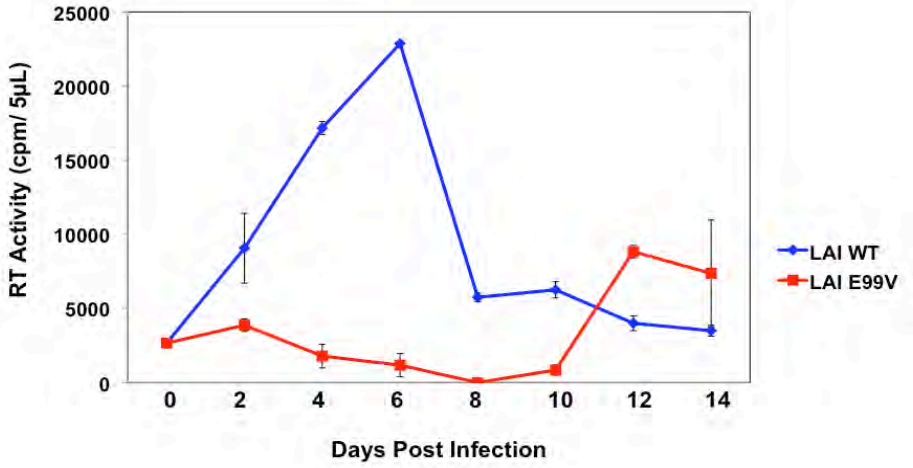
RT Activity (cpm/ 5μL)
25000
20000
15000
10000
5000
0
0 2 4 6 8 10 12 14
Days Post Infection
LAI WT
LAI E99V

C

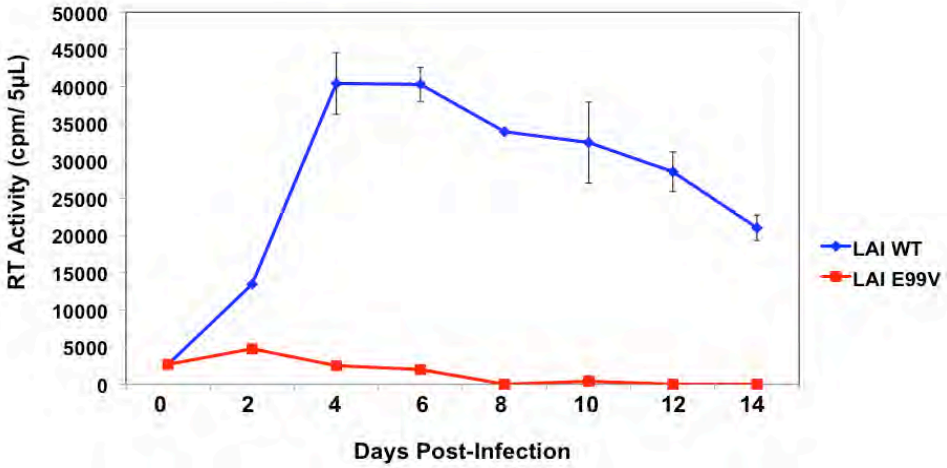
RT Activity (cpm/ 5μL)
50000
45000
40000
35000
30000
25000
20000
15000
10000
5000
0
0 2 4 6 8 10 12 14
Days Post-Infection
LAI WT
LAI E99V

Figure 3.5 Replication kinetics of LAI-derived virus in Human T-cell lines. Virus stocks generated in 293T cells by transfection with the indicated pLAI molecular clones were normalized based on RT activity and used to infect MT-4 (**A)**, C8166 (**B**) or M8166 (**C**) cells. Fresh cells and media were added to each culture on day seven. RT activities in cell culture supernatants were monitored every other day for two weeks. The data shown is representative of two independent experiments performed in duplicate.

3.2.3 LAI-derived particles bearing the E99V or E99K MA mutations have a severe defect in Env incorporation

Because certain amino acid substitutions in MA have been shown to disrupt Env incorporation in nascent particles (68, 69, 72, 111, 150), I next examined whether this process might be impaired in viruses lacking a glutamate at position 99 in MA. HeLa cells were transfected with the proviral clones pLAI-WT, pLAI-E99V, pLAI-E99A, pLAI-E99K, pLAI-E99D, pLAI-E99G, pLAI-K32E, pLAI-L21K, pLAI-L13E, and pLAI-ΔEnv, or an LAI proviral clone with two stop codons proximal to the start of the *gag* reading frame [pLAI-Gag(-)]. After 48 hours, transfected cells were harvested and culture supernatants were normalized based on RT activity. Cellular and viral lysates were prepared and analyzed for Env expression and particle incorporation, respectively, by immunoblotting with an anti-HIV-1 Env mAb as previously described (52).

The data shown in Figure 3.6 (Top Panel) indicate that Env precursor proteins were expressed in all cultures transfected with a proviral clone containing an intact *env* open reading frame. The bottom panel of Figure 3.6 shows results from the immunoblot analysis of Env proteins of the corresponding viral lysates. The absence of Env in the LAI-Gag(-) culture confirms that the signals detected represent virus-associated Env, and not viral glycoproteins trapped in intracellular vesicles. Similar to a previous study, LAI-L13E was found to be completely devoid of Env proteins, a result consistent with a defect in Env incorporation (72). Also as previously reported, the level of Env incorporated into L21K particles was comparable to that of LAI-WT (104). On the other hand, I observed a

marked reduction in the amount of Env in LAI-K32E particles, a finding that does not agree with the initial characterization of this virus (111). Of the mutations at E99, I found the amount of Env in LAI-E99A, LAI-E99D, or LAI-E99G particles was comparable to that in LAI-WT particles. However, I found that the LAI-E99V and LAI-E99K particles were devoid of viral glycoproteins. Given that cells transfected with pLAI-E99V or pLAI-E99K expressed wild-type levels of Env (Figure 3.6, Top Panel), I conclude that the E99V and E99K MA mutations disrupt incorporation of Env into nascent particles.

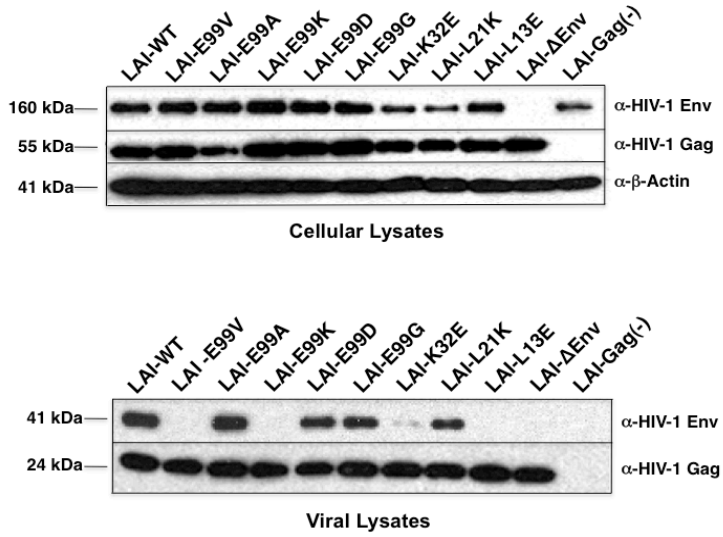

Figure 3.6 Effects of MA mutations on HIV-1 Env incorporation in LAI-derived virus. Transfected HeLa cells **(Top Panel)** or virus particles **(Bottom Panel)** were harvested, and cellular or viral lysates were prepared as previously described (119). The levels of Env proteins in lysates were analyzed by SDS-PAGE and immunoblotting using monoclonal antibodies directed against HIV-1 p24, HIV-1 gp41 and β-actin, or against HIV-1 p24 and HIV-1 gp41.

3.2.4 LAI-derived particles bearing the E99V or E99K MA mutations are markedly impaired for fusion with target cells

Although the immunoblotting results were consistent with a severe disruption in Env incorporation for LAI-E99V and LAI-E99K, I considered that some Env glycoproteins could still be incorporated into particles at a level below the detection limit of this assay, which could facilitate some target-cell fusion events. Indeed, a previous study has demonstrated that striking reductions in Env incorporation do not always correlate with a proportional defect in fusion capacity (43). Therefore, I examined whether LAI-E99V and LAI-E99K are also defective in their ability to fuse with target-cell membranes. I used a recently modified fusion assay that measures β-lactamase (BLaM) activity as an indicator of virus-cell fusion events in living TZM-bl cells after fusion with virus containing chimeric BLaM-Vpr proteins (32, 133). In parallel, I monitored single-cycle infectivity of WT or mutant viruses using the Beta-Glo® assay. Representative data from virus-cell fusion assays and the corresponding viral infectivity studies, using LAI-E99V, LAI-E99K, LAI-L13E, and LAI-K32E are shown in Figures 3.7A and B. At 80 minutes and later times, I observed high levels of BLaM activity in cells incubated with LAI-WT. In contrast, minimal BLaM activity was detected in mock- or LAI-ΔEnv-treated cells, even at late times (180 minutes). Overall, there was a direct correlation between the fusion capacity of each virus and its level of infectivity. Notably, few discernable fusion events were detectable at each sampling time for cells incubated with LAI-E99V, LAI-E99K or LAI-L13E particles, each of which is devoid of Env

proteins. These results suggest that similar to LAI-L13E, the LAI-E99V and LAI-E99K viruses are defective in membrane fusion and infectivity due to a disruption in Env incorporation.

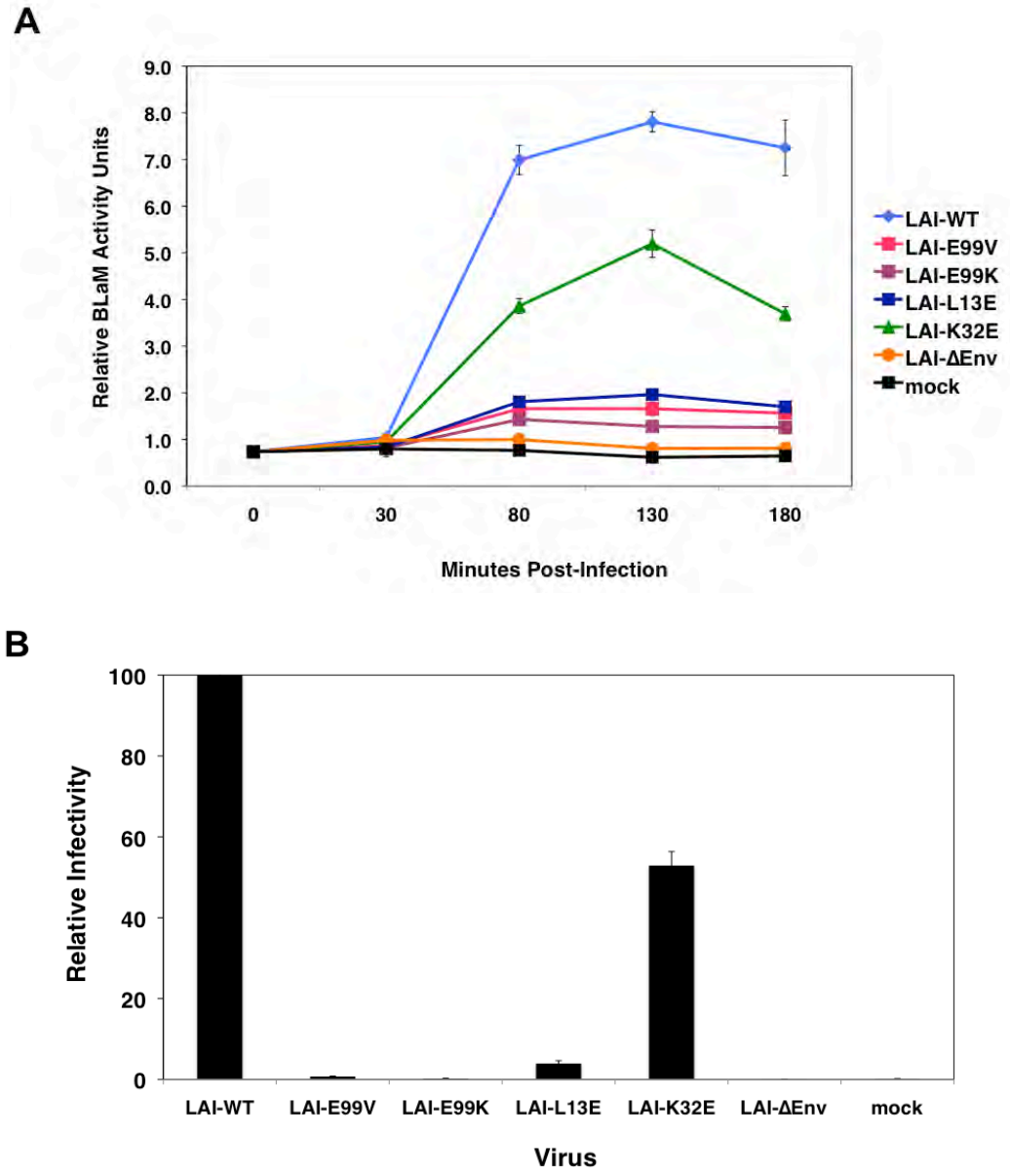

<u>Figure 3.7</u> Effects of MA mutations on virus-cell membrane fusion capacity in LAI-derived virus. Equal amounts of virus were added to TZM-bl cells grown in 96-well plates. The plates were centrifuged at room temperature for 30 minutes, and then incubated further at 37°C for 50, 100 or 150 minutes, or 24 hours. The data shown are representative of three independent experiments performed in

duplicate. **(A)** Virus-cell fusion events. Cells were washed with 1X PBS at the indicated times post-infection and the BLaM substrate was added to the culture media. Plates were incubated overnight at room temperature to allow cleavage of the loaded substrate. Cellular BLaM activity was monitored as an indicator of virus-cell fusion events using a fluorometer. **(B)** Single-cycle infectivities of LAI-derived MA mutants from the virus-cell fusion assay. Relative infectivities of the indicated viruses were assayed 24 hours post-infection as described in Figure 3.4. The assessment of infectivity is based on the level of LAI-WT.

3.2.5 Defects associated with the E99V MA mutation are mitigated when expressed in the NL4.3 strain

Although particle production and Gag processing was normal in LAI-E99V particles, these results indicate that these mutant particles had pronounced defects in Env incorporation, membrane fusion, and infectivity. To determine whether the E99V mutation affects similar processes in a different strain of HIV, I introduced the E99V mutation into an NL4.3 proviral clone (pNL4.3-E99V).

As described for Figure 3.2, HeLa cells were transfected with either pNL4.3-WT or pNL4.3-E99V. Transfected cell supernatants were collected 48 hours later, and then equal volumes were analyzed for virus production by p24 ELISA and RT assay (Figure 3.8). There was a slight reduction in particle production from the pNL4.3-E99V transfection when compared to that generated from transfection of pNL4.3-WT. Although this modest difference was observed in both the p24 quantification and in RT activity of transfected cell supernatants, it seemed that NL4.3-E99V particles were efficiently produced by transfection.

I also compared Gag processing of the NL4.3-derived viruses. Equal RT units of LAI- or NL4.3-, wild-type or E99V viruses were pelleted, resuspended in RIPA buffer, and then resolved on an SDS-polyacrylamide gel. Gag processing was analyzed by immunoblotting using an anti HIV-1 p24 mAb. Shown in Figure 3.9, I observed a slight difference in Gag processing between the two viruses. Levels of fully processed p24 were high in all lanes, while immature Gag, running at 55 kDa, was slightly greater in NL4.3-

WT. Interestingly, the stronger signal corresponding to a MA-CA processing intermediate (p41) was observed in the NL4.3-WT particle analysis, similar to that detected earlier in L21K-containing particles (Figure 3.3). I reasoned that although Gag processing may be slightly enhanced with NL4.3-WT, fully processed p24 was similar to levels detected with LAI-WT, and therefore the significance of such a processing difference might be low. Overall, it seems that the E99V MA mutation does not cause significant differences in Gag processing for NL4.3 virus.

Next, single-cycle infectivity for LAI-WT, LAI-E99V, NL4.3-WT, NL4.3-E99V, and LAI-ΔEnv was monitored at 24 and 48 hours using the Beta-Glo® assay, as described in Figure 3.4. In the LAI-E99V infection, I observed a major defect in infectivity at both the 24- and 48-hour time points, specifically a 32- and 22-fold reduction, respectively. However, while a 23-fold reduction in infectivity was observed at 24 hours with NL4.3-E99V, the infection improved significantly by 48 hours to a modest 2.3-fold reduction compared to NL4.3-WT (Figure 3.10A). Replication of LAI-ΔEnv was undetectable, confirming the specificity of the assay (data not shown). Thus, the infectivity defect associated with the E99V mutation appears to be mitigated in NL4.3-derived particles when compared to the defects seen in LAI.

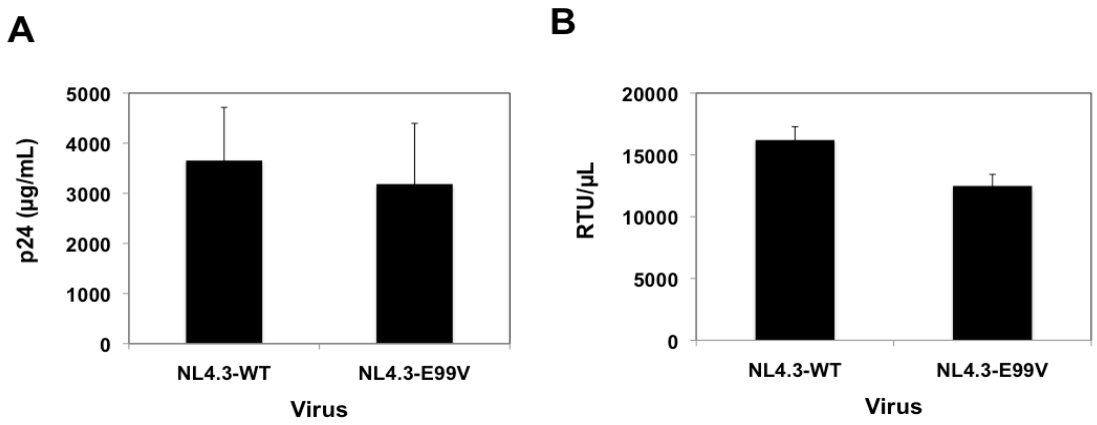

Figure 3.8 Effect of the E99V MA mutation on NL4.3 particle production. Virus was generated by transient transfection of 293T cells with proviral clones pNL4.3-WT and pNL4.3-E99V. Particle yield was determined by both p24 ELISA **(A)** and RT analysis **(B).** The data represent the average of two independent transfections.

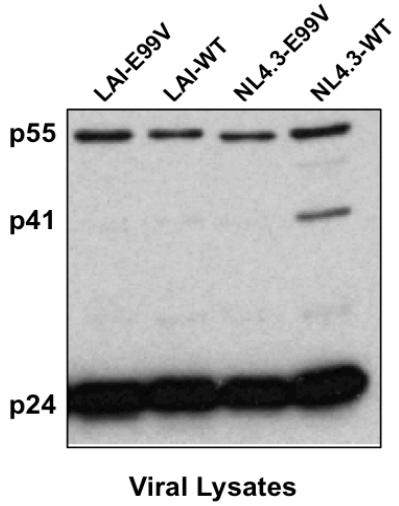

Figure 3.9 Western blot analysis of Gag processing in NL4.3- and LAI-derived viruses. Equal RT units of the indicated virus particles were harvested and then resuspended in RIPA buffer, as previously described (119). Gag processing was analyzed by SDS-PAGE and immunoblotting using monoclonal antibodies directed against HIV-1 Gag, as in Figure 3.3.

Next, I examined whether NL4.3-E99V could initiate a spreading infection in MT-4 cells. Cells were inoculated with NL4.3-WT, NL4.3-E99V or LAI-ΔEnv and incubated for fifteen days. An aliquot of each culture supernatant was obtained every other day and the level of RT activity in each aliquot was measured using the RT assay. Figure 3.10B shows the results from this viral infectivity study. Robust levels of viral replication were detected in cultures incubated with NL4.3-WT, but not LAI-ΔEnv.

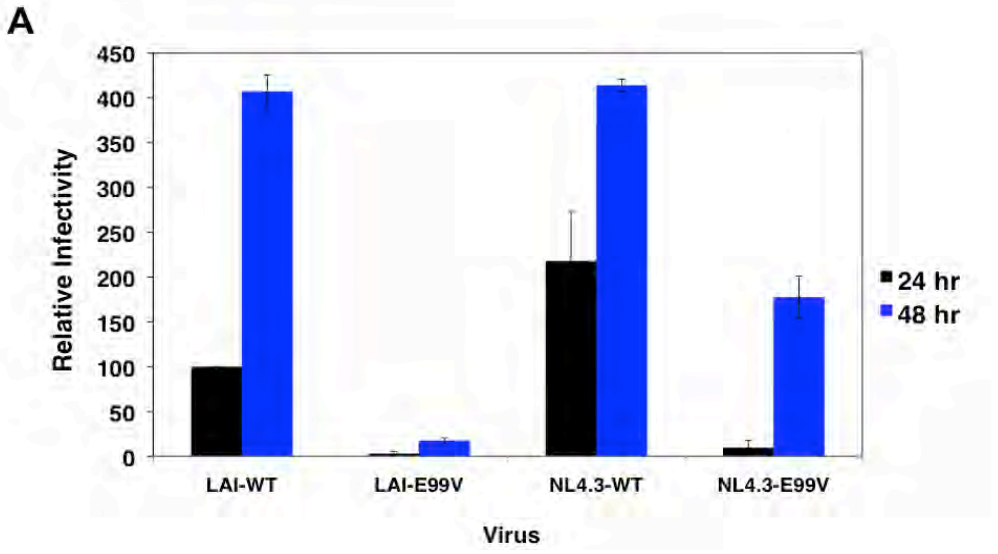
A
Relative Infectivity
450
400
350
300
250
200
150
100
50
0
LAI-WT
LAI-E99V
NL4.3-WT
NL4.3-E99V
Virus
24 hr
48 hr

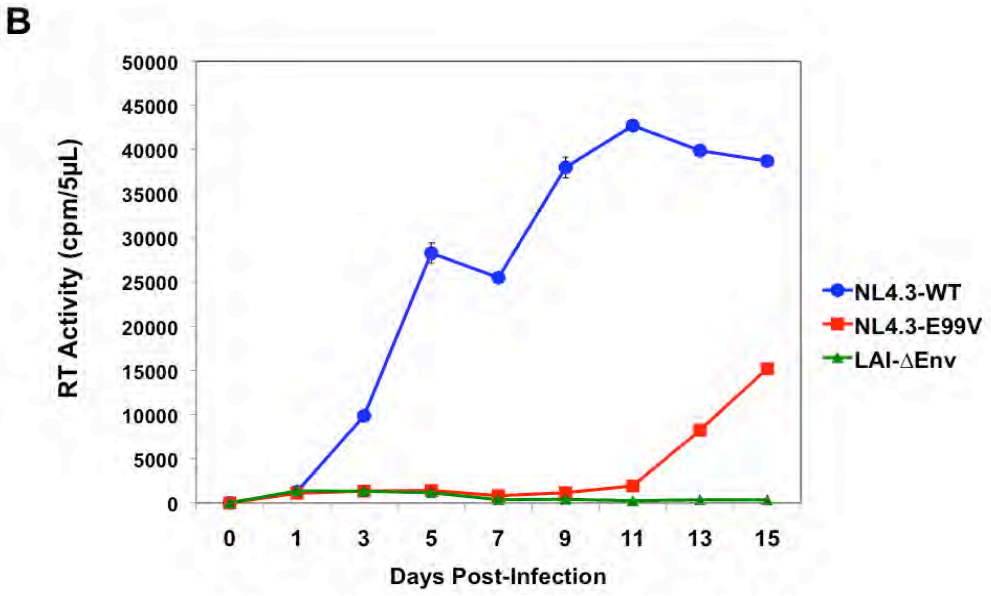
B
RT Activity (cpm/5µL)
50000
45000
40000
35000
30000
25000
20000
15000
10000
5000
0
0
1
3
5
7
9
11
13
15
Days Post-Infection
NL4.3-WT
NL4.3-E99V
LAI-ΔEnv

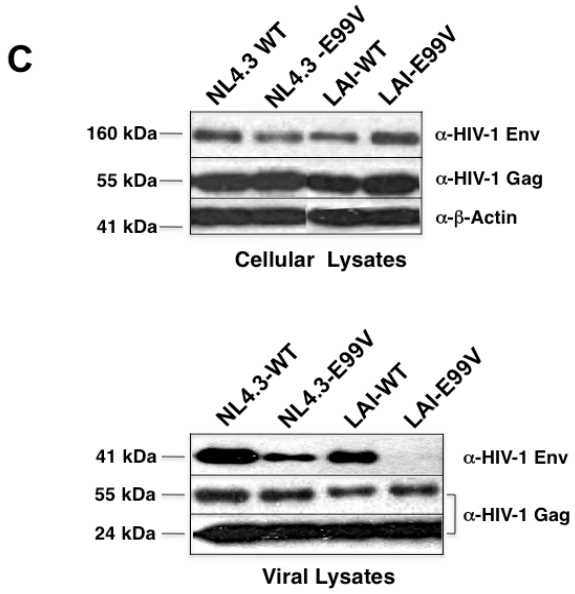

Figure 3.10 Effects of the E99V MA mutation in LAI- and NL4.3-derived particles. (A) Single-cycle infectivities of LAI- and NL4.3-derived viruses, with and without the E99V MA mutation**,** were assayed at 24 or 48 hours post-infection as described in Figure 3.4. The assessment of infectivity was based on the level of LAI-WT determined at 24 hours post-infection. The data is representative of three independent experiments performed in duplicate. **(B)** Replication kinetics of NL4.3-E99V in the MT-4 cell line. Virus stocks were generated in 293T cells by transient transfection, normalized based on RT activity and then used to infect MT-4 cells, as in Figure 3.5. A representative graph of two independent experiments is shown. **(C)** Effects of the E99V MA mutation on Env incorporation in LAI- and NL4.3-derived particles. Lysates from transfected HeLa cells **(Top Panel)** or virus particles **(Bottom Panel)** were prepared and analyzed as described in Figure 3.6.

Interestingly, I did not detect replication in the NL4.3-E99V infected culture until day 13. Supernatant from the NL4.3-E99V infected culture was added to fresh MT-4 cells and permitted to incubate for longer. After a week's time, only minimal RT activity was detected in this new culture, and the cells were harvested. Total DNA was extracted and primers specific for HIV-1 MA were used to amplify MA from proviral DNA. Upon sequencing, I found that the E99V mutation was still present and had not reverted back to E99. Thus, consistent with the data from single-cycle infectivity assays, I observed a significant reduction in NL4.3-E99V infectivity. However, instead of being abolished, virus replication may have been delayed.

I also examined whether Env incorporation might be disrupted in NL4.3-E99V particles. HeLa cells were transfected with pNL4.3-WT, pNL4.3-E99V, pLAI-WT, or pLAI-E99V. At 48 hours, virus and the transfected cells were harvested and analyzed for Env incorporation and expression, respectively, as described in Figure 3.6. Immunoblot analyses show that Env precursor proteins were expressed at comparable levels in the transfected cell cultures (Figure 3.10C, Top Panel). The corresponding viral lysates indicate that NL4.3-E99V, but not LAI-E99V particles, contained a detectable amount of Env proteins (Figure 3.10C, Bottom Panel). Repeatedly, I found that while the level of Env incorporation was markedly reduced in NL4.3-E99V particles compared to that of NL4.3-WT, it was substantially higher than that of LAI-E99V particles.

3.3 Discussion

In this chapter, I examined whether a highly conserved glutamate at MA position 99 is required for the function of the protein in HIV-1 replication. I found that both production and processing of LAI-E99V particles were comparable to that in the wild-type virus. However, analyses of single-cycle and spreading infection showed a significant infectivity defect. After introducing additional substitutions at this position, I discovered that a lysine for glutamate change (E99K) also imposed a similar reduction in infectivity. I observe a severe disruption of Env incorporation into LAI-E99V and LAI-E99K particles through immunoblotting analyses, and then correlated this assembly defect to a marked reduction for fusion capacity. Next, the role for E99 in another HIV-1 strain was analyzed, and I found that in the context of NL4.3, the E99V substitution imposed somewhat mitigated defects compared to those observed in LAI. Interestingly, the infectivity defect observed in NL4.3-E99V was consistent with a possible delay compared to the course of an NL4.3-WT infection. The results described here are summarized in Table 3.1.

Table 3.1 Summary of Results from Chapter 3

Virus	Assay Performed			
	Env Incorporation	Virus-Cell Fusion	Single-cycle Infectivity	Spreading Infection
LAI-WT	++++	++++	++++	++++
LAI-E99V	-	-	-	-
LAI-E99K	-	-	-	ND
LAI-E99A	++++	++++ (NS)	++++	ND
LAI-E99D	++++	++++ (NS)	+++++	ND
LAI-E99G	+++	++++ (NS)	++++	ND
LAI-L13E	-	-	+	ND
LAI-L21K	+++	++++ (NS)	+++	++ (NS)
LAI-K32E	+	++	++	+ (NS)
NL4.3-WT	++++	++++	++++*	++++
NL4.3-E99V	++	-	++*	+

+++++	better than WT	++	25-60% of WT
++++	90-100% of WT	+	5-25% of WT
+++	60-90% of WT	-	0-5% of WT

Single-cycle infectivities of eleven different viruses were analyzed in this chapter, and additional assays were performed to further characterize those defective for virus replication. Viruses are listed in the left hand column. The assays performed are given in the top row, and the findings relative to results of WT virus are shown. Single-cycle infectivity was determined in TZM-bl cells 24 hours post-infection, unless indicated otherwise. Relative Env incorporation was approximated by Western blot using anti-gp41 mAb (Chessie 8). Spreading infection results refer to analysis in MT-4 cells. ND = assay not done. NS = assay performed but results not shown. * = infectivity results from 48 hours post-infection.

To validate my findings, viral mutants with substitutions at residue 99 were compared to other single amino acid substitutions in MA that had been previously characterized. For example, a slight enhancement in Gag processing was observed in the L21K mutant, consistent with results from an earlier study (104). Similarly, the significant reduction in Env incorporation previously reported for HIV-1 particles containing the L13E MA mutation was also observed in my studies (72). These findings were substantiated by directly correlating the impairments in Env incorporation with marked reductions in virus-cell fusion capacity. Although several earlier studies had demonstrated significant MA-imposed Env incorporation defects, the corresponding virus-cell fusion capacities were not always analyzed. I, and others have found that oddly, such reductions in Env incorporation do not always correlate with an equally severe defect in virus-cell fusion (14, 43). Because of this phenomenon, it seems that virus-cell fusion assays should be directly analyzed to accurately validate a correlation between disrupted Env incorporation and compromised fusion.

While most of my results using previously characterized mutants were consistent with earlier reports, I observed a different phenotype of the K32E MA mutant that had been published previously. In contrast to the 1997 study published by Lee *et al*., I observed a reduction in Env incorporation in particles generated from a K32E-containing clone (111). A modest defect in virus-cell fusion, observed with my LAI-K32E virus, was consistent with such a disruption in Env incorporation. I believe that the discrepancy between my findings and those from the previous report might be attributed to several

differences between the two studies. First, I analyzed the K32E substitution in the context of an LAI background, whereas the previous study examined the mutation in an HXB2R3 clone. Second, I evaluated virus produced in HeLa cells, rather than COS-7 cells. Third, the Lee study did not include a Gag(-) control, which is necessary to determine whether the Env detected is virion associated, or from cellular vesicles pelleted along with the virus. And fourth, an α-gp120 Ab had been used to detect Env in the Lee study, while I used Chessie 8, an α-gp41 Ab. In spite of these differences, it is worth noting that my results are consistent with an Env incorporation defect associated with a different substitution in MA residue 32 (14, K32I mutant).

NMR and X-ray crystallographic studies have determined that this highly conserved glutamate at MA residue 99 resides in the protein's C-terminal helix, a domain that encompasses residues 96 through 121 (93, 124). Although substitutions of residue 99 have not been previously examined, several groups have observed various defects caused by other mutations in this region. One study reported that transfection of an HIV-1 clone encoding an A100E MA point mutation failed to produce virus (72). Later, the same group produced a K98E MA mutant and although virus particles were produced, there was an increase in membrane bound Gag in producer cells and replication was delayed (150). Other studies have suggested that MA residues T97 and K98 may both be involved in PI(4,5)P_2 binding at the cell membrane (150, 174). Finally, an Env incorporation defect was associated with an HIV-1 mutant containing a deletion in MA amino acids 98-100. Taken together, these findings suggest that the beginning of the C-terminal helix is involved in Gag targeting and assembly.

My studies indicate that MA E99 might specifically be involved in the Env incorporation step during virus assembly. One possibility is that E99 is necessary for maintaining the overall structure of MA, and certain substitutions at this position might indirectly affect Env incorporation by preventing the correct folding of the MA protein. Conversely, E99 may have a direct function in Env incorporation via a specific interaction with viral glycoproteins. It has been suggested that during assembly, MA trimers form a lattice structure containing an arrangement of spaces large enough to accommodate the cytoplasmic tails of gp41 trimers (93, 124, 165). Additionally, others have speculated that the C-terminal tail of gp41 might bind to several different MA protein surfaces within the hexameric lattice (124). Although the crystal structure of MA in the context of Gag has not yet been deciphered, antibody-mapping studies have suggested that E99 in Gag is solvent-exposed (124, 157). Therefore, E99 might be considered as a potential binding site for the C-terminal tail of gp41. Alternatively, E99 might interact with cellular or other viral proteins that stabilize Gag: Env complexes required for the retention of Env in virus particles. The human protein TIP47 has been previously reported to be involved in Gag: Env interactions (116). Although this study identified MA residues L12, W15 and E16 to interact with TIP47, the authors note that this association might involve other portions of MA as well. Therefore, TIP47 might be a cellular factor that selectively binds to E99.

CHAPTER IV: IDENTIFICATION OF A COMPENSATORY MUTATION AT MA RESIDUE 84

4.1 Introduction

When characterizing viral mutants containing single amino acid substitutions, several groups have identified second-site changes that can rescue the phenotype conferred by the original mutation. The identification of compensatory changes can offer valuable insight into the relationship between protein structure and function by defining possible inter- and intra-molecular interactions. There are several ways a second-site change can offset the original mutation when the two residues occur in the same protein. First, the two amino acids may directly interact in the context of a single functional or structural domain, and one mutation may restore the association that was disrupted by the other. In this case, the two residues may be close to one another in the primary sequence of the protein, or they could be distant in primary structure but proximal in the tertiary structure. Alternatively, the residues may be distant in the tertiary structure of the molecule, but interact in the quaternary structure of the functional protein, possibly through an interface between monomers. The second way a mutation might compensate for the original defect is if it falls within a domain that is separate from, but functionally linked to the region containing the primary-site mutation. For example, the two residues may interact with a common host or viral factor, and the second-site change may restore this interaction. In the third way, the compensatory mutation may offset a global conformational change brought about by the first substitution, restoring the original function of the protein.

By isolating and sequencing emergent viruses, previous groups have identified second-site compensatory changes in MA that specifically reverse a primary defect in Env incorporation. For example, one study determined that the impairment in Env incorporation imposed by the MA L13E mutation is reversed by a V35I substitution in the same protein (69). Similarly, the phenotype of a different substitution at MA residue 35 (V35E), which also abrogated Env incorporation into virus particles, could be offset by the single amino acid change Q63R (150). Interestingly, neither the V35E nor the Q63R secondary substitutions alone abrogated Env incorporation. Such observations suggest the possibility that second-site mutational analyses can also reveal residues in the protein with more subtle involvements in a particular process, as their role may only be evident in the context of the primary site mutation.

I used a molecular genetic approach to identify a residue that compensates for the defects associated with substitutions at MA E99 in LAI. With the identification of this second-site mutation, located at MA position 84, I was able to broaden my initial hypothesis that implicated the MA C-terminal helix in Env incorporation. Here, I present evidence that also associates a C-terminal hydrophobic pocket of MA in facilitating HIV-1 Env incorporation.

4.2 Results

4.2.1 Identification of MA residue 84 in potentially modulating E99V-associated defects

In the previous chapter, I showed that the E99V MA mutation, when introduced into an LAI-WT proviral clone, causes severe defects in Env incorporation, virus-cell fusion and infectivity. However, I found that the E99V-associated Env incorporation and infectivity defects appeared to be mitigated in the context of the NL4.3 strain. Therefore, I considered whether the phenotypic discrepancies observed between the two viruses (LAI-E99V and NL4.3-E99V) might be due to an inherent amino acid difference in their respective MA proteins.

I aligned the amino acid sequences of the LAI- and NL4.3-MA proteins, and found non-conservative changes at four positions: 28, 84, 124, and 125 (Figure 4.1A). Using PyMOL, I then established the positions of these residues on a published 3-dimensional structure of HIV-1 MA [PDB ID code 1UPH, (191)], and examined their positions relative to residue E99 (Figure 4.1B). My studies revealed that of these four amino acids, residue 84, a threonine in LAI and a valine in NL4.3, lies in close proximity to the glutamate at position 99.

A

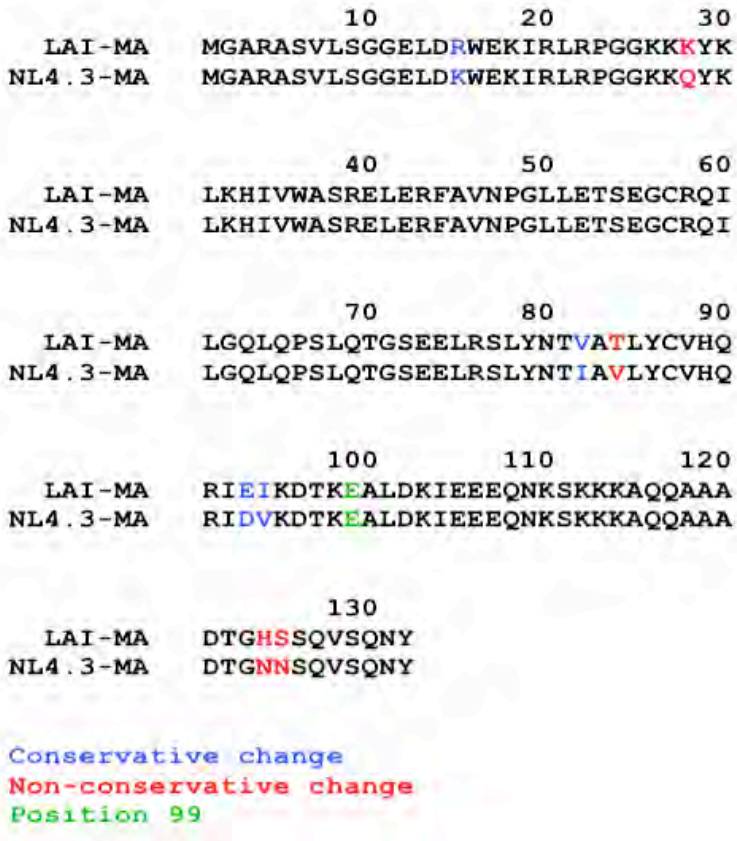
10 20 30
LAI-MA MGARASVLSGGELDRWEKIRLRPGGKKKYK
NL4.3-MA MGARASVLSGGELDKWEKIRLRPGGKKQYK
40 50 60
LAI-MA LKHIVWASRELERFAVNPGLLETSEGCRQI
NL4.3-MA LKHIVWASRELERFAVNPGLLETSEGCRQI
70 80 90
LAI-MA LGQLQPSLQTGSEELRSLYNTVATLYCVHQ
NL4.3-MA LGQLQPSLQTGSEELRSLYNTIAVLYCVHQ
100 110 120
LAI-MA RIEIKDTKEALDKIEEEQNKSKKKAQQAAA
NL4.3-MA RIDVKDTKEALDKIEEEQNKSKKKAQQAAA
130
LAI-MA DTGHSSQVSQNY
NL4.3-MA DTGNNSQVSQNY
Conservative change
Non-conservative change
Position 99

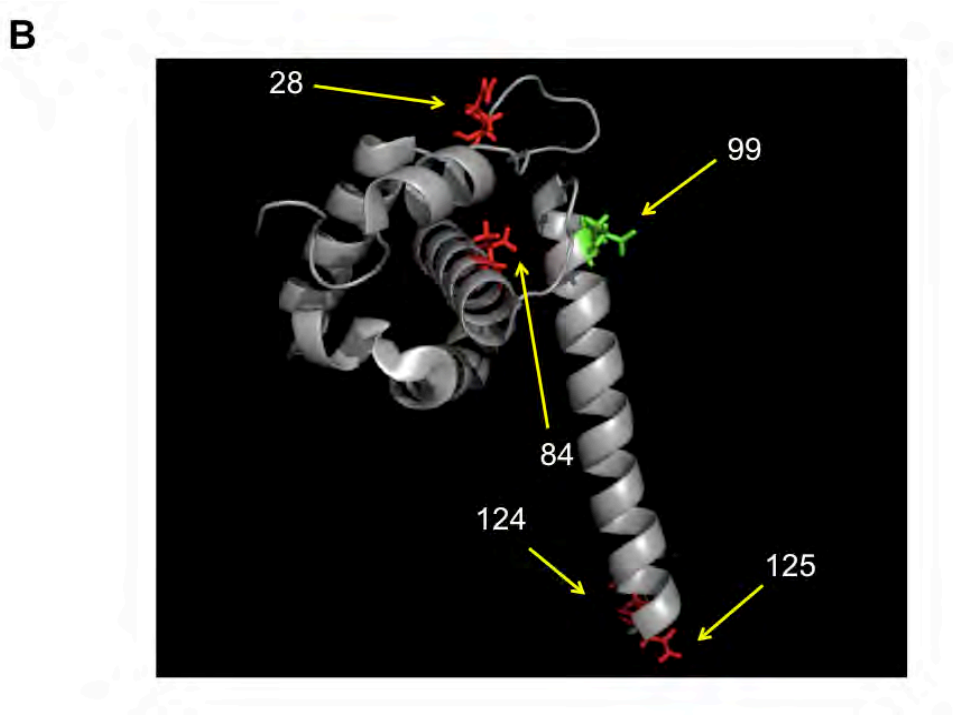

Figure 4.1 Amino acid differences between the LAI and NL4.3 MA proteins and their locations relative to E99. (A) Alignment of the LAI and NL4.3 MA protein sequences showing four non-conservative amino acid differences, highlighted in red. Conservative differences are highlighted in blue, and the common glutamate at residue 99 is shown in green. **(B)** A ribbon diagram of the HIV-1 MA structure [PDB ID code 1UPH, (191)] showing that residue 84, a threonine in LAI and a valine in NL4.3, has closest proximity to residue 99, compared to the positions of the three other non-conservative changes.

4.2.2 MA V84 modulates the E99V-associated defects

Because of its relative proximity, I considered whether the amino acid difference at position 84 might affect the degree to which the E99V substitution imposes its defects in these two HIV-1 strains. To test this possibility, I use PCR-based site-directed mutagenesis to introduce a T84V mutation into pLAI-WT and pLAI-E99V, or the reciprocal mutation, V84T, into pNL4.3-WT and pNL4.3-E99V. Each mutant proviral clone, pLAI-WT, or pNL4.3-WT, were individually transfected into 293T or HeLa cells. After 48 hours, virus in culture supernatants and the HeLa producer cells were harvested. The viruses were then subjected to analyses by the single-cycle infectivity assay, Western blot or the virus-cell fusion assay.

Figure 4.2 shows results from Beta-Glo® infectivity assays in TZM-bl cells using the indicated viruses. On its own, the threonine to valine change at MA position 84 in LAI (LAI-T84V) resulted in particles that were slightly more infectious than those containing the wild-type protein (upper graph). Conversely, the level of infectivity for NL4.3-derived particles with the solo mutation at position 84 in MA (NL4.3-V84T) was somewhat lower than that for NL4.3-WT (lower graph). These data suggest that in the context of an otherwise wild-type MA protein, a valine rather than threonine at position 84 might be more conducive for virus infectivity.

Examination of viruses with changes at both positions 84 and 99 in MA revealed that inclusion of the V84T substitution in NL4.3-E99V particles (NL4.3-V84T/E99V) completely ablated viral infectivity (lower graph). Strikingly, the addition of the reciprocal T84V MA mutation into LAI-E99V particles (LAI-T84V/E99V) restored

infectivity to wild-type levels (upper graph). These data strongly suggest that a valine at position 84 in MA is sufficient to rescue the infectivity defect associated with the E99V MA mutation in both of these HIV-1 strains, although to varying extents.

Immunoblot analyses of the indicated viral lysates using an anti-Env mAb are shown in Figure 4.3A. No disruption in Env incorporation was observed for the LAI- or NL4.3-derived viruses with a single amino acid substitution at MA residue 84. By contrast, NL4.3-V84T/E99V particles were nearly devoid of Env proteins (lower panel). Consistent with the infectivity data, Env incorporation into LAI-T84V/E99V particles was indistinguishable from that of LAI-WT (upper panel). Env precursor proteins were expressed at comparable levels in the corresponding transfected HeLa cell lysates (Figure 4.3B).

Results from the corresponding membrane fusion assays are shown in Figure 4.4. I found that amino acid substitutions in residue 84 of MA in LAI- or NL4.3-derived viruses had no discernible effect on their ability to fuse with cell membranes. Similar to LAI-E99V and NL4.3-E99V, BLaM activity was deficient in cells incubated with NL4.3-V84T/E99V (lower graph). Most important, cells treated with LAI-T84V/E99V contained levels of BLaM activity comparable to those produced with LAI-WT (upper graph). Thus, a valine at residue 84 in MA is sufficient to restore membrane fusion capability in LAI- or NL4.3- derived particles containing an E99V substitution.

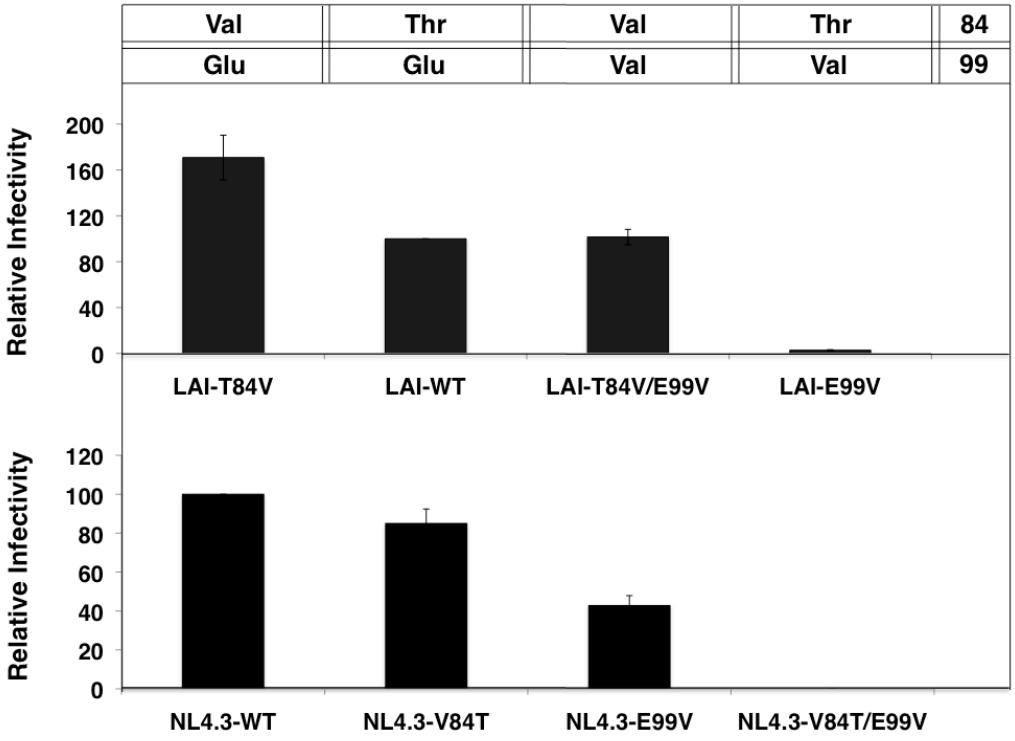

Figure 4.2 Single-cycle infectivities of LAI- or NL4.3-derived viruses bearing single or double mutations at MA positions 84 and 99. TZM-bl cells were infected with LAI- **(upper graph**) or NL4.3- (**lower graph**) derived viruses. Single-cycle infectivities were monitored 48 hours post-infection, using the Beta-Glo® reporter assay, as described in Figure 3.4. The assessment of infectivity for each mutant virus was based on the level of LAI-WT **(upper graph)** or NL4.3-WT **(lower graph)**, which represented 100% infectivity. The amino acid identities at positions 84 and 99 in each virus are indicated above the bars of both graphs. The data shown is representative of two independent experiments performed in duplicate.

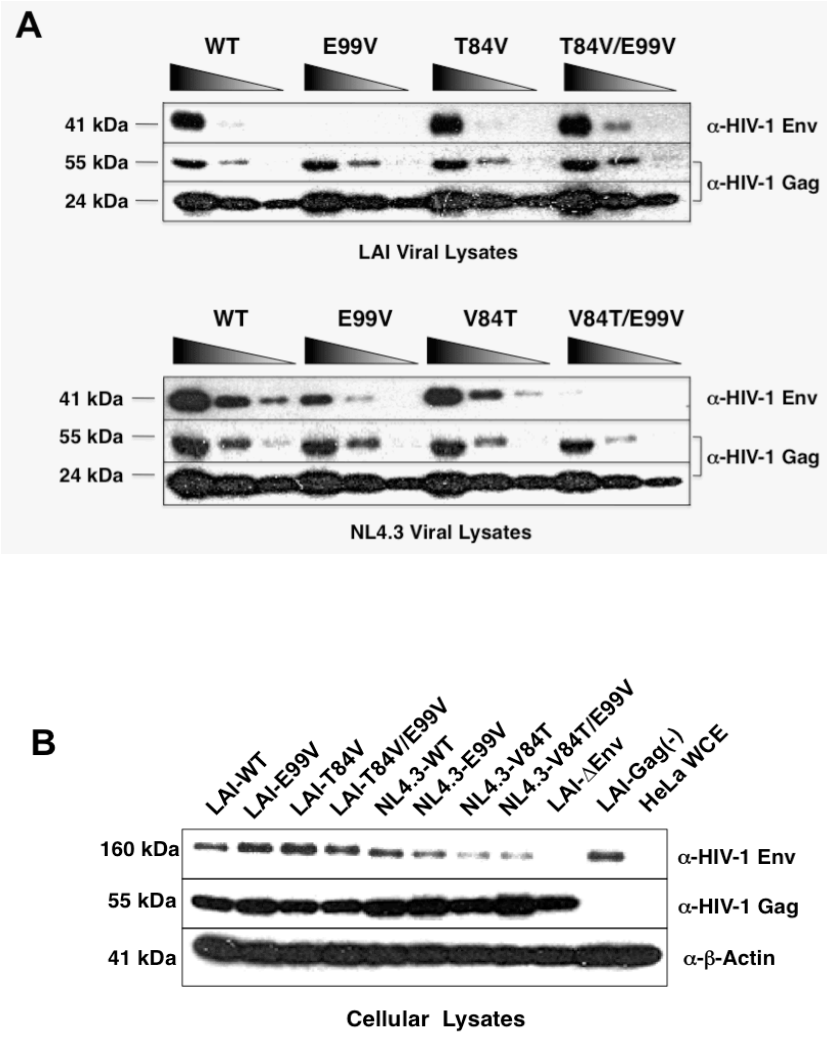

Figure 4.3 Effects of mutations at MA position 84 on Env incorporation in LAI- and NL4.3-derived particles bearing the E99V MA substitution. Lysates from LAI- **(upper panel)** or NL4.3- **(lower panel)** derived viruses **(A),** and their corresponding transfected HeLa cell lysates **(B),** were prepared and analyzed as in Figure 3.6.

4.2.3 MA V84 modulation is specific for MA E99 mutations

From the data presented in Figure 4.2, I showed that valine, rather than threonine, at position 84 of MA was more favorable for virus infectivity in the context of both LAI and NL4.3 strains. However, the improvement observed in infectivity in an otherwise wild-type MA protein was far less dramatic than what I had observed in the context of E99V. Therefore I considered whether the rescue by the T84V mutation was specific for changes at E99, or whether it was a more general phenomenon that could dramatically rescue defects imposed by substitutions of other MA residues.

To determine the specificity of rescue for residue 99 by T84V, I next investigated whether the T84V mutation in LAI could similarly rescue the defects observed with E99K, L13E or K32E MA mutations. Using PCR-based site-directed mutagenesis, the T84V MA mutation was introduced into pLAI-E99K, pLAI-K32E, and pLAI-L13E to generate pLAI-T84V/E99K, pLAI-T84V/K32E and pLAI-T84V/L13E proviral clones, respectively. Each LAI-based clone encoding the double amino acid substitutions were individually transfected into 293-T in parallel to their counterparts containing the single MA mutations. At 48 hours post-transfection, virus in culture supernatants were harvested and normalized for subsequent analysis as in previous experiments.

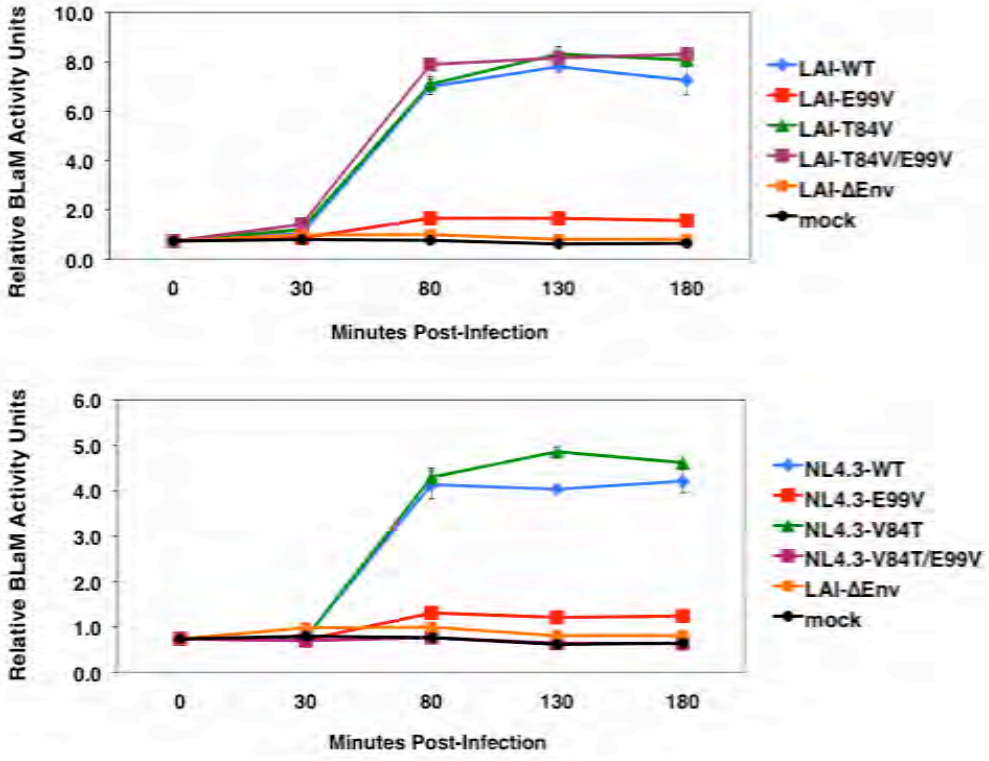

Figure 4.4 Effects of single and double MA substitutions on virus-cell membrane fusion capacity in LAI- and NL4.3-derived viruses. Virus-cell fusion events in TZM-bl cells, using LAI- **(upper graph)** or NL4.3- (**lower graph)** derived viruses, were assayed as described in Figure 3.7. The data shown is representative of three independent experiments performed in duplicate.

Single-cycle infectivity was monitored in TZM-bl cells 24 hours after inoculation with each virus. The results were assessed with the Beta-Glo® reporter assay and are presented in Figure 4.5. I found that in addition to enhancing infectivity of LAI containing an otherwise wild-type MA protein, the threonine to valine change at position 84 also improved infectivity of viruses bearing each of the E99K, L13E or K32E MA mutations. Aside from virus encoding the E99V substitution, the T84V mutation most significantly enhanced infection of the LAI-E99K virus, which improved from about 2% to 40% of WT levels. In contrast to the considerable augmentation of infectivity in the context of the E99V or E99K substitutions, the T84V mutation only modestly boosted virus replication in the context of the L13E or K32E MA mutations.

To determine whether the degree of rescue in infectivity by the T84V mutation is a function of virus titer, I performed similar Beta-Glo® assays across four, two-fold dilutions of virus. The specific fold-increase in infectivity conferred by the T84V mutation was calculated in the context of each primary MA substitution, and the data across different viral inputs is presented in Table 4.1.

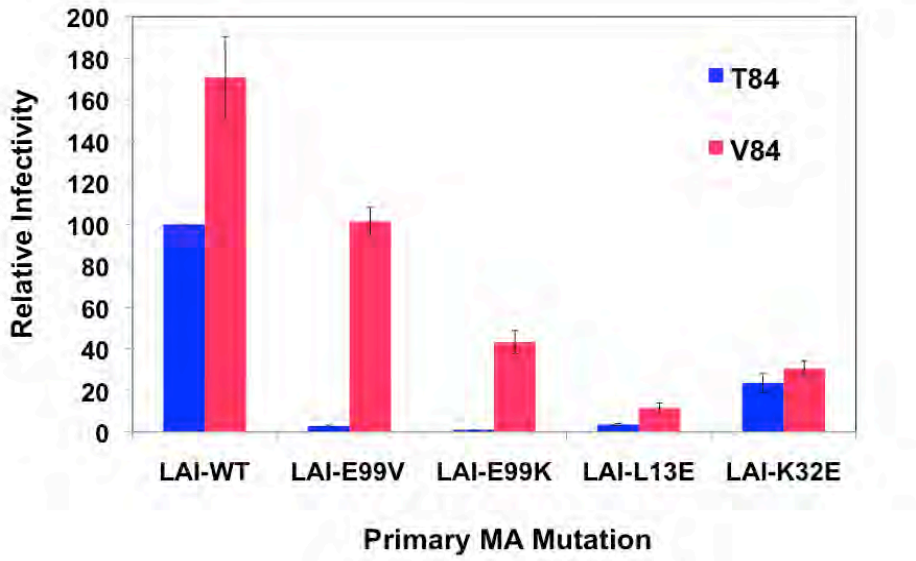

Figure 4.5 Effects on infectivity by the T84V MA mutation on LAI- derived particles bearing primary MA mutations. LAI-derived viruses bearing primary MA mutations in the presence or absence of the T84V MA substitution were used to infect TZM-bl cells. Single-cycle infectivities were monitored 24 hours post-infection using the Beta-Glo® reporter assay. The assessment of infectivity for each mutant virus is based on the level of LAI-WT, which represents 100% infectivity. Data is the average of four independent experiments performed in duplicate.

Table 4.1 Fold enhancement in relative infectivity of LAI-derived viruses bearing the T84V MA substitution

Virus titer	Primary MA mutation				
	-	E99V	E99K	L13E	K32E
20K	1.7	34.0	43.0	3.0	1.3
10K	1.9	35.3	42.0	2.0	1.3
5K	1.7	31.0	39.0	2.3	1.3
2.5K	1.6	32.0	20.0	2.2	1.4

The data is presented as fold improvement between viruses with primary MA mutations (as indicated in the top row) with, and without, the additional T84V change, at four serial dilutions (indicated in the left column as RT units of virus per well). Data shown are the averages of four independent Beta-Glo® infectivity assays analyzed 24 hours post-infection, performed in duplicate.

Overall, I did not observe any changes in relative infectivities that corresponded to viral titer. At each virus dilution, I observed a 1-2-fold enhancement in infectivity when the T84V MA mutation was expressed in the context of an otherwise wild-type MA protein. Similarly, I observed a modest 1-3-fold enhancement in viral infectivity when T84V was expressed alongside either of the L13E or K32E mutations. However, when presented in this way, the significance of T84V-imposed enhancements in the contexts of E99V or E99K MA substitutions was quite evident. Specifically, the relative luciferase units (RLU) of infections with LAI-E99K/T84V were improved by 20- to 43-fold when compared to TZM-bl infections with LAI-E99K. These findings were similar to the E99V rescues, which ranged from a 31- to 35-fold enhancement at each titer. In general, I found that a valine at residue 84 confers a modest improvement in infectivities in most MA contexts. However, these data strongly suggest that the rescue observed alongside an E99V or E99K MA mutation is unique and specific.

Next, to determine whether the T84V mutation specifically improves Env incorporation in Env-deficient MA mutants, pLAI-WT, pLAI-E99V, pLAI-E99K, pLAI-L13E pLAI-K32E, pLAI-T84V, pLAI-T84V/E99V, pLAI-T84V/E99K, pLAI-T84V/L13E, pLAI-T84V/K32E and pLAI-Gag(-) were transfected into HeLa cells. The viral supernatants and producer cells were individually collected 48 hours later and processed as described previously (52).

Immunoblot analyses of the corresponding viral and cellular lysates are shown in Figure 4.6. Again, Env precursor proteins were expressed at comparable levels in each of

the corresponding transfected HeLa cell lysates (bottom panel). In the vial lysate blots shown in the top panel, slight differences in viral content were demonstrated by the anti-p24 mAb blot, despite equal amounts of virus loaded in each lane. For example, it appeared as though more virus was present in the LAI-E99V/T84V lane, compared to the virus in LAI-T84V or LAI-WT lanes. Overall, less virus RT units were used per lane in this blot, compared to the viral RT units loaded in the immunoblot from Figure 3.6, which might explain why Env was not detected in this LAI-K32E lane. Nevertheless, a distinct band at 41 kDa was detected in both the LAI-WT and LAI-E99V/T84V viral lysates, demonstrating the efficient processing and packaging of gp41 in these particles. Although not at levels equal to the LAI-E99V/T84V lysate, gp41 was clearly detected in LAI-E99K/T84V particles. This demonstrates a partial, but significant rescue in Env incorporation by the T84V mutation in the context of an E99K MA mutation, and agrees with the partial, but significant rescue observed in the infectivity studies. Interestingly, a similar band was observed in the LAI-K32E/T84V virus, and might represent a slight improvement in Env incorporation over the LAI-K32E particles. However, loading differences in the LAI-K32E and LAI-K32E/T84V lanes may also account for this observation. It is interesting to note that the similar gp41 bands observed in the LAI-K32E/T84V and LAI-E99K/T84V lanes mimicked the comparable infectivities of these viruses that were demonstrated in Figure 4.5A. By contrast, Env was not detected in the LAI-L13E/T84V virus, again suggesting that the T84V mutation does not rescue the Env incorporation defect conferred by the L13E MA mutation. Taken together, these results agree with the infectivity data, demonstrating that while a T84V mutation confers a

modest improvement in defects associated with many MA mutations, a quite significant recovery is observed in the context of E99 substitutions.

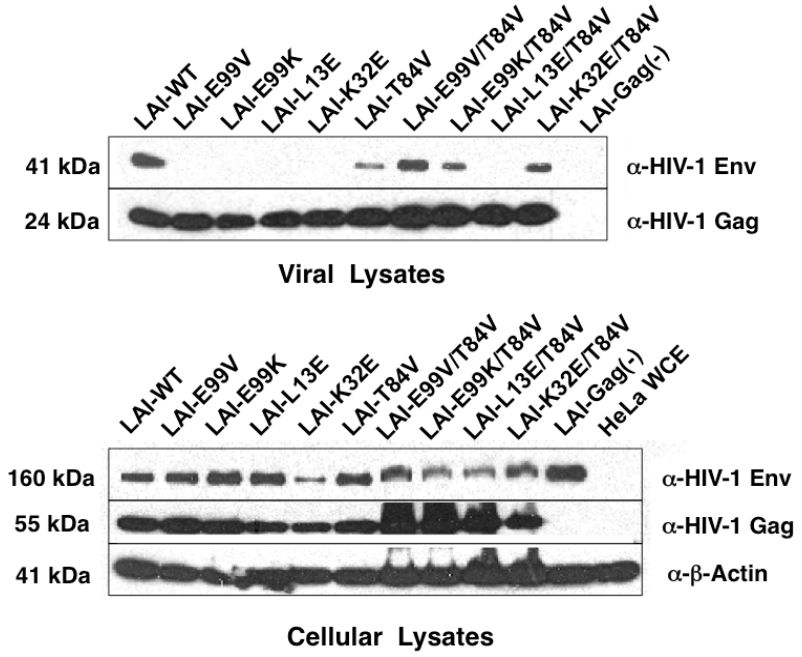

Figure 4.6 Effects of the T84V MA substitution on Env incorporation in LAI-derived particles containing WT MA or other MA mutations. Lysates from virus particles (**top panel**), or transfected HeLa cells (**bottom panel**) were prepared and analyzed by Western blotting, as in Figure 3.6.

Lastly, to determine whether the T84V mutation could rescue fusion defects in various MA mutants, pLAI-WT, pLAI-E99V, pLAI-E99K, pLAI-L13E, pLAI-K32E, the corresponding T84V double mutants, and pLAI-ΔEnv were individually transfected into 293T cells, along with the pBLaM-Vpr expression plasmid. Viruses were harvested and processed as previously described, and equal amounts were used to infect TZM-bl cells for the fusion assay.

Results from this fusion experiment are shown in Figure 4.7. Similar to the infectivity data, a valine at residue 84 appears to improve the capacity for membrane fusion in cells incubated with each virus tested. However, the degree of improvement varied, and was most evident in the context of the E99V and E99K mutations. Fusion of LAI-E99K/T84V particles with cells was significantly greater than that in the LAI-ΔEnv infection, improving to levels of about 50% that in the LAI-T84V infection, and demonstrates a greatly improved fusion capacity compared to that with LAI-E99K particles (fusion of LAI-E99K was presented in Figure 3.5). Only a slight enhancement of fusion was observed between LAI-L13E/T84V virus and target cells, when compared to that with LAI-ΔEnv, which corresponded to the minor improvement observed in the infectivity results. Lastly, although fusion appeared to be completely rescued in the LAI-K32E/T84V infection, only a modest fusion defect was observed in the original LAI-K32E virus infection, and therefore the improvement may only be about 2-fold (fusion of LAI-K32E was presented in Figure 3.5).

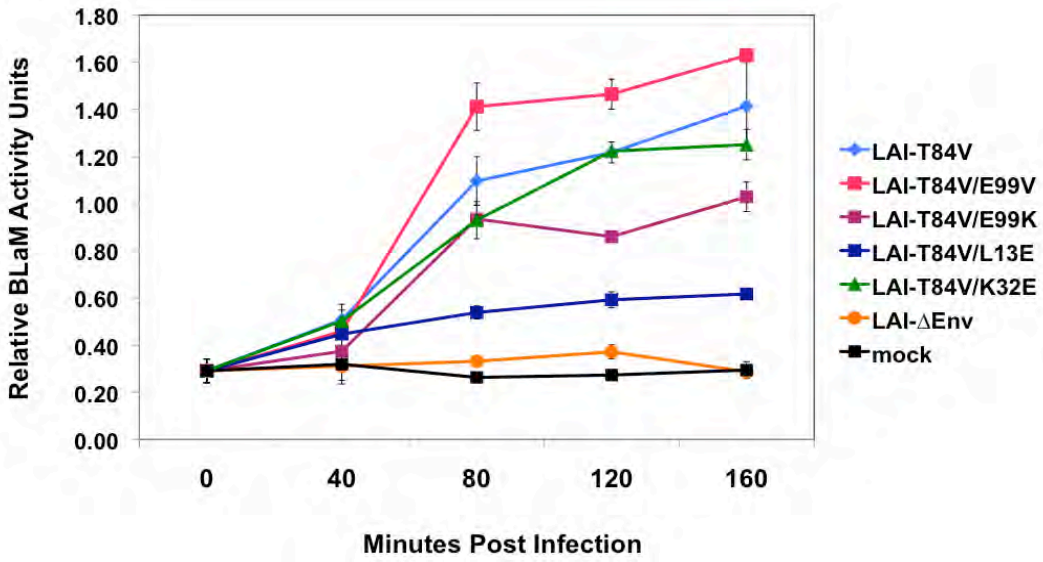

Figure 4.7 Effects of single and double MA substitutions on virus-cell membrane fusion capacity in LAI-derived viruses. Virus-cell fusion events in TZM-bl cells were assayed as described in Figure 3.7. The data shown is representative of three independent experiments performed in duplicate.

4.3 Discussion

Using a molecular genetic approach, I identify a substitution at MA residue 84 that counteracts the E99V-imposed defects in the LAI HIV-1 strain. Introduction of this T84V change in the context of the original E99V mutation caused a significant improvement in Env incorporation, virus-cell fusion and single-cycle infectivity assays. These findings indicate that T84V is sufficient to reverse the defects imposed by the original E99V amino acid change in LAI. I also demonstrated that in the NL4.3 background, a valine at residue 84 only partially compensates for the severe infectivity defects imposed by the T84, V99 combination in MA. Finally, analyzing the T84V mutation in the context of individual MA substitutions L13E, K32E or E99K demonstrates that V84 seems to specifically improve defects conferred by E99 mutations, above the enhancements it confers in the context of wild-type MA. The results from each clone analyzed in this chapter are summarized in Table 4.2.

Table 4.2 Summary of Results from Chapter 4

Virus	Assay Performed		
	Env Incorporation	Virus-Cell Fusion	Single-cycle Infectivity
LAI-T84V	+++	++++	+++++
LAI-T84V/E99V	++++	+++++	++++
LAI-T84V/E99K	++	++	++
LAI-T84V/K32E	+++	++++	++
LAI-T84V-L13E	-	+	+
NL4.3-WT	++++	++++	++++*
NL4.3-E99V	+	-	++*
NL4.3-V84T	++++	+++++	+++*
NL4.3-V84T/E99V	-	-	-*

+++++	better than WT	++	25-60% of WT
++++	90-100% of WT	+	5-25% of WT
+++	60-90% of WT	-	0-5% of WT

The different viruses analyzed in this chapter are listed in the left hand column. The assays performed and individual findings relative to results from the wild-type parental virus are indicated. Single-cycle infectivity was determined 24 hours post-infection, unless indicated otherwise. Relative Env incorporation was approximated by Western blot using anti-gp41 mAb (Chessie 8). * results from 48 hours

Both NMR and X-ray crystallographic techniques have determined that residue 84 falls within the fourth helix of MA, a region almost entirely buried inside the tightly packed globular core of the MA protein (31, 93, 124). This fourth helix makes up part of a hydrophobic pocket, created by the N-terminus of MA Helix V packing alongside residues of Helix IV (30, 93). It has been suggested that instability of this pocket, which includes residues V84, Y86, I92, V94, A100, and K103, might compromise the overall structure of the MA core domain (30). Based on these residues and the determined structure of MA, I recognized that E99 also appears to fall in the vicinity of the pocket. I speculated that this region may have a role in Env incorporation, and that in addition to V84, E99 may be necessary for its stabilization. However, as a polar amino acid, E99 is unlikely to contribute to the hydrophobicity of this domain. Therefore, it seems unlikely that maintaining the Env incorporation function of this C-terminal MA hydrophobic pocket may necessitate either an interaction between the side chains of residues 84 and 99, or possibly between these residues and a host or viral bridging protein. It is also possible that these two residues somehow compensate for the overall changes, in pocket stability or function, incurred by mutations at either position.

It is worth noting that I consistently found a valine at residue 84 to be more conducive to viral replication compared to a threonine. Since this was observed in the context of an otherwise wild-type virus, it was not surprising that marginal improvement in infectivity correlated to the introduction of V84 in both the LAI-K32E and LAI-L13E mutants. However, it is apparent that the rescues observed when T84V is expressed alongside the E99V or E99K mutations were notably more conspicuous. Specifically,

while V84 improved the K32E- or L13E-imposed infectivity defects by 1- or 2- fold, V84 enhanced the infection of viruses containing E99K or E99V by about 35- and 32-fold. The overall improvements seen in each virus when residue 84 is a valine is consistent with the hypothesis that this residue is critical for stabilization of the hydrophobic pocket. However the specific improvement observed with the E99 mutations suggest that either E99 is also critical for the stabilization of this pocket, or V84 improves E99 mutations by a mechanism independent of this hydrophobic pocket stabilization.

Although a valine at residue 84 correlates with enhanced infectivity, I was surprised to find that a threonine is present more frequently at this position in MA. Sequence alignment of >1100 MA proteins from HIV-1 Group M, subtypes A through K, reveals a threonine and a valine in this position in 82% and 17% of the strains, respectively. I also find it interesting that two amino acids associated with vastly different polarities and sizes could be present at one position 99% of the time. Also curious is that the residue correlated with enhanced infectivity (V84) is present less frequently than the amino acid linked to inferior replication kinetics (T84). In considering this, I reasoned that enhanced infectivity, as measured with laboratory assays using cells in culture, may not confer an advantage in virus replication *in vivo*. For example, if a valine at residue 84 does vastly enhance single-cycle infectivity *in vivo,* then the incidence of super-infection (defined here as multiple viruses infecting a single cell) may occur too frequently. It is possible that super-infection events are more easily detected by the host cell, in comparison to the recognition of a single virus entering into a cell. In turn, apoptosis may be triggered before nascent particles are ready for release, which would negatively affect

the fitness of that virus. Alternatively, V84 may cause an overall structural change in MA, and while this may be advantageous for infectivity in cell culture, it may establish an epitope more easily neutralized by host immunity.

The E99V-associated defects observed with V84 in NL4.3-derived particles, but not in LAI, reveal a greater degree of complexity between these two residues in Env incorporation, virus-cell fusion and infectivity. Data gathered from single-cycle and spreading infection assays of NL4.3-E99V suggest a delay in the replication kinetics of this virus. Consistent with this possibility, a considerable defect in virus-cell fusion was evident for NL4.3-E99V at each of the time points analyzed (Figure 4.5, lower graph), despite a relatively modest Env incorporation defect, as assessed by Western blot (Figure 4.4, upper panel). Observing a greater level of BLaM activity in cells after extended incubation with NL4.3-E99V, but not with LAI-E99V, would provide more evidence for a delay in virus-cell fusion. The phenotypic variation observed between LAI- and NL4.3-derived viruses containing valines at both positions 84 and 99 might be the result of additional amino acid dissimilarities between the two strains. For example, positions 28, 124 and 125 also differ in LAI-MA and NL4.3-MA, and these non-conservative amino acid differences may contribute to the dissimilar phenotypes (Figure 4.1A). Alternatively, variations encoded within other viral proteins could also be responsible for the observed phenotypes.

CHAPTER V: IDENTIFICATION OF AN ADDITIONAL DEFECT IMPOSED BY E99 MA MUTATIONS AT AN EARLY, POST-FUSION STEP

5.1 Introduction

As discussed in Chapter 1, the incorporation of full-length Env into HIV-1 particles seems to be dependent upon an interaction between the viral gp41 cytoplasmic tail (CT) and the MA domain of Gag. In contrast, the packaging of heterologous viral envelopes into HIV-1 seems to occur through a MA-independent mechanism. Many believe that this discrepancy is linked to the unusually long CT of HIV-1 Env, as it has been suggested that the extraordinary length of HIV-1 gp41 may sterically hinder its incorporation into virus particles in a way that only the HIV-1 MA can accommodate (71, 93). In general, extended cytoplasmic domains are a unique property of many lentiviral envelope glycoproteins, when compared to those of other retroviruses. For example, most simple retroviruses have CTs of 20 to 50 amino acids in length, whereas the lentiviruses HIV-1, HIV-2 and SIV all have cytoplasmic domains of about 150 residues (53).

Previously, it has been observed that the Env incorporation defects in HIV-1 MA mutants can be overcome by pseudotyping particles with heterologous envelopes bearing shorter CTs (14, 43, 52, 69, 71, 104, 214). The glycoprotein of the Vesicular Stomatitis Virus (VSV-G) is commonly used in such pseudotyping experiments, as its short CT permits packaging into many different viruses, and its use of a common receptor confers a broad cellular tropism to the pseudotyped particle. To facilitate virus entry, the VSV glycoprotein binds to a phospholipid receptor at the surface of a target cell (10, 210). This

interaction promotes the formation of clathrin-coated pits, which enables the virus to be internalized via endocytosis. Fusion activity of the glycoprotein is then activated within the endosome by the eventual decrease in pH inside the vesicle. This process deposits the viral core into the cytoplasm of the cell, often at a site proximal to the nuclear periphery (2).

Although VSV-G pseudotyping can be a useful way to restore fusion in a mutant virus, this endocytic entry can obscure analyses regarding the nature of the initial impairment. This is because it not only overcomes a fusion block, but also may bypass a post-entry restriction that would be encountered if fusion were to take place at the PM. To mimic the normal mode of HIV-1 entry, and in turn examine the presence of an early post-entry block, many studies have relieved Env incorporation defects in MA mutants through truncation of the HIV-1 gp41 CT (14, 43, 69, 71, 104, 118, 142). Thus, the truncated Env is packaged via a MA-independent mechanism, in a manner similar to the incorporation of other glycoproteins bearing shorter CTs. It is believed that *in vivo,* the extended length of the Env CT is beneficial for HIV-1 replication (70, 180). This hypothesis is based on the fact that very few primary isolates have been found with extensive deletions in the gp41 CT (180). However, its importance for infection in cell culture has been questioned, since many cell lines, such as MT-4 and those derived from HeLa cells, can support productive infections of HIV particles containing gp41 truncations (118, 142, 205). In this chapter, I used the Env truncation and VSV-G pseudotyping methods to further characterize the infectivity defects imposed by the E99V and E99K MA mutations.

5.2 Results

5.2.1 HIV-1 Env truncation restores fusion but not infectivity of viruses with mutations at MA E99

To examine whether the fusion and infectivity defects imposed by MA mutations E99V and E99K can be reversed by truncating sequences within the long cytoplasmic domain of HIV-1 gp41, PCR-based site-directed mutagenesis was used to introduce two consecutive stop codons into the gp41 coding sequences of pLAI-WT, pLAI-E99V, pLAI-E99K, pLAI-K32E or pLAI-L13E. The gp41 proteins generated from transfection of the resulting proviral clones (pLAI-Δ144, pE99V-Δ144, pE99K-Δ144, pK32E-Δ144, and pL13E-Δ144, respectively) contain an abbreviated CT that is six residues in length, instead of the normal 150 amino acids. Each mutant proviral clone, or pLAI-ΔEnv, was individually transfected into 293T cells. Viruses in culture supernatants were harvested 48 hours post-transfection, and then normalized by RT content for subsequent analysis.

The Beta-Glo® assay system was used to monitor single-cycle infectivity of viruses with either full length or truncated HIV-1 gp41. Four serial dilutions of each virus were used to infect TZM-bl cells, and their relative infectivities were analyzed 24 hours post-infection. Upon comparison of the raw data, I found that the LAI-Δ144 particles were more infectious than LAI-WT, at each dilution (data shown in Appendix B, Tables B.1 and B.2). This result was consistent with previous studies (205, 208), and is likely due to the removal of a tyrosine-based endocytic motif normally present in the gp41 cytoplasmic domain. In the absence of this signal, Env expression is increased at the

surface of producer cells, which likely favors more efficient packaging of Env into particles (173).

To evaluate virus infection across the four dilutions, I assigned the infectivity values of the LAI-WT or LAI-Δ144 infections to represent 100%, and then infections with the other viruses were adjusted accordingly at each titer. These normalized values for each virus bearing either full-length or truncated gp41 are presented in Tables 5.1 and 5.2, respectively. Adjusted in this way, it is evident that the truncated Env augmented infectivity of each MA mutant consistently across the different titers. However, it was also apparent that the extent of rescue varied among the different MA mutations. The presence of a short gp41 CT rescued the infectivity defects associated with each of the L13E and K32E MA mutations to levels comparable to the WT-Δ144 infection. By contrast, only a modest enhancement was observed with viruses bearing the E99V or E99K mutations. Therefore, I concluded that truncation of the gp41 CT was not able to reverse the infectivity defects associated with either of the E99 MA substitutions.

Table 5.1 Relative infectivities of LAI-derived viruses bearing single amino substitutions in MA

Virus	Titer (RT units per well)			
	20K	10K	5K	2.5K
LAI- WT	100	100	100	100
LAI- E99V	0.8	1.4	1.3	1.6
LAI- E99K	0.5	0.6	1.0	1.6
LAI- L13E	2.4	3.4	3.3	5.4
LAI- K32E	21.2	22.9	17.6	21.3
LAI-ΔEnv	0.1	0.2	0.1	0.5

The data shown are normalized from the RLU values presented in Table 8-2, and represent averages of four independent Beta-Glo® infectivity assays analyzed 24 hours after TZM-bl cells were infected with four serial dilutions of the indicated virus. The normalized values are based on results from the LAI-WT infection, which represents 100% infectivity at each titer.

Table 5.2 Relative infectivities of LAI-derived double mutants bearing gp41 cytoplasmic domain truncation and individual substitutions in MA

Virus	Titer (RT units per well)			
	20K	10K	5K	2.5K
WT-Δ144	100	100	100	100
E99V-Δ144	9.8	9.8	9.0	7.3
E99K-Δ144	12.8	12.5	13.3	16.3
L13E-Δ144	112.3	105.8	114.3	96.5
K32E-Δ144	84.0	76.3	86.0	74.8
LAI-ΔEnv	0.0	0.0	0.3	0.5

The data shown are normalized from the RLU values presented in Table 8-3, and represent averages of four independent Beta-Glo® infectivity assays analyzed 24 hours after TZM-bl cells were infected with four serial dilutions of the indicated virus. The normalized values are based on results from the WT-Δ144 infection, which represents 100% infectivity at each titer.

Since the data demonstrate that LAI-Δ144 was more infectious than equal RT units of LAI-WT, I decided to compare dilutions of the two viruses that resulted in similar values, which would likely correspond to a comparable MOI in each infection. I determined that the average RLU value from infection with 5K RTU of LAI-WT was similar to the RLU values from the 2.5K RTU LAI-Δ144 infection, and the relative infectivities of each virus are shown in Figure 5.1A.

Although low levels of infection were detected in TZM-bl cells inoculated with E99V-Δ144 and E99K-Δ144, the possibility remained that these viruses might still have the capacity to initiate a spreading infection. To examine this, equal RT units of LAI-Δ144, E99V-Δ144 or LAI-ΔEnv were used to infect MT-4 cells in a 24-well plate. The cells were washed after four hours, and then replated in fresh media. Small aliquots of the culture supernatants were collected every other day for two weeks, and then analyzed for RT activity. The data, shown in Figure 5.1B demonstrates that robust levels of virus replication were detected in cells incubated with LAI-Δ144, but not in LAI-ΔEnv. Overall, spreading infection was markedly reduced with particles bearing the E99V MA substitution, compared to the cells inoculated with LAI-Δ144. However, after 11 days, some RT activity was detectable in the E99V-Δ144 infected cultures. Supernatant from the E99V-Δ144 day 15 culture was then used to infect fresh MT-4 cells. Minimal RT activity was detected after a week (data not shown), and the cells were harvested at that time. Total cellular DNA was extracted and proviral DNA was sequenced using primers specific for the MA region. Although the E99V mutation was still present, the continuously low levels of infection led me to conclude that overall, particles bearing the

E99V MA substitution had a reduced capacity to initiate single–cycle and spreading infections, even with the gp41 truncation.

Since the impairments in single-cycle infectivity associated with the L13E and K32E MA mutations were both rescued by Env truncation, I concluded that functional Env trimers were indeed expressed and incorporated into these particles. However, since the possibility remained that the MA mutations were somehow reducing expression or packaging of truncated Env, I decided to analyze Env incorporation in the E99V-Δ144 or E99K-Δ144 particles. Pseudotyped viruses with truncated CTs were generated through transient transfection of HeLa cells. After 48 hours, viruses and producer cells were harvested and processed for immunoblot analysis, as descried earlier. I found that the Chessie 8 antibody used in previous experiments could not detect the truncated glycoproteins, probably due to the loss of a required epitope. Two different antibodies directed against gp120 (Clone VT-21 and Chessie 6, both from NIH AIDS Research & Reference Reagent Program), and serum from an HIV-seropositive patient (a gift from K. Luzuriaga), were also used to detect Env in producer cells and viral lysates. Unfortunately, the Env glycoproteins with short cytoplasmic tails were not detected in any of the particles or producer cells, even though the infectivity data indicated proper expression and packaging into LAI-Δ144 particles. Since an antibody to detect the truncated form of gp41 was unavailable, I was unable to determine whether truncated Env was expressed and incorporated into E99V-Δ144 or E99K-Δ144 particles.

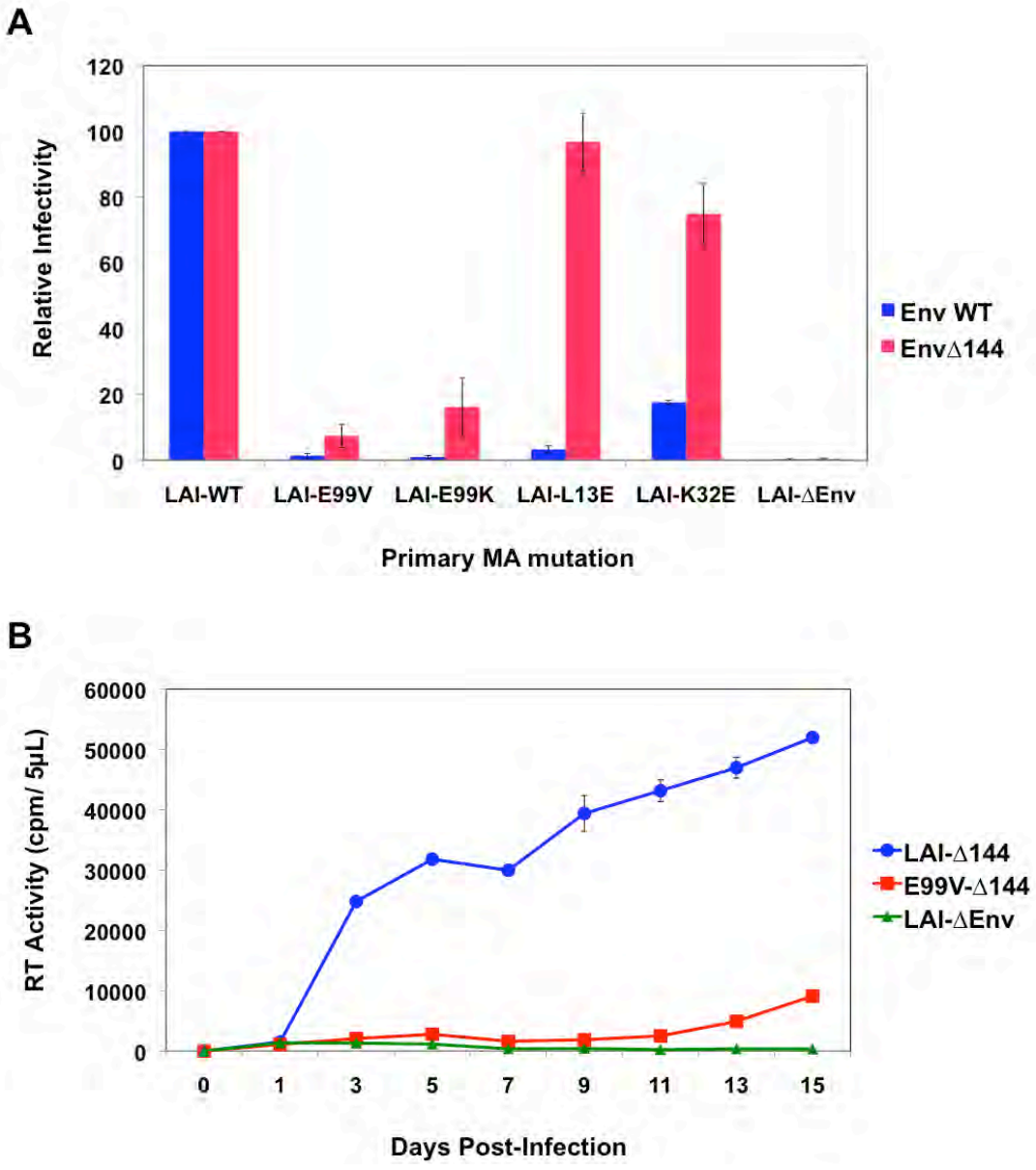

<u>Figure 5.1</u> Effects on infectivity by Env truncation in LAI-derived particles bearing individual MA mutations. (A) Single-cycle infectivities of LAI-derived viruses, containing either full length (**blue bars**, inoculated at 5K RTU/well) or truncated (**red bars**, inoculated at 2.5K RTU/well) HIV-1 Env, were monitored in

TZM-bl cells 24 hours post-infection using the Beta-Glo® reporter assay. The assessment of infectivity for each mutant virus was based on the levels in LAI-WT or LAI-Δ144 infections, which represented 100% infectivity. The data shown is the average of four independent experiments performed in duplicate. **(B)** Equal RT units of the indicated viruses were used to infect MT-4 cells, and virus replication kinetics were monitored every other day for two weeks, as described in Figure 3.5. Fresh cells and media were added to each culture on day seven. A representative graph of two independent experiments, performed in duplicate, is shown.

Next, the fusion capacity of these particles were analyzed, using the BLaM assay described previously. Each proviral clone with a truncated Env, or pLAI-ΔEnv, was co-transfected into 293T cells with an expression vector for BLaM-Vpr. Equal amounts of each virus were used to infect TZM-bl cells, and virus-cell fusion was monitored, as described for Figure 3.6. The data from this virus-cell fusion assay is shown in Figure 5.2. Supporting my infectivity results, I found that BLaM activity was comparable in cells incubated with particles containing truncated Env and MA mutations K32E or L13E, or WT MA. Remarkably, the levels of BLaM activity in cells treated with E99V-Δ144 or E99K-Δ144 were also comparable to the LAI-Δ144 infection at each time point analyzed. Therefore, despite an inability to monitor Env packaging by Western blot, the high capacity to initiate virus-cell fusion, as detected with this assay, suggests that truncated Env was indeed incorporated into E99V-Δ144 and E99K-Δ144 particles at levels comparable with WT-Δ144. Most important, these results suggest that although Env truncation could not rescue their infectivity defects, this modification was able to reverse the diminished fusion capacity imposed by the E99V and E99K MA substitutions.

The incongruity between my fusion and infectivity data for the E99V-Δ144 and E99K-Δ144 particles suggests that in addition to disruptions in Env incorporation, the E99V and E99K MA mutations might also impose a post-entry restriction to productive infection. To evaluate the early step for which E99V-Δ144 particles might be defective, early products (EP) were analyzed in target cells incubated with E99V-Δ144. EPs are the first part of the viral genome to be reverse transcribed, and they are used as a marker for

reverse transcription initiation. Prior to infection, equal amounts of LAI-Δ144 or E99V-Δ144 viruses (as determined by RT analysis) were treated with DNase, to eliminate any contaminating DNA carried over from the transfection procedure. MT-4 cells were then challenged with the DNase-treated viruses in a 12-well plate, and equal volumes of cells were harvested from each well at 1, 5, 8 or 24 hours post-infection. When cells from each time point were collected, total DNA was extracted using the DNeasy kit (Qiagen). Primers that target a region within the R and U5 portions of the HIV-1 LTR were used to amplify and quantitate EPs (minus-strand strong stop viral DNA) by qPCR. To normalize the cell counts in each sample, an additional set of primers were used to quantify copies of the cellular CCR5 gene, which is present in two copies of each cell. The data, presented as EPs per million cells is shown in Figure 5.3. Significant levels of EPs were detected in cultures infected with LAI-Δ144, and these levels increased with time. However, an 8-fold reduction in EP synthesis was observed in the E99V-Δ144 infection at 24 hours, compared to those produced by LAI-Δ144. Thus, although E99V-Δ144 particles were competent for fusion with target cells, they were markedly impaired for the production of EPs. These results suggest that the E99V-Δ144 particles were unable to overcome a post-entry block that occurs at, or prior to, the initiation of reverse transcription.

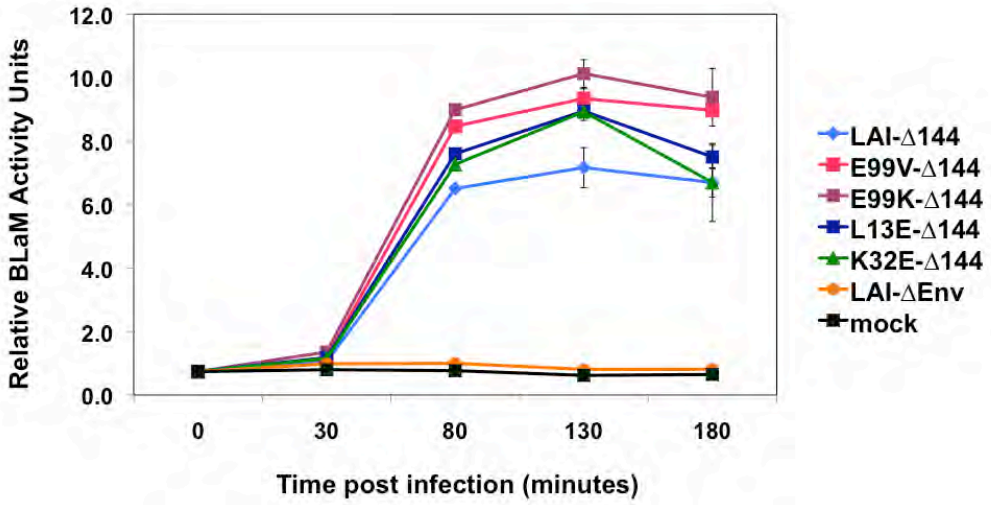

Figure 5.2 Effects of Env truncation on virus-cell membrane fusion capacity in LAI-derived viruses bearing MA substitutions. Virus-cell membrane fusion events were assayed in TZM-bl cells as described in Figure 3.7. The data shown is representative of three independent experiments performed in duplicate.

5.2.2 VSV-G pseudotyping can partially rescue the post-entry block

In the previous section, I showed that the E99V and E99K MA mutations conferred an infectivity defect, even when fusion was permitted at the plasma membrane of target cells. To determine whether endosomal entry could rescue the infectivity defect of these particles, I next decided to analyze particles that were pseudotyped with the glycoprotein from the Vesicular Stomatitis Virus (VSV-G). To create proviral clones encoding the MA mutations but lacking the ability to make HIV-1 Env, mutagenic primers were used to introduce individual MA substitutions E99V, E99K, K32E or L13E into the proviral clone pLAI-ΔEnv, to produce pE99V-ΔEnv, pE99KΔEnv, pK32EΔEnv and pL13EΔEnv, respectively. The individual clones, or pLAI-ΔEnv, were cotransfected into 293T cells with an expression vector encoding VSV-G. Virus-containing supernatants were harvested 24 and 48 hours post-transfection, and then normalized by RT assay.

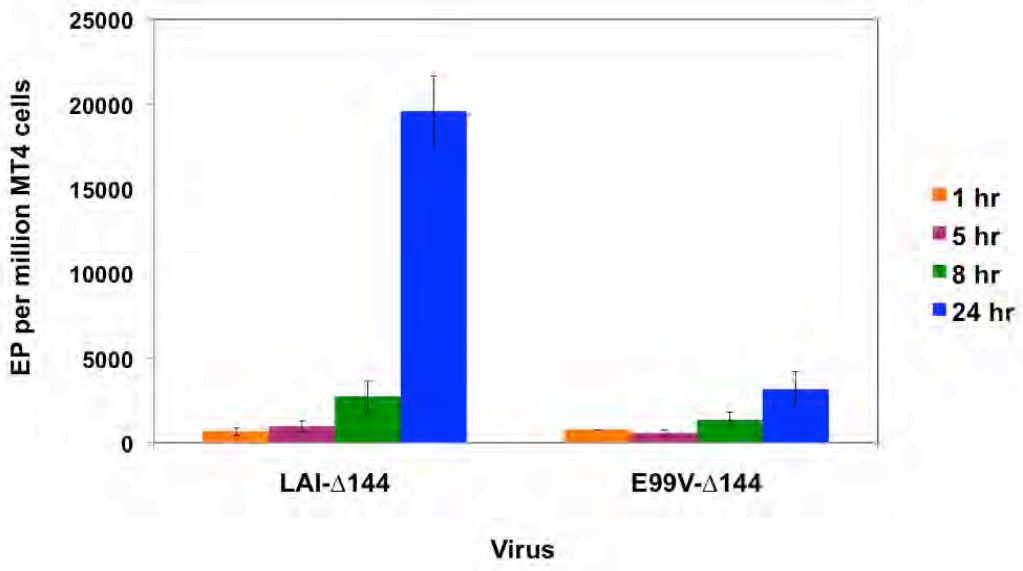

Figure 5.3 Early reverse transcription products in cells infected with LAI-derived virus containing truncated HIV-1 Env with and without the E99V MA substitution. MT-4 cells were infected with equal RT units of the indicated virus. At 1, 5, 8 or 24 hours post-infection, cells were lysed and EPs were quantified directly by real-time PCR using primers specific for strong-stop viral DNA. Data was normalized by quantification of the cellular CCR5 gene in each sample. Data shown is the mean of two separate experiments performed in duplicate.

To determine whether the pseudotyped viruses were competent for a single round of infection, 2-fold serial dilutions were incubated with TZM-bl cells and analyzed with the Beta-Glo® assay system at 24 hours. In parallel, similar infections were performed using viruses with wild-type HIV-1 Env. Non-pseudotyped LAI-ΔEnv particles were used as a negative control. In analyzing the average raw RLU values from four separate experiments, it is apparent that each dilution of the VSV-G-pseudotyped particles containing wild-type MA (VSV-G-LAI-ΔEnv) was substantially more infectious than LAI-WT (presented in Appendix B Table B.3).

To normalize the data, an infectivity value of 100 was assigned to the VSV-G-LAI-ΔEnv infection, as done in the analyses of viruses bearing a truncated Env. The normalized data for infections with VSV-G-pseudotyped viruses is presented in Table 5.3. It was apparent that overall, pseudotyping with VSV-G enhanced infection of each virus, however, the degree of enhancement varied depending on the MA mutation. VSV-G pseudotyping rescued infectivities of viruses bearing the L13E or K32E MA mutations, to at least 50% of the levels achieved using VSV-G-LAI-ΔEnv.

Across each titer, I observed a partial rescue for both the VSV-G-E99V-ΔEnv and VSV-G-E99K-ΔEnv infections (Table 5.3). However, the raw data suggests that the VSV-G-LAI-ΔEnv virus was saturating at higher titers. For this reason, I concluded that the 20K RTU or 10K RTU viral inputs might not represent accurate enhancement for infections with a-VSV-G-E99V-ΔEnv or a-VSV-G-E99K-ΔEnv. Nevertheless, the data for the VSV-G-LAI-ΔEnv infections at dilutions of 5K RTU and less declined linearly in relation to the titer. With saturation unlikely at these intermediate titers, the data suggests

that VSV-G pseudotyping improved infectivities of viruses with E99V or E99K MA mutations from less than 2% of infection of LAI-WT when bearing HIV-1 Env, to levels of around 40% or 22% of VSV-G-LAI-ΔEnv when pseudotyped with VSV-G, respectively.

Table 5.3 Relative infectivities of LAI-derived MA mutants pseudotyped with VSV-G Env

Virus	Titer (RT units per well)							
	20K	10K	5K	2.5K	1.25K	625	312.5	156
WT-ΔEnv + VSV-G	100	100	100	100	100	100	100	100
E99V-ΔEnv + VSV-G	72.5	58.0	45.3	37.0	37.2	35.7	36.4	51.0
E99K-ΔEnv + VSV-G	51.0	35.5	27.3	21.8	19.0	19.0	13.8	20.8
L13E-ΔEnv + VSV-G	82.3	70.8	61.0	57.0	41.5	34.7	64.6	62.7
K32E-ΔEnv + VSV-G	91.0	84.5	77.8	74.8	63.2	51.4	101.8	63.3
LAI-ΔEnv	0.5	0.5	1.0	0.3	0.2	0.3	0.0	0.0

The data shown are normalized from the RLU values presented in Table 8-4, and represent averages of four independent Beta-Glo® infectivity assays analyzed 24 hours after TZM-bl cells were infected with four serial dilutions of the indicated virus. The normalized values are based on results from the VSV-G-LAI-ΔEnv infection, which represents 100% infectivity at each titer.

To analyze the rescues observed with comparable MOIs (as determined by the titers of LAI-WT and VSV-G-LAI-ΔEnv that resulted in similar raw RLU values), I evaluated the normalized data using virus with WT HIV-1 Env at 10K RTU per well, to the infections with VSV-G pseudotyped particles at 2.5K RTU per well. With this data, shown in Figure 5.5, I concluded that VSV-G pseudotyping facilitates moderate improvements in infectivity in viruses containing MA substitutions E99V or E99K.

Next, I sought to analyze the fusion capacities of these VSV-G pseudotyped particles. Proviral clones pLAI-ΔEnv, pE99V-ΔEnv, pE99KΔEnv, pK32EΔEnv or pL13EΔEnv were cotransfected into 293T cells, along with the BLaM-Vpr expression construct, and the VSV-G vector, as described in Materials and Methods. At 24 hours and 48 hours after the transfection, virus-containing supernatants were harvested and normalized according to RT content. Equal titers of each virus were used to infect TZM-bl cells, and virus-cell fusion was monitored as described previously in Figure 3.7.

Results from this fusion assay are shown in Figure 5.6. Despite only a partial rescue in infectivity, I found that the fusion capacity for VSV-G-E99V-ΔEnv or VSV-G-E99K-ΔEnv with target cells was completely restored. In fact, BLaM activity in cells infected with VSV-G-E99V-ΔEnv or VSV-G-E99K-ΔEnv was markedly higher than cells challenged with VSV-G-LAI-ΔEnv at each time point. Interestingly, I found that BLaM activity in cells challenged with VSV-G-K32E-ΔEnv or VSV-G-L13E-ΔEnv, while consistently above background, did not reach the levels observed in cells challenged with VSV-G-LAI-ΔEnv. However, the fusion capacity for VSV-G-L13E-ΔEnv was improved when compared to that of LAI-L13E particles. By contrast, the

virus-cell fusion for VSV-G-K32E-ΔEnv particles was not augmented when compared to that of LAI-K32E. Most important, these results reveal that although VSV-G pseudotyping could not fully rescue the E99V- and E99K- associated infectivity defects, it was able to completely reverse the E99V- and E99K- associated fusion defects. These findings were consistent with my Env truncation data, as they suggest the existence of a post-fusion restriction to particles bearing the E99V or E99K MA mutations.

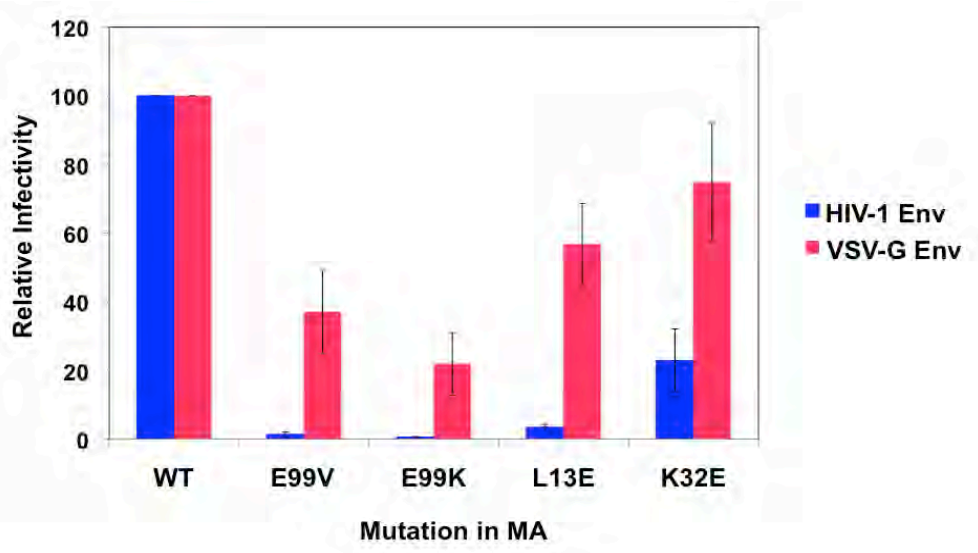

Figure 5.4 Single-cycle infectivities of LAI-derived MA mutants, containing either WT HIV-1 Env, or pseudotyped with VSV-G. Pseudotyped virus was generated by co-transfection of a pLAI-based Env deficient proviral clone and an expression plasmid encoding the VSV-G heterologous envelope. Infectivity was monitored 24 hours post-infection using the Beta-Glo® reporter assay, as described in Figure 3.4. The assessment of infectivity for each mutant virus is based on the level of LAI-WT (**blue bars**, 10K RTU/well) or VSV-G-LAI-ΔEnv (**red bars**, inoculated at 2.5 RTU/well), which represents 100% infectivity. Data is the average of four independent experiments performed in duplicate.

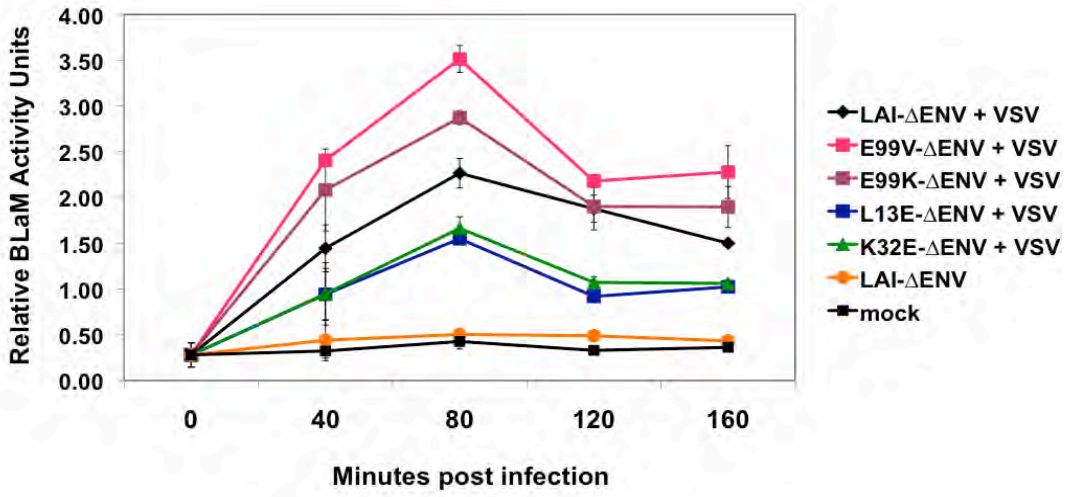

Figure 5.5 Effects of VSV-G pseudotyping on virus-cell membrane fusion capacity in LAI-derived viruses bearing MA substitutions. Fusion events of VSV-G-pseudotyped particles were assayed in TZM-bl cells as described in Figure 3.7. The data shown is representative of three independent experiments performed in duplicate.

To further analyze the post-entry step that may be interrupted by the E99 MA mutations, I investigated the extent to which the VSV-G-E99V-ΔEnv particles were competent for reverse transcription. Proviral clones pLAI-ΔEnv and pE99V-ΔEnv were individually transfected into 293T cells with an expression vector encoding VSV-G. Virus-containing supernatants were harvested 24 and 48 hours post-transfection as before, and then normalized by RT content. DNase-treated virus was then used to infect MT-4 cell cultures. At the indicated time points, cells were harvested, and total DNA was extracted. Specific primers were used to quantify EPs and CCR5 copy number, as in the PCR analysis of the previous section. The data, shown in Figure 5.7A, is presented as copies of EP per million cells. EPs were detected in both cultures, and while the levels were lower in the VSV-G-E99V-ΔEnv infected cells compared to those from the VSV-G-LAI-ΔEnv infections, the values increased over time. These data agree with the partial rescue observed with the infectivity assays.

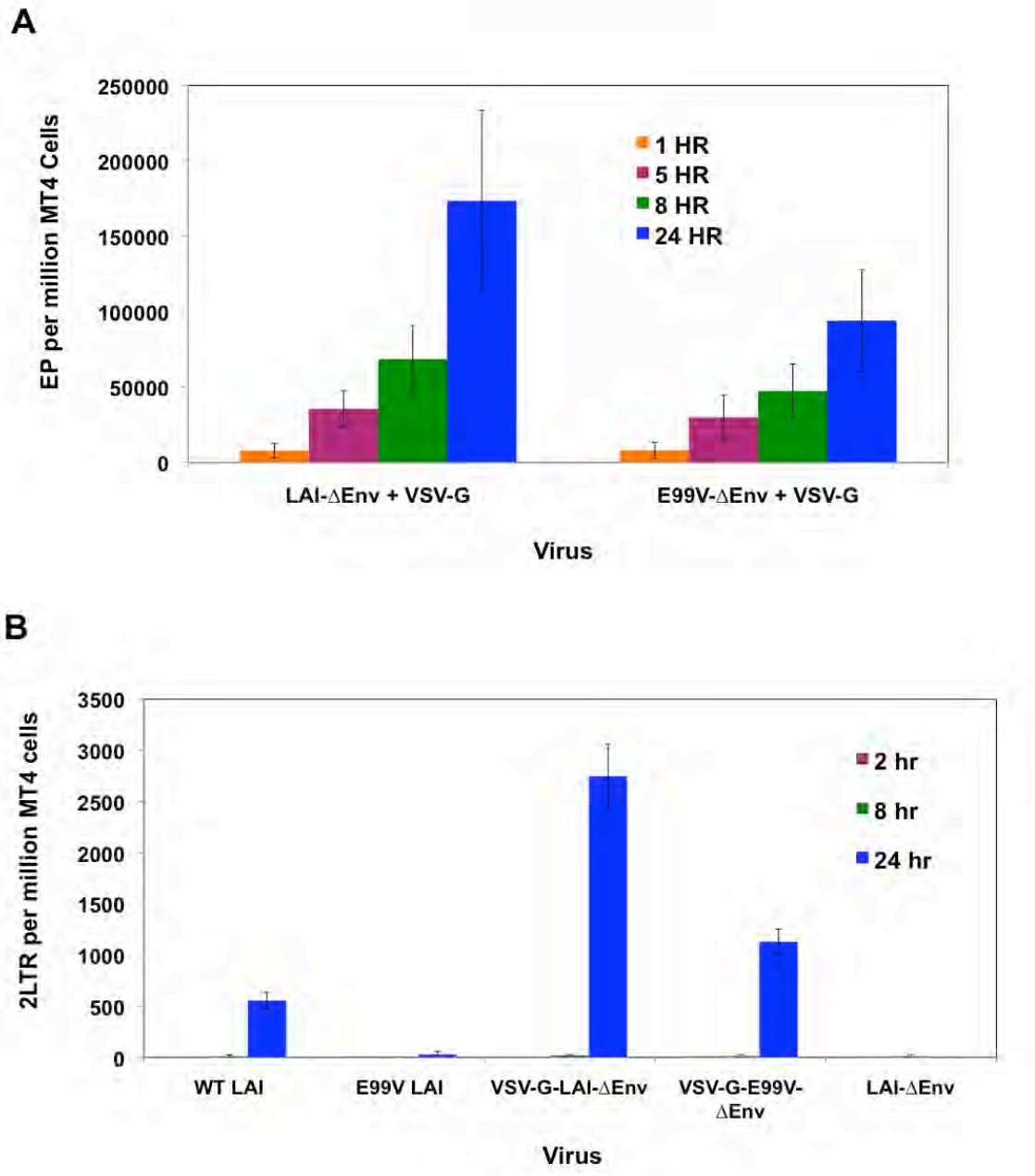

Figure 5.6 Analysis of reverse transcription products in cells infected with VSV-G-pseudotyped MA mutants. MT-4 cells were infected with equal RT units of LAI-derived MA mutants containing WT HIV-1 Env, or pseudotyped with VSV-G. At the specified times post-infection, cells were lysed and total

DNA was extracted. **(A)** EPs were directly quantified by real-time PCR, using primers specific for strong-stop viral DNA. Data was normalized by quantification of the cellular CCR5 gene in each sample. Data shown are the mean of two separate experiments performed in duplicate. **(B)** 2LTR circles were directly quantified by real-time PCR, using primers specific for the HIV-1 LTR-LTR junction. Data was normalized by quantification of the cellular CCR5 gene in each sample. Data shown are the mean of two separate experiments performed in duplicate.

Next I analyzed the production of 2LTR circles in infected cells. 2LTR circles are a form of viral DNA found only in the nucleus of cells. Although they are dead-end products of reverse transcription and cannot be integrated into the host cell genome, their detection in infected cells is a useful marker for the successful completion of reverse transcription and nuclear import (23, 27). MT-4 cells were incubated with LAI-WT, LAI-E99V, LAI-ΔEnv, VSV-G-LAI-ΔEnv and VSV-G-E99V-ΔEnv particles. Infected cells were collected at 2, 8 and 24 hours and then total DNA was extracted from each sample. Q-PCR was performed, using primers to specifically amplify the LTR-LTR junction used to identify 2LTR circles. The data was normalized according to CCR5 copy numbers, and is presented in Figure 5.7B as 2LTR circles per million cells. By 24 hours, cells from the LAI-ΔEnv or LAI-E99V infections gave no signal, while significant levels of 2LTR circles were detected in the LAI-WT infection, findings that correlate with my previous infectivity data. Most important, 2LTR circles were also present in the VSV-G-E99V-ΔEnv infection at levels that correlate to the partial rescue observed with the single-cycle reporter assay. Overall, the detection of both EPs and 2LTR circles in cells infected with VSV-G-E99V-ΔEnv supports my hypothesis that VSV-G pseudotyping confers a partial rescue of the post-fusion block imposed by the E99V MA mutation.

5.3 Discussion

Here, I employed single-cycle infectivity, fusion, and PCR assays to determine whether restoring the incorporation of a functional envelope is sufficient to reverse the infectivity defects conferred by the E99V or E99K MA mutations in HIV-1 particles. My results from the BLaM fusion assays indicate that truncation of the HIV-1 gp41 CT, or

pseudotyping with VSV-G were sufficient methods to restore the fusion capacities of HIV-1 viruses containing the E99V or E99K MA substitutions. However, my infectivity data suggests that the specific route of entry utilized by the virus is critical for reinstating infectivity in these viruses. I found that when particles were permitted to fuse at the PM of a target cell, the infectivity defects imposed by the E99V or E99K MA mutations were not reversed. By qPCR, I determined that E99V-Δ144 particles were unable to initiate reverse transcription, which suggests the presence of an early, post-fusion restriction inside cells. Conversely, my results demonstrated that this putative post-entry block was partially bypassed when virus entry was shunted through an endosomal route, as facilitated by VSV-G pseudotyping. It has been speculated that this alternate delivery method could protect the virus from certain entry- and post-entry restrictions that would be encountered if fusion were to occur at the PM. Indeed, this partial rescue was confirmed with detection of early products and 2LTR circles in VSV-G-E99V-ΔEnv infected cells. Since VSV-G-mediated fusion would not bypass a restriction at nuclear import or integration, I speculate that this post-entry defect must be encountered soon after fusion with the PM.

My results were validated with parallel studies analyzing rescues of previously characterized MA mutations. Consistent with earlier reports, I observed that Env truncation and VSV-G pseudotyping were sufficient modes of restoring infectivity defects imposed by L13E or K32E MA mutations (72, 111). This suggests that a disruption in Env incorporation during particle assembly is the only, or at least the most prominent, defect imposed by the L13E and K32E MA mutations. However, since these

methods failed to completely restore the infectivity defects associated with the E99V and E99K substitutions, I conclude that in addition to a role in Env incorporation, the glutamate at MA residue 99 is critical for an early, post-fusion function of MA. A summary of the findings from this chapter are shown in Table 5.4.

MA has previously been implicated in a number of post-entry steps, including uncoating, reverse transcription, PIC migration, nuclear import and even integration (23, 31, 72, 88, 101, 104, 166, 198, 213). It is possible that MA E99 has a specific role in facilitating one or more of these early steps, such as engaging with a cellular cofactor or a virally encoded protein in the HIV core. Another possibility is that E99 could be important for the dissociation of MA molecules from the PM, either by a direct mechanism or through an indirect one, such as promoting a MA conformation that sequesters the myristoyl moiety. Such a disruption in MA membrane detachment during early events could have several consequences that might prevent productive infection of the particle. For example, MA has been shown to associate with the viral core, and failing to dissociate from the PM could tether the complex to the membrane, and in turn inhibit proper trafficking of the reverse transcription complex (RTC) towards the nucleus. Such membrane adherence may prevent critical interactions with the cytoskeleton, which could be detrimental for efficient nuclear migration. Moreover, an association between the RTC and actin filaments has been linked to efficient reverse transcription (21). Another possibility is that proper capsid uncoating could be linked to the location of the complex within the cell, and membrane tethering of the viral core might impair the uncoating step.

Finally, one might imagine that such sequestration at the cell's periphery could expose the viral core to cellular degradative pathways.

Table 5.4 Summary of Results from Chapter 5

Virus	Assay Performed				
	Virus-Cell Fusion	Early Products	2LTR Circles	Single-Cycle Infectivity	Spreading Infection
LAI-Δ144	++++	++++	++++ (NS)	++++	++++
E99V-Δ144	+++++	+	+ (NS)	+	+
E99K-Δ144	+++++	ND	ND	+	ND
K32E-Δ144	+++++	ND	ND	+++	ND
L13E-Δ144	+++++	ND	ND	+++++	ND
VSV-G-LAI-ΔEnv	++++	++++	++++	++++	ND
VSV-G-E99V-ΔEnv	+++++	+++	++	++	ND
VSV-G-E99K-ΔEnv	+++++	ND	ND	+	ND
VSV-G-K32E-ΔEnv	++	ND	ND	+++	ND
VSV-G-L13E-ΔEnv	++	ND	ND	++	ND

+++++	better than WT	++	25-60% of WT
++++	90-100% of WT	+	5-25% of WT
+++	60-90% of WT	-	0-5% of WT

The different viruses analyzed in this chapter are listed in the left hand column. The assays performed and individual findings relative to results from the wild-type parental virus are indicated. Single-cycle infectivity was determined 24 hours post-infection. Relative Env incorporation was approximated by Western blot using anti-gp41 mAb (Chessie 8). Spreading infection was analyzed in MT-4 cells. EP and 2LTR circle data represents the 24-hour time point. ND = assay not done. NS = assay performed but results not shown.

Indeed, it has been suggested that the membrane affinity of MA must be precisely balanced to facilitate its roles in early and late phases of the HIV-1 life cycle (151, 170). One study speculated that in particular, the N-terminal region of the MA fifth helix exerts a negative affect on the overall membrane affinity of MA (151). Structural studies have suggested that the N-terminal region of this C-terminal helix lies in proximity with the PM (4, 93). Therefore, I propose that the polar, negatively charged glutamate at residue 99, which happens to lie within this precise location of the molecule, may be critical in antagonizing this membrane affinity. In agreement with this hypothesis is the finding that both valine and lysine substitutions disrupt this post-fusion role for MA. It is likely that valine, a large hydrophobic amino acid, would enhance the overall hydrophobicity of the MA C-terminal helix and thereby promote membrane affinity. Similarly, the positively charged lysine could increase membrane association by interacting with negatively charged phospholipids embedded in the cell's PM. In Chapter 3 (section 3.2.2), I also showed that substitution of this glutamate with aspartate, glycine or alanine (mutations E99D, E99G and E99A) did not reduce virus infectivity. These findings might be explained by the presence of other residues in the MA C-terminal helix that are also important in antagonizing MA membrane affinity, and these substitutions (E99D, E99G or E99A) may either be too conservative or not strong enough to negate the membrane disassociation properties of proximal residues. Based on these speculations, I would propose that other substitutions of residue 99, such as glutamate for arginine, phenylalanine, isoleucine or leucine (E99R, E99F, E99I or E99L), would also impart a post-entry defect in viruses that have an Env truncation.

CHAPTER VI: DEVELOPMENT OF AN ASSAY TO MONITOR RTC TRAFFICKING IN INFECTED CELLS

6.1 Introduction

In Chapter 5, I demonstrated that in addition to an Env incorporation defect, the E99V and E99K MA mutations might also confer post-entry blocks to productive infection. My results using a mutant with a truncated Env (E99V-Δ144) suggested that this defect likely occurs prior to the reverse transcription step (refer to Figure 5.2.1). Interestingly, a similar phenotype was observed when wild-type virus was incubated with H9 cells expressing siRNAs that knockdown the Arp2/3 actin-nucleator complex, a structure necessary for the polymerization of actin microfilaments (107). This result is consistent with another study, which indicated that virus interaction with the actin microfilaments alone might stimulate efficient reverse transcription (21). In addition, fluorescent imaging techniques have indicated that the RT complex (RTC) likely uses microtubules to move long distances within the cell (129). Thus, it appears that an association with the cytoskeleton during early events might be crucial for the productive infection of HIV-1. Although the viral proteins that interact with host-cell transport machinery at this step are unknown, MA is a candidate (21, 201). Therefore, it is possible that the E99V and E99K MA mutations might interrupt RTC interaction with the host cytoskeletal system, thwarting proper intracellular trafficking of the complex. The accumulation of these mutant RTCs at the PM, or inside a subcellular compartment, may then inhibit viral DNA synthesis, ultimately blocking infection.

A variety of techniques have been established to monitor the progress of many early events of the retroviral life cycle. However, a standard assay for evaluating whether retroviral RTCs are competent for migration through the cell to the nucleus is lacking. As a result, the pathways that nucleoprotein complexes follow after virus-cell fusion are not clearly defined. Such a technique might be useful for identifying viral proteins or cellular factors involved in the putative interaction between the RTC and the host cytoskeletal system. To address this, and to characterize the early block encountered by the E99V-Δ144 mutant virus, I sought to develop and validate a PCR-based method that would allow for the investigation of a possible defect in RTC nuclear trafficking.

6.2 Results

6.2.1 Experimental rationale and overview of the methods

The processes of HIV-1 reverse transcription and nuclear translocation are thought to proceed concurrently. However, nucleoprotein complexes can arrive at the host cell nucleus as early as 1 hour after infection (21), while reverse transcription of the viral RNA genome into DNA is generally completed in 8 to 12 hours (59). Therefore, it is likely that a vast majority of nuclear RTCs are undergoing reverse transcription (21). I reasoned that if viral RNA genomes (gRNA) could be extracted and quantified from different subcellular compartments within infected cells, then it would be possible to distinguish between normal and aberrant RTC trafficking based on different levels of RTCs over time.

My proposed methods are outlined in Figure 6.1. Cells are first incubated with equal amounts of virus at 4° C, which allows viral binding to the cellular receptors but not internalization. Next, the cells are moved to 37° C to permit synchronized entry of bound particles into the cells. Cells are then harvested and subjected to fractionation. Total RNA is extracted from each of the fractions containing different cellular components, and then HIV-1 gRNAs are reverse transcribed into cDNA using a primer specific for the full-length HIV-1 genome. Finally, quantitative PCR is used to quantify the cDNA copies in each sample.

6.2.2 Optimization of fractionation techniques

Originally, I intended to analyze RTC migration by comparing the quantity of gRNA in membranous, cytoskeletal, cytosolic and nuclear components of the cell. However, early attempts to do this consistently were unsuccessful, and it became clear that clean separation of these fractions would be critical to ensure the accuracy of my results. Therefore, I compared additional methods used for isolating nuclei from cytoplasmic extracts. For these experiments, I used the CD4+ HeLa-derived MAGI cell line as target cells, since their adherent nature would allow for uniform infection.

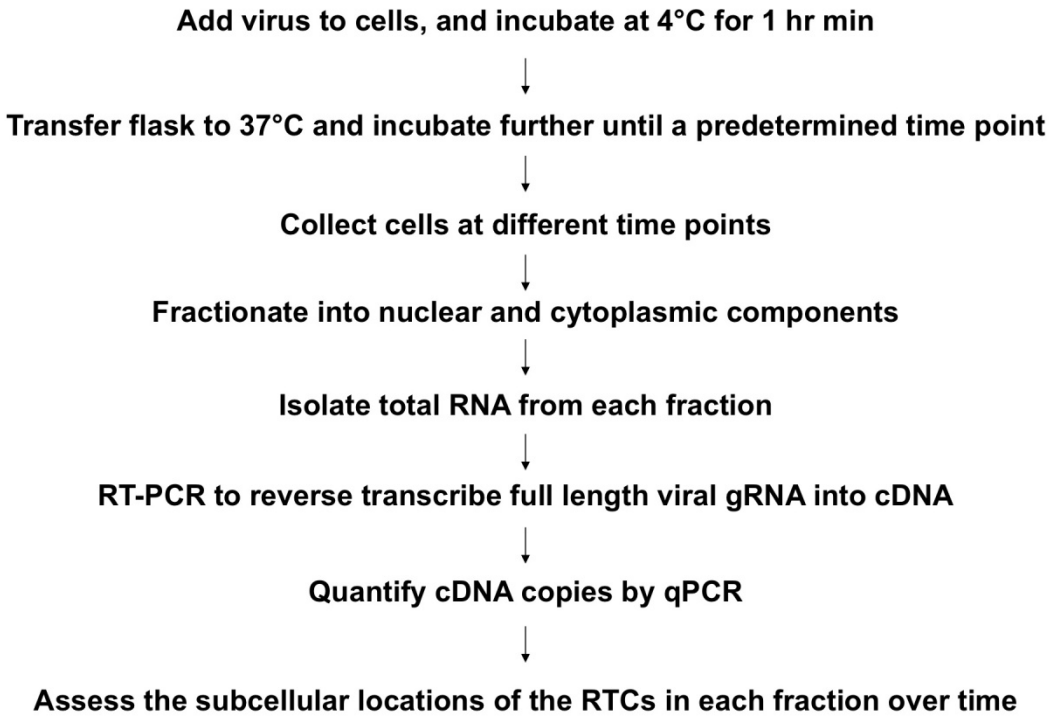

Figure 6.1 Schematic representation of the proposed RTC migration assay. Equal amounts of virus are added to cells, and virus-cell fusion events are synchronized by a one-hour pre-incubation at 4° C before moving the flasks to a 37° C incubator. After specified times, cells are harvested and fractionated. Total RNA is isolated from each of the cellular components, and then HIV-1 gRNAs are reverse transcribed into cDNA using a primer specific for the full-length viral genome. Finally, quantitative PCR is used to quantify the cDNA copies in each sample.

Initially, I compared mechanical disruption to chemical disruption of the cell. Both protocols called for an initial swelling of cells in hypotonic media. The mechanical protocol then involved 10-15 strokes with mini-dounce homogenizers to disrupt plasma membranes. The chemical technique used the nonionic detergent digitonin, which is reported to permeabilize cell membranes and mitochondria while preserving nuclei and most other organelles (134). After swelling, cell permeabilization was initiated upon exposure to a diluted digitonin solution. After thirty minutes on ice, the reaction was stopped by the addition of casein.

Nuclei were pelleted using centrifugation, and the cytoplasmic supernatants were carefully removed and transferred to another tube. Total protein content was calculated for each fraction using the BCA Protein Assay kit (Pierce) as directed, and extract purities were analyzed by Western blot. To distinguish between the two cellular components, a polyclonal antibody for Sam68 was used as a nuclear marker, and monoclonal antibodies specific for β-actin and pyruvate kinase were used as cytoplasmic determinants. In addition, I determined the integrity of the nuclear membrane with a monoclonal antibody directed against Nup62, a protein normally associated with the nuclear pore complex. In the resulting blots (Figure 6.2A), I found that nuclear extracts from both methods were enriched for Sam68, but only the pyruvate kinase antibody seemed to show specificity for the digitonin-derived cytoplasmic fraction. Although a significant amount of Nup62 was also detected in this extract, I cannot exclude the possibility that this was newly synthesized protein not yet inserted into the nuclear

envelope. Neither method was successful in isolating pure cellular components, however, since β-actin was detected in all samples.

Next, I tested a chemical-based protocol that used the nonionic, non-denaturing detergent Nonidet P-40 (NP-40). Although higher concentrations of NP-40 are often used to lyse both cellular and nuclear membranes, more dilute solutions are reported to permeabilize plasma membranes while keeping nuclear membranes intact (56). Cells were incubated in a 0.63% solution of NP-40 on ice with periodic vortexing. In parallel, I repeated the digitonin lysis protocol, using two different concentrations of digitonin. In the Western blot analysis of the resulting fractions, I used antibodies directed against HSP90 and GAPDH as cytoplasmic markers. The results, shown in Figure 6.2B, indicated that the NP-40 method generated cleaner fractions than either dilution of digitonin.

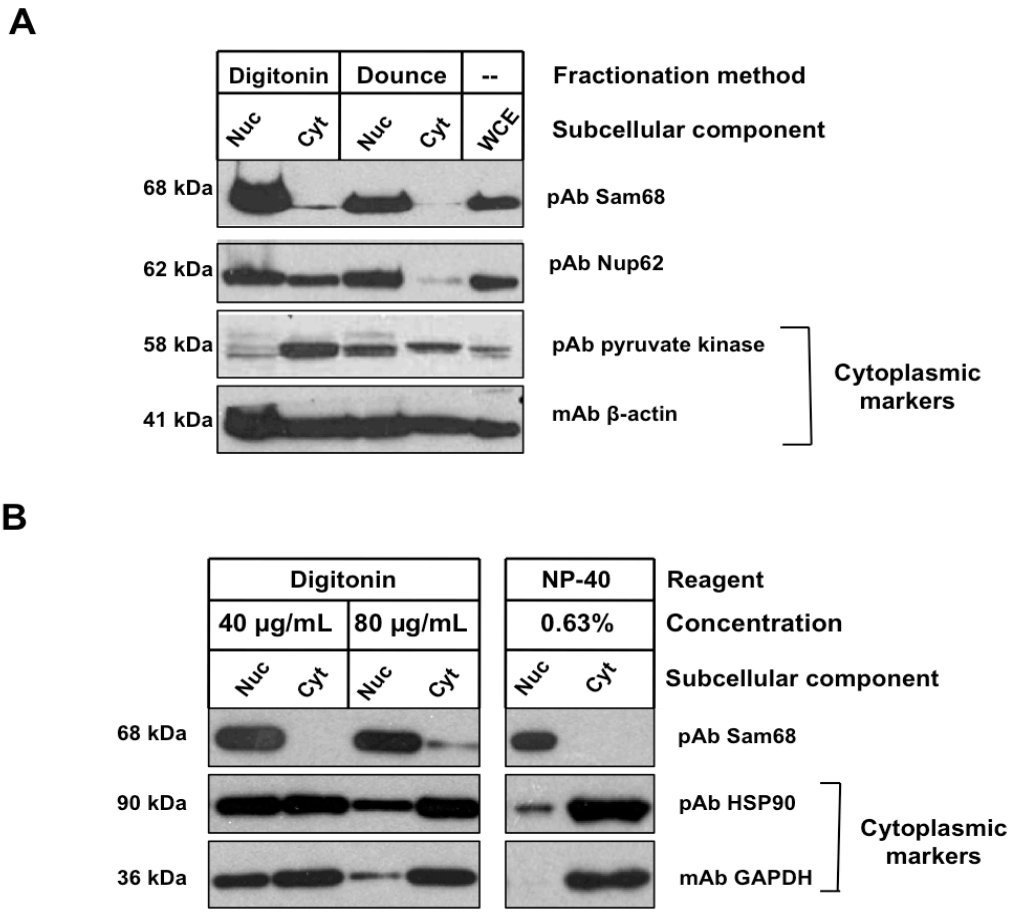

Figure 6.2 A comparison of the efficiencies of fractionation procedures designed for separating cytoplasm from intact nuclei. MAGI cells were subjected to dounce homogenization, digitonin treatment, or NP-40 exposure, and then centrifuged to separate the nuclei from cytoplasm, as described in the text. Equal µg of protein from each fraction, or from whole cell lysates, were separated by SDS-PAGE. Extract purity was analyzed by immunoblotting. **(A)** Comparison of dounce homogenization and digitonin treatment. Antibodies were directed against Sam68 (nuclear), Nup62 (nuclear envelope), pyruvate kinase (cytoplasmic), or β-actin (cytoplasmic). **(B)** Comparison of 40µg/mL or 80µg/mL

digitonin treatment, or 0.63% NP-40 exposure. Antibodies were directed against Sam68 (nuclear), HSP90 (cytoplasmic), or GAPDH (cytoplasmic).

To further optimize the NP-40 method, fractionations made with a variety of dilutions of NP-40 were compared. Western blot analysis indicated that each of the cellular component fractions were pure using all but the GAPDH-specific antibodies (Figure 6.3A). The GAPDH blot suggested that some cytoplasmic proteins were contaminating the nuclei pellets. This experiment was unable to distinguish whether the contaminating GAPDH was due to small amounts of cytoplasm that had carried over after the centrifugation step, or incompletely lysed cells that had been pelleted down with the nuclei. To distinguish between these two possibilities, I repeated the experiment using the 0.6% and 0.9% NP-40 solutions and compared the purities of washed and unwashed nuclei at each concentration. As shown in Figure 6.3B, washing the intact nuclei in 1X PBS reduced cytoplasmic contamination, as indicated by the markers HSP90
and GAPDH, without significantly lowering Sam68 levels. These results demonstrated that contamination of the nuclear fractions was due to carry over of soluble cellular components, and not inefficient cell lysis.

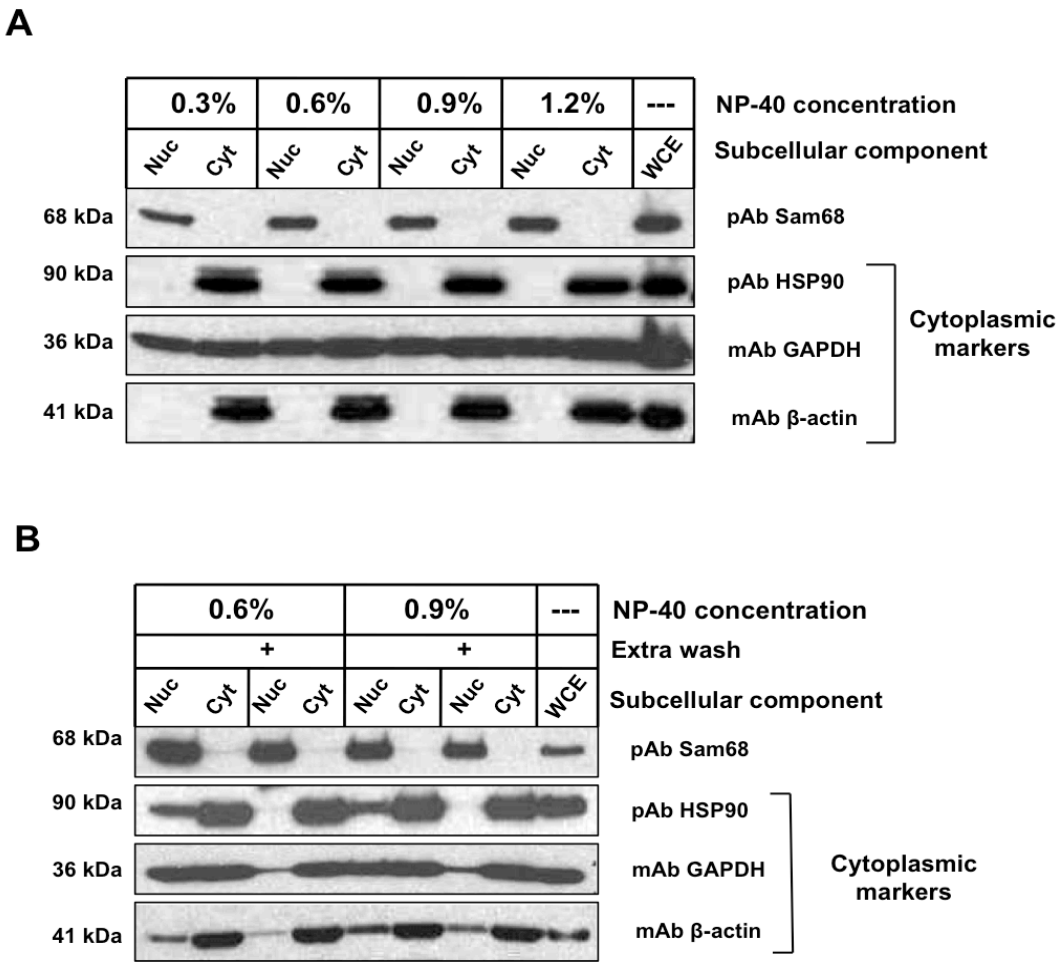

Figure 6.3 Optimization of the NP-40 fractionation method. MAGI cells were treated with the indicated concentrations of NP-40, and then nuclear and cytoplasmic fractions were prepared as described in the text. Equal μg of protein were separated by SDS-PAGE and analyzed by immunoblotting with antibodies directed against Sam68 (nuclear), HSP90 (cytoplasmic), GAPDH (cytoplasmic) or β-actin (cytoplasmic). **(A)** Cells were exposed to 0.3%, 0.6%, 0.9%, or 1.2% NP-40 solutions. **(B)** Cells were exposed to 0.6% or 0.9% NP-40 solutions, and then intact nuclei were isolated and either washed with 1X PBS (lanes 3 and 7) or left unwashed (lanes 1 and 5).

6.2.3 Characterization of positive and negative controls

Although VSV-G pseudotyping is known to enable a more efficient infection of HIV-1 particles than those with wild-type HIV Env, I wanted to ensure the physiological relevance of HIV particle trafficking observed with this assay. Therefore, I decided to use non-pseudotyped LAI-WT as my positive control. For negative controls, I used LAI-ΔEnv, as well as exogenously-added soluble CD4 (sCD4) to inhibit LAI-WT infection.

During HIV-1 infection, the majority of viral particles are internalized into cells via endocytosis. Although a portion of these endocytosed particles may indeed fuse and be competent for infection (133), I decided that limiting endocytic internalization was necessary to reduce any background from the non-specific recycling of particles in and out of the cells. Therefore, I chose to perform the infections in media containing 0.45 M sucrose, which is known to block endocytosis of ligands and receptors (159).

MAGI cells were cultured in T-25 flasks until about 80-90% confluency. The media was removed and cold virus was added to each culture, one flask for each time point. Virus-receptor binding, but not internalization, was permitted by the pre-incubation of cells at 4°C for one hour. Every 5 minutes, the flasks were manually rocked back and forth, to enhance virus-cell binding efficiency. After one hour, the supernatant was removed and fusion events were synchronized with the addition of pre-warmed, sucrose-containing media. The flasks were then placed in a 37° C incubator. Because sucrose can be toxic to cells upon sustained exposure (159), I replaced the hypertonic media with normal media after 20 minutes. Cells were further incubated at 37° C for either 25 or 160 minutes.

Cells were harvested, washed and divided into two aliquots. One aliquot was stored for subsequent extraction of total cellular DNA. The other aliquot was fractionated using 0.6% NP-40. Total cellular RNA was isolated from the nuclear and cytoplasmic extracts using the RNeasy kit (Qiagen) as directed. RNA from each sample was then subjected to RT-PCR using the Superscript 1st Strand System kit (Invitrogen), and a primer specific for the 5' end of the viral genome (primer BB). This region was targeted because it is the last portion to be destroyed by RNase H during reverse transcription in the cell. To validate the specificity of the PCR, I also set up reactions omitting the RT enzyme. I quantified the cDNA products with qPCR, using primers W and LA17/r, and a probe that targeted a region between these qPCR primers. The data was then normalized by quantifying CCR5 gene copy number in the total DNA extracted from the aliquot of unfractionated cells. The primers and probe that targeted the HIV-1 genome are depicted in Figure 6.4.

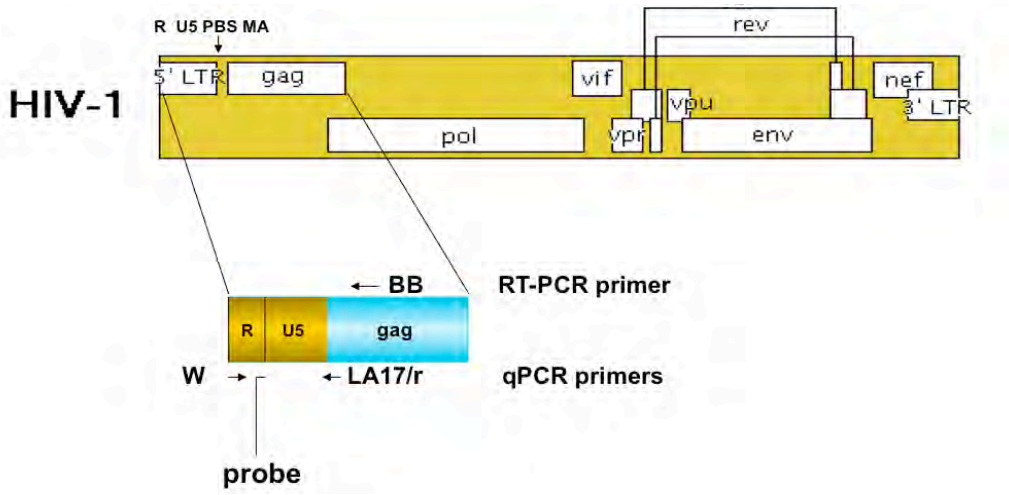

Figure 6.4 A schematic representation of the locations in the HIV-1 genome targeted by the RT-PCR and qPCR steps. Primer BB, located in Gag was used to generate cDNA from HIV-1 gRNA. Since this region is the last part of the genome to be degraded by the RNase H activity of RT, window of detection is maximized. Primers W and LA17/r, targeting sequences in R and Gag respectively, were used to amplify and quantitate cDNA molecules from each sample. The probe selectively binds to a region in U5.

The results from this experiment are shown in Figure 6.5. The lack of detectable cDNA in any of the no-RT controls, demonstrated that the quantified cDNA copies in other samples represented gRNA extracted from cells. As expected, cells infected with the LAI-ΔEnv virus had fewer gRNA copies than infection with WT virus. Addition of sCD4, however, did little to inhibit infection by WT-LAI. Control experiments indicated that, by 2LTR circle analysis, sCD4 was effective in inhibiting WT-LAI infection in MAGI cells (data not shown). Therefore, it is unclear why efficient entry and migration events occurred in the LAI-WT/sCD4 samples in this assay.

A significantly greater number of gRNA was detected in the cytoplasmic fraction compared to the nuclear preparation from each infection condition. This finding may be evidence of the limited number of viral cores that successfully reach the nucleus after fusion into the cell. I also detected an increase in cytoplasmic-associated gRNA, and a reduction in nuclear-associated gRNA, over time, which may indicate incomplete synchronization of fusion events. It was also possible that delayed fusion was an unintended consequence of the sucrose exposure. I also considered that the decrease in nuclear gRNA at the later time point might be from its degradation by RNase H activity.

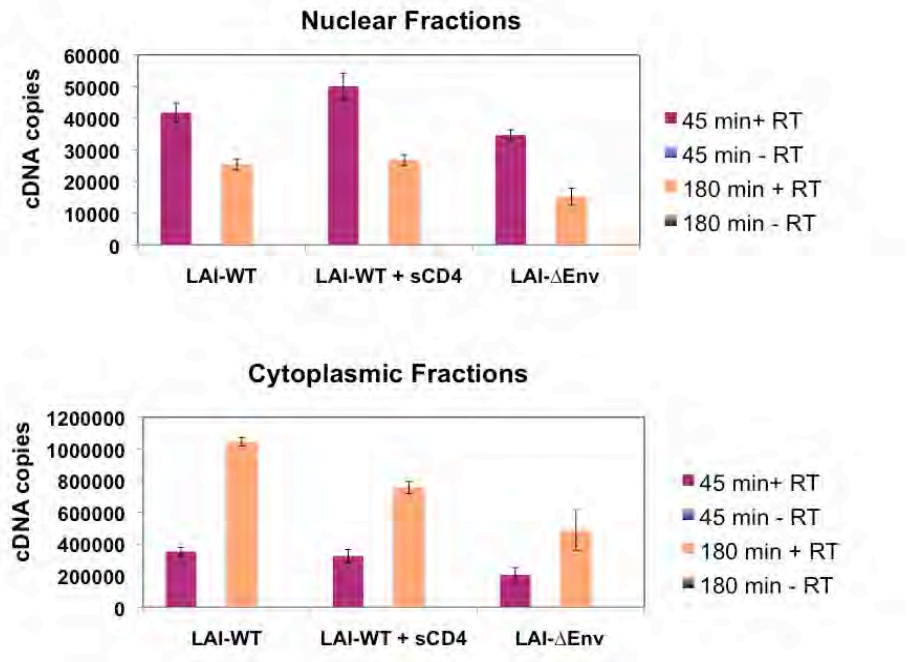

Figure 6.5 Analysis of potential positive and negative controls in the RTC migration assay. Distribution of RTCs in nuclear **(top graph)** or cytoplasmic **(bottom graph)** fractions of MAGI cells infected with equal RT units of LAI-WT, LAI-WT in the presence of soluble CD4 (sCD4), or LAI-ΔEnv. Cells were incubated for 1 hour at 4 °C, followed by 45 or 180 minutes at 37 °C. Endocytosis was inhibited with 0.45 M sucrose added to the cell culture media for the first 20 minutes of the 37 °C incubation. Cells were harvested, washed and then exposed to 0.6% NP-40 before centrifugation at 6500 RPM. Intact nuclei were washed after separation from the cytoplasmic supernatant. RNA from each sample was then subjected to standard RT-PCR using primer BB. Control reactions were performed in parallel in the absence of reverse transcriptase. The cDNA product was quantified in duplicate wells by qPCR using primers W and LA17/r. +RT = reaction performed in the presence of reverse transcriptase, -RT = control reaction performed in the absence of reverse transcriptase.

Although fewer gRNA copies were detected in LAI-ΔEnv infected cells than in those infected with LAI-WT, I still detected a substantial amount of viral RNA in the nuclei of LAI-ΔEnv infected cells. 2LTR analysis had determined that LAI-ΔEnv was not competent for a productive infection (data not shown), but incomplete washing of the cells after harvesting may have lead to contamination by residual free or receptor-bound virus.

6.2.4 Effectiveness of endocytosis inhibition

To evaluate the degree to which 0.45 M sucrose prevented endocytosis, I compared both LAI-WT and LAI-ΔEnv infections in the presence or absence of sucrose. Higher amounts of gRNA were detected in the cytoplasmic fractions of cells not exposed to sucrose, compared to those exposed to sucrose (Figure 6.6), consistent with the known ability of sucrose to limit entry of endocytosed virus (159). In the LAI-WT infection, the peak number of cytoplasmic gRNA was occurred at 90 minutes post-infection in the presence of sucrose, whereas peak cytoplasmic gRNA was detected at 30 minutes post-infection when endocytosis was permitted. These results suggest that sucrose may confer a delay in fusion, which may reflect the time needed by cells to recover from hypertonic media exposure. Conversely, it may indicate that the majority of endocytic entry events occur prior to membrane fusion, at which time other processes required for efficient membrane fusion, such as specific intracellular signaling, might also be taking place.

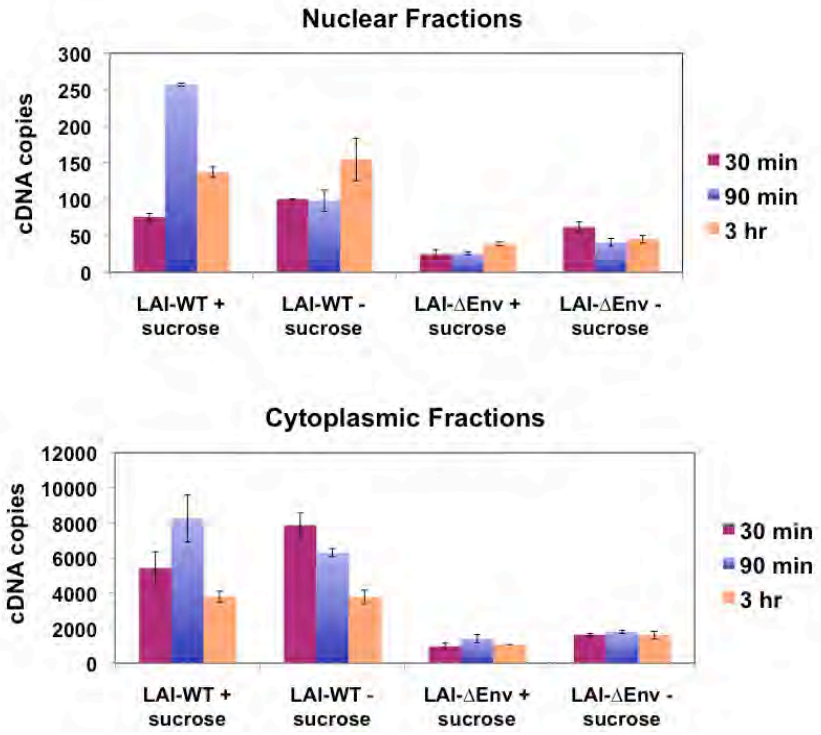

Figure 6.6 The effect of sucrose exposure on blocking virus endocytosis. Distribution of RTCs in nuclear **(top graph)** or cytoplasmic **(bottom graph)** fractions of cells infected with LAI-WT or LAI-ΔEnv, as described above, with or without the 20-minute sucrose incubation. Cells were harvested at 30 minutes, 90 minutes, or 3 hours post-infection.

Nuclear-associated gRNA peaked at 90 minutes in the presence of sucrose but was highest at 3 hours without sucrose during LAI-WT infection (Figure 6.6). This suggests that limiting endocytosis may enhance the efficiency of RTC trafficking, despite the corresponding delay in membrane fusion.

Since prolonged sucrose exposure can be toxic to cells, I also used dynasore (Sigma) to inhibit endocytosis. Dynasore is a small molecule GTPase inhibitor that blocks dynamin-dependent endocytosis, and its use is associated with less cytotoxicity than observed with other reagents (106). Cells were infected with LAI-WT virus in the presence of either 0.45 M sucrose, or 80 μM dynasore, and then harvested 45 or 180 minutes post-infection. The qPCR data suggested that dynasore was far more effective than sucrose in limiting endocytic entry of virus (Figure 6.7), however the use of dynasore also reduced cell recovery during harvesting. I therefore concluded that sucrose was less toxic and therefore better suited than dynasore in this assay.

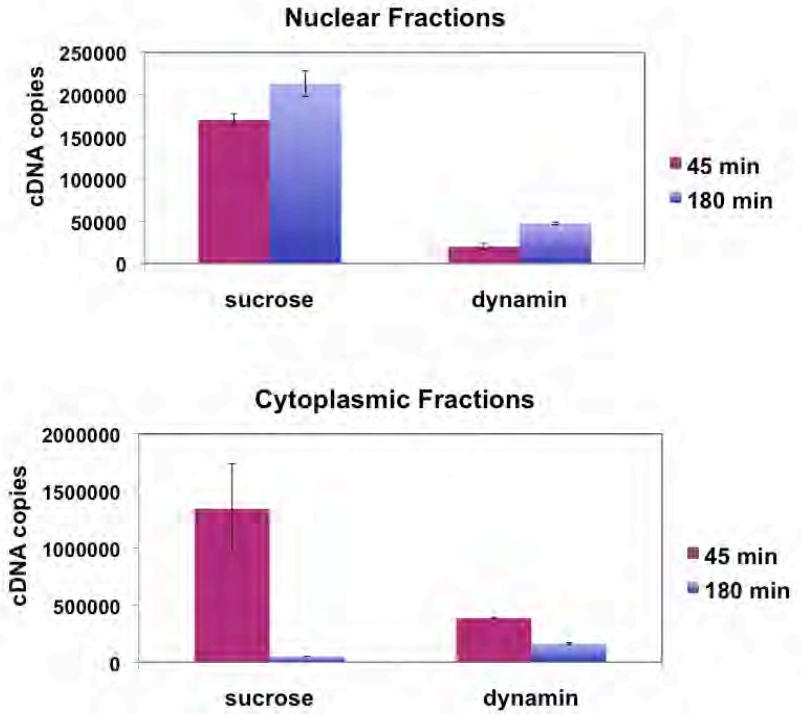

Figure 6.7 Comparison of two methods for inhibiting endocytosis. Distribution of RTCs in nuclear **(top graph)** or cytoplasmic **(bottom graph)** fractions of cells infected with equal RT units of LAI-WT, in the presence of either 0.45 M sucrose or 80 μM dynasore, at two time points. Sucrose was washed away after 20 minutes whereas the dynasore concentration was kept constant throughout the infection. Cells were harvested 45 or 180 minutes post-infection.

6.2.5 RTC trafficking in the absence of reverse transcription

While previous studies have demonstrated that efficient reverse transcription is dependent on cytoskeletal interactions (21), it is unclear whether efficient trafficking events require reverse transcription. I therefore tested whether intracellular RTC migration could proceed in the absence of efficient reverse transcription, using the RT inhibitor AZT. As a thymidine analog, AZT is incorporated into cDNA by the viral RT enzyme. Its insertion prevents further strand synthesis as the compound lacks the 3'OH group required for cDNA elongation. I incubated MAGI cells with media containing 10 μM AZT for two hours before the addition of virus, after which the infection protocol preceded as above. The trafficking profile of cytoplasmic RTCs was similar with and without AZT (Figure 6.8), consistent with its inhibitory effects occurring independently of virus entry. On the other hand, in the absence of AZT, nuclear gRNA quantities reached a high point at 90 minutes and its peak at 24 hours. The two peaks likely reflected RTC migration to the nucleus and the synthesis of new viral genomes, respectively. Reduced gRNA detected in the cytoplasmic fraction at 24 hours, suggested that the majority of unspliced viral RNA is translated and degraded by this time, as opposed to being stabilized for packaging into nascent particles. In contrast, gRNA decreased over time in the nuclear fraction of cells infected in AZT-containing media. This observation is consistent with a role for the central DNA flap in nuclear targeting and likely represents reduced efficiency of RTC nuclear entry in the absence of reverse transcription.

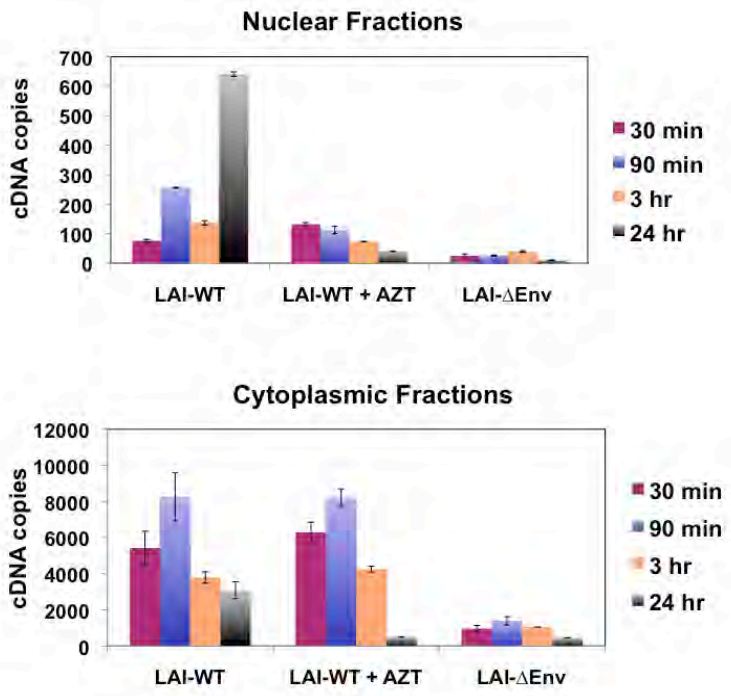

Figure 6.8 Analysis of RTC migration in the absence of efficient reverse transcription. Distribution of RTCs in nuclear **(top graph)** or cytoplasmic **(bottom graph)** fractions of cells infected with LAI-ΔEnv, or LAI-WT virus in the presence or absence of 10 μM AZT. Cells were harvested at 30 minutes, 90 minutes, 3 hours or 24 hours post-infection.

6.3 Discussion

The development of additional techniques for identifying and characterizing the post-entry steps required for a productive retroviral infection is crucial for the advancement of HIV research. My efforts in developing a technique to monitor RTC trafficking is one important step in addressing this technical gap, though further optimization is required.

In addition to the experiments described above, I also evaluated various cell harvesting techniques. I found that trypsin exposure was the safest and most consistent way to harvest intact cells, compared to scraping with a plastic or rubber scraper. As small differences in cell recovery could confound my results, and I also tested ways to normalize the data. In one experiment, I analyzed gRNA in the unfractionated cells, instead of CCR5 copy number. cDNA copies in each fraction were then compared to the total number of cDNA copies quantified in whole cell lysates. Final gRNA equivalent numbers were then reported as a percentage of total cDNA per cell. Unfortunately, my results were inconsistent and in some cases total cDNA content from the fractionated samples far exceeded that extracted from unfractionated cells.

I also recognize fundamental limitations of the experimental design, as described here. This study was conceived of prior to 2009, when it was widely believed that endocytosed virus was unable to fuse and productively infect cells. I therefore found it appropriate to inhibit endocytic internalization events. However, a study published by Miyauchi and colleagues in 2009 demonstrated that productive infection does in fact occur by HIV-1 fusion within endosomes, and that this may even be the predominant

mode of entry in some cell types (133). Considering my data in light of these recent findings, I speculate that reducing endocytosis may have diminished the efficiency of infections, which could minimize the validity of my results. While RTC migration defects may certainly arise in some mutants, a mutation that prevents proper mobility through the cortical actin layer at the cell periphery might be overcome by delivery of the viral core within an endosome.

Finally, another limitation that might confound interpretation of the data is the RNase H function of RT. Since RNase H degrades the viral RNA during reverse transcription, viral genomic RNA may not be a proper marker for RTC migration in this assay. It is likely that many RTCs in the nucleus are still undergoing reverse transcription at earlier time points, however the inevitable destruction of gRNA obscures the analysis of low cDNA copies from cells harvested at later time points. For example, the detection of low nuclear-associated gRNA at later time points may reflect aberrant nuclear trafficking of complexes, or more efficient reverse transcription. Therefore, more rigorous testing is needed to define the optimal times post-infection for analyzing migration. The ideal window would be after a high number of RTCs reach the nucleus, but before RNase H activity degrades a significant portion of the nuclear associated gRNAs. To define this window, one might analyze the RTC migration of an RNase H mutant virus. A 1999 study identified the P236L mutation in the RNase H domain of RT in inhibiting RNase H activity in HIV-1 particles (79). However, one must determine whether defective RNase H activity negatively impacts RTC trafficking.

CHAPTER VII: DISCUSSION

7.1 Summary of results

The results from this thesis implicate E99, a glutamate residue located in the C-terminal helix of the HIV-1 MA protein, in Env incorporation during particle assembly as well as early post-entry steps. I demonstrated that virus particles bearing a substitution of this glutamate by either a valine (E99V) or lysine (E99K) are devoid of Env proteins and unable to fuse with target cell membranes. More conservative substitutions of this residue, such as aspartate, glycine or alanine (E99D, E99G or E99A) do not confer any substantial changes in Env incorporation or infectivity. Comparing the extent of infectivity defects in particles bearing the E99V or E99K substitutions to previously published MA mutants L13E, L21K or K32E, suggested that residue E99 plays a more important role in virus infection. I used a genetic approach to identify a second-site mutation in MA, T84V, which successfully rescued the Env incorporation, fusion, and infectivity impairments associated with the E99V or E99K substitutions. However, the degree to which a valine at position 84 rescued mutations at position 99 depended on the particular residue that replace E99 and the particular virus strain in which it was expressed. I also utilized a MA-independent method to facilitate the incorporation of various envelope proteins into virus particles that contained the E99V or E99K MA mutations. Although one approach, truncation of the HIV-1 gp41 protein, successfully restored virus-cell fusion at the cell's plasma membrane, it was not sufficient to reverse the infectivity defects incurred by the E99V or E99K MA mutations. A lack of viral DNA in these cells indicated that HIV-1 cores were unable to initiate reverse transcription after

entry. Interestingly, pseudotyping E99V- or E99K- containing particles with VSV-G, which mediates virus-cell fusion events by a pH-dependent endosomal route, was able to partially rescue the reverse transcription and infectivity impairments. Therefore, in addition to mediating Env incorporation during nascent HIV particle assembly, MA residue E99 is also critical in early, post-entry functions of the protein. Finally, I addressed the lack of methods available for analyzing early events of the retroviral life cycle. Specifically, I developed a novel technique for distinguishing between aberrant and successful trafficking of reverse transcription complexes (RTCs) after entry.

7.2 Potential mechanism for E99 in Env incorporation

The mechanism for HIV-1 Env incorporation into nascent particle assembly has not yet been fully defined. However, it remains clear that the MA domain of Gag somehow mediates this process, which is required for the production of infectious HIV-1 particles. It has been hypothesized that MA might somehow accommodate packaging of the lengthy C-terminal tail of gp41 into particles. Previous reports have identified specific residues in the N-terminal portion of MA that are required for this process, however deletion studies suggest that additional regions outside of the MA N-terminal domain are also utilized in Env incorporation (43, 52, 53, 69, 116, 118, 141, 142, 162, 200, 214). To my knowledge, this thesis is the first study to identify a specific residue in the C-terminal helix of MA required for nascent particles to acquire Env glycoproteins. I considered both direct and indirect mechanisms by which the E99V or E99K MA mutations might confer a defect in Env incorporation.

First, residue 99 may directly contribute to Env incorporation via a specific interaction with viral glycoproteins. The glutamate residue typically at this MA position may be critical for MA-Env binding, and a non-conservative valine or lysine substitution could therefore abolish an association between the two proteins. X-ray crystallographic studies of HIV-1 and SIV MA structures suggest that MA trimers may form a hexameric lattice with an arrangement of spaces large enough to accommodate the cytoplasmic tails of gp41 trimers (4, 93, 165). While the precise residues that make up the putative MA-Env binding site have yet to be defined, it has been suggested that any solvent-exposed amino acids are candidates (93). Indeed, antibody mapping studies suggested that E99 is present at the surface of MA molecules, and therefore it may be available as a potential binding site for the C-terminal tail of gp41 (124, 157). Alternatively, this residue may directly interact with cellular or other viral proteins that are essential for stabilizing Gag:Env complexes. For example, the human protein TIP47 has been reported as a cellular cofactor required for Env incorporation during HIV-1 assembly, as it interacts with both Gag and gp41, and its expression is necessary for Env packaging into particles (116). It was speculated that TIP47 might interact with Env inside endosomes during its retrograde transport from the PM, and that a TIP47-MA interaction might redirect Env from this endosome to the Golgi pathway back to the PM (116). Although this study identified MA residues L12, W15 and E16 as binding sites for TIP47, the authors noted that additional sites on MA may also be involved in TIP47 binding. Gag has also been implicated in facilitating viral particle budding through the recruitment of the host cell's ESCRT machinery, and so host proteins within this complex could also be considered as

factors that might interact with MA E99 (99). Finally, recent siRNA screens have implicated new cellular proteins in HIV-1 particle assembly, and these studies may provide other candidate factors for mediating or stabilizing an interaction between MA and Env (18, 108).

It is also possible that residue 99 is indirectly providing support for the structure of MA that is required for Env incorporation. For example, certain E99 mutations could result in local or global misfolding of MA, preventing the formation of a functional domain required for Env packaging into HIV-1 particles. E99 is located in close proximity to a C-terminal hydrophobic pocket in MA, created by the N-terminus of Helix V packing alongside Helix IV (30, 93). It has been suggested that mutation of particular residues within this pocket, particularly V84, Y86, I92, V94, A100, and K103, might compromise the overall structure of the MA core domain (30). While it is unlikely that E99 contributes to the hydrophobicity of this pocket, it may be necessary to stabilize the region. Since I demonstrated that a valine at MA position 84 (V84) rescued the E99V- and E99K-associated Env incorporation defects, I propose that V84 stabilizes the hydrophobic pocket, such that it prevents or mitigates any structural distortions made by a valine or lysine at position 99.

7.3 Potential mechanisms for E99 in membrane dissociation of MA

My results demonstrated that in addition to conferring an Env incorporation defect, the E99V and E99K mutations also imposed a post-fusion impairment, specifically at a step prior to reverse transcription. Previous studies have shown that the glutamate at position 99 is located in a region of MA that likely associates with the PM

(93, 124, 174). Despite the physical proximity, the hydrophilic nature and negative charge of this amino acid suggests that E99 is not involved in a direct association with the PM. Although certain residues at this membrane-proximal side of the C-terminal MA helix may associate with the cellular membrane- such as K95, T97 and K98- it has been proposed that this region exerts an overall negative effect on membrane binding (150). The hydrophilic and basic properties of glutamate, together with the vital role for position 99 in MA function demonstrated in these studies, suggest that E99 might be involved in antagonizing the membrane association of MA.

The many functions of HIV-1 MA require it to have both a high affinity for the plasma membrane, but also the ability to dissociate from it. The strong membrane binding properties of MA have been well established, and are attributed to the attachment of a myristate moiety and the clustering of basic residues at the surface of the protein's globular core. On the other hand, particular MA residues that are involved in detachment from the PM have not been well characterized. Dissociation from the membrane during early entry events is critical for MA association with the viral core, as well as its potential roles in uncoating, reverse transcription, nuclear localization and integration. Failure to detach from the PM, while binding to the viral core, would cause MA to tether the complex to the membrane and prevent proper trafficking required for productive infection.

The ability of MA to reduce its affinity for the PM has been related to possible sequestration of the myristoyl group inside the hydrophobic core of MA (90, 191, 206, 217). Consistent with this hypothesis is the observation that MA monomers that associate

with the viral core seem to adopt a “tense” conformation (191, 206, 217). The concealment of the hydrophobic moiety may then allow exposure of basic residues on the outside of MA that account for its karyophilicity (217). Such a scenario suggests that residues within MA that are involved in sequestering the myristate group are critical for membrane dissociation. I hypothesize that E99 is critical in facilitating the membrane dissociation of MA monomers during early events in HIV infection. This residue could promote the sequestration of myristate, which may lead to a reduced membrane binding, as detailed above. Alternatively, E99 could act prior to the myristoyl switch, initiating membrane detachment through a different mechanism altogether.

Considering both possibilities, my initial analysis of the E99V and E99K mutations indicated that either a large hydrophobic or a basic residue at MA position 99 was sufficient to cause the post-fusion defects. However, I also found that the phenotype caused by the E99K MA substitution was more severe than that of the E99V mutant. For example, the T84V secondary mutation compensated for the Env incorporation, fusion and infectivity defects of the E99V mutation to a greater extent than those of the E99K substitution. Similarly, facilitating MA-independent fusion was consistently more effective in restoring the replication defect of E99V than that of E99K. Somewhat surprising was my finding that several other amino acids could be tolerated at position 99, despite the high conservation of a glutamate at this position in primary HIV isolates. Specifically, I found that virus containing the E99A substitution demonstrated comparable levels of infection as the wild-type virus, despite the uncharged, hydrophobic nature of alanine. I reasoned that the difference between an alanine substitution at

position 99 and a valine substitution is that the former is considerably smaller than the latter, which could potentially minimize negative effects on viral infection. Regardless, position 99 appears to tolerate neutral and hydrophobic substitutions while disallowing the likes of lysine. As positively charged amino acids such as lysine enable interaction with membrane phospholipids, I hypothesize that E99 is more important for destabilizing the membrane affinity of MA than for mediating the myristoyl switch.

7.4 Future Studies

This thesis identified a single conserved residue in the MA protein of HIV that is multifunctional, and utilized at both early and late stages of the viral life cycle. Several mechanisms through which this residue might act are proposed here, and my results suggest that the reduced infectivity of viruses bearing the E99V or E99K MA mutations are due to the cumulative effects of several disrupted MA functions. Further functional and structural analyses of this residue and others in the MA C-terminal helix are necessary to more fully understand the pleiotropic roles of this region in MA.

In my experiments, I observed that E99V-associated Env incorporation and infectivity defects were evident in the NL4.3 strain, even in the presence of a valine at MA position 84. Since a valine at this position was sufficient to completely rescue the E99V phenotype in LAI, these results may reflect an additional amino acid difference between LAI-MA and NL4.3-MA. I identified other non-conservative differences between the two strains at MA positions 28, 124 and 125. In addition to residues 84 and 99, these amino acids could also be critical for stabilizing a structure in MA that is required for the protein to facilitate Env incorporation during assembly, or influence its

membrane affinity. Additionally, sequence differences within the second α-helix of the NL4.3 and LAI gp41 C-terminal tails may be important, as this particular region has been implicated in an interaction with MA (141).

To further characterize a role for E99 in Env incorporation, one could analyze the stability and persistence of gp41 or gp120 at the surface of LAI-E99V or LAI-E99K producing cells by labeling cells with specific antibodies and monitor surface expression of Env with FACS. A previous study demonstrated that certain MA residues could affect the non-covalent association of gp120 and gp41 on the surface of particles, possibly by changing the structure of the gp41 ectodomain (43). Another method to analyze E99 in Env packaging is to examine the ability of Gag to associate with lipid rafts of virus producing cells. Previous studies have shown that the association of Gag with lipid microdomains is important for Env incorporation during virus assembly (15, 50, 60). Gag association with detergent resistant membrane domains can be analyzed using membrane flotation assays, as described in a 2003 study by Feng, et. al (60). In this technique, cytoplasmic lysates are obtained from cells transfected with mutant proviral clones, and treated with or without detergent. The lysates are then separated through sucrose gradients, and the association of Gag with lipid rafts can be determined by Western blotting fractions of the gradient (14, 60).

My data suggested that the E99V or E99K substitutions might alter the overall structure of MA. To investigate this possibility, one might compare changes in the 3D solution structure of recombinant mutant MA proteins to that of the wild-type MA

protein. Major or slight shifts detected by NMR spectroscopy, or X-ray crystallography could help identify changes in biochemical properties or structure.

Finally, to further characterize the post-entry defect conferred by E99 mutations, one could use a previously published method that has potential for monitoring virus uncoating, which is thought to precede the reverse transcription step (187). This technique involves pelleting particulate capsid proteins from newly infected cells through a sucrose gradient. By removing the middle sucrose layer, one can separate out capsid found within endosomes and lysosomes. The top layer and the resulting pellet can then be analyzed by Western blot to measure the relative levels of soluble and particulate capsid molecules, respectively. This technique could be performed on cells infected with HIV bearing a gp41 CT truncation, and either a wild type- or E99V/K-containing- MA coding region. Comparing differences in the fates of capsid between these viruses could reflect accelerated or restricted uncoating of the viral core, and would support the potential role of MA E99 in the viral core uncoating process.

7.5 Implications for the development of a novel anti-HIV therapeutic

Today, there are no approved drugs that target Gag or any aspect of the virus assembly pathway. However, small molecule compounds targeting the putative MA nuclear localization signal are currently being developed to inhibit HIV-1 nuclear import (87). While the importance of its nuclear localization function has been disputed (48, 63, 120, 209), the Env incorporation or other post-entry functions of MA could represent another class of anti-MA targets. Considering the results of this study, drugs that mimic

the defects conferred by the E99V or E99K MA mutations would likely display significant antiviral activity.

In addition to small molecule inhibitors, gene therapy is another approach to designing novel antiviral agents. For example, dominant negative forms of an HIV protein or cellular cofactor expressed in a lentiviral vector may be effective in hindering HIV replication. An attractive feature of such an approach is that the introduction of multiple mutations would limit the emergence of resistance, and their co-expression may have cumulative effects on their potency (61, 97). Indeed, the oligomeric property of Gag makes it a promising candidate for use in a gene therapy vector, and certain amino acid substitutions in MA and CA have already been shown to act in a dominant negative fashion by inhibiting production of wild type virus (34, 102, 139, 179, 195). Although it is currently unknown whether the E99V or E99K MA substitutions act in a dominant negative fashion, a 1998 study demonstrated that viral replication can proceed in the absence of MA (168). Since virus replication can proceed in the absence of MA, and I show here that mutation of a single amino acid in MA can inhibit replication, the E99V or E99K MA mutations may have the potential to act in a dominant negative fashion.

7.6 Conclusions

Great strides have been made in the management of HIV disease since the first cases were reported thirty years ago. Yet, current estimates report that there are still about 34 million people living with HIV worldwide. Unfortunately, the majority of these individuals do not have access to existing treatments. On the other hand, many of those who do receive antiviral therapy must endure the debilitating side effects of treatment. In

addition, poor adherence to strict treatment schedules combined with the rapidly mutating nature of the virus has led to the emergence of drug resistant strains. Thus, the development of better anti-retroviral drugs, ones with fewer side effects and that use novel mechanisms of action, is critical in the ongoing fight against HIV.

The studies in this thesis demonstrate that a highly conserved glutamate residue at position 99 in HIV-1 MA is essential for both early and late steps in the virus life cycle. Although the precise mechanisms by which this residue carries out these pleiotropic functions are unknown, future studies will lead to a greater understanding of MA-dependent processes that are required for productive HIV infection. Most important, this critical residue in the viral MA protein may prove to be an effective drug target, and its identification, presented here, could bring the world one step closer to a cure.

CHAPTER VIII: References

1) **Adachi, A., H. E. Gendelman, S. Koenig, T. Folks, R. Willey, A. Rabson and M. A. Martin.** 1986. Production of acquired immunodeficiency syndrome-associated retrovirus in human and nonhuman cells transfected with an infectious molecular clone. *J. Virol.* **59**(2):284-291.

2) **Aiken, C.** 1997. Pseudotyping human immunodeficiency virus type 1 (HIV-1) by the glycoprotein of vesicular stomatitis virus targets HIV-1 entry to an endocytic pathway and suppresses both the requirement for Nef and the sensitivity to cyclosporin A. *J. Virol.* **71:**5871-5877.

3) **Alcami, A., R. Chazal and J. W. Yewdell.** 2002. Viruses in control of the immune system. *EMBO Rep*. **3:**927-932.

4) **Alfadhli, A., R.L. Barklis and E. Barklis.** 2009. HIV-1 matrix organizes as a hexamer of trimers on membranes containing phosphatidylinositol-(4,5)-bisphosphate. *Virology* **387**(2):466-72.

5) **Alfadhli, A., A. Still and E. Barklis**. 2009. Analysis of Human Immunodeficiency Virus Type 1 Matrix Binding to Membranes and Nucleic Acids. *J. Virol.* **83**:12196 - 12203.

6) **Aloia, R.C., H. Tian and F.C. Jensen.** 1993. Lipid composition and fluidity of the human immunodeficiency virus envelope and host cell plasma membranes. *Proc. Natl. Acad. Sci. U.S.A.* **90**(11)**:**5181-5.

7) **Arhel, N., A. Genovesio, K. A. Kim, S. Miko, E. Perret, J. C. Olivo-Marin, S. Shorte and P. Charneau.** 2006. Quantitative four-dimensional tracking of cytoplasmic

and nuclear HIV-1 complexes. *Nat. Methods* **3:**817-824.

8) **Auewarakul, P., P. Wacharapornin, S. Srichatrapimuk, S. Chutipongtanate and P. Puthavathana.** 2005. Uncoating of HIV-1 requires cellular activation. *Virology* **337:**93-101.

9) **Barre-Sinoussi, F., J. Chermann, F. Rey, M. Nugeyre, S. Chamaret, J. Gruest, C. Dauguet, C. Axler-Blin, *et al*.** 1983. Isolation of a T-lymphotropic retrovirus from a patient at risk for acquired immune deficiency syndrome (AIDS). *Science* **220** (4599): 868–871.

10) **Bartz, S. R., and M.A. Vodicka.** 1997. Production of high-titer human immunodeficiency virus type 1 pseudotyped with vesicular stomatitis virus glycoprotein. *Methods* **12:**337-342.

11) **Basavapathruni, A., and K.S. Anderson.** 2007. Reverse transcription of the HIV-1 pandemic. *The FASEB Journal* **21** (14): 3795–3808.

12) **Batonick, M., M. Favre, M. Boge, P. Spearman, S. Honing and M. Thali**. 2005. Interaction of HIV-1 Gag with the clathrin-associated adaptor AP-2. *Virology* **342**:190-200.

13) **Benaroch, P., E. Billard, R. Gaudin, M. Schindler and M. Jouve.** 2010. HIV-1 assembly in macrophages**.** *Retrovirology* **7:**29.

14) **Bhatia, A., N. Campbell, A. Panganiban and L. Ratner.** 2007. Characterization of replication defects induced by mutations in the basic domain and C-terminus of HIV-1 matrix. *Virology* **369**:47–54.

15) **Bhattacharya, J., A. Repik and P.R. Clapham**. 2006. Gag regulates association of human immunodeficiency virus type 1 envelope with detergent-resistant membranes. *J. Virol.* **80**:5292–5300.

16) **Blot, G., K. Janvier, S. Le Panse, R. Benarous and C. Berlioz-Torrent.** 2003. Targeting of the human immunodeficiency virus type 1 envelope to the *trans*-Golgi network through binding to TIP47 is required for *env* incorporation into virions and infectivity. *J. Virol.* **77:**6931-6945.

17) **Bouyac-Bertoia, M., J.D. Dvorin, R.A. Fouchier, Y. Jenkins, B.E. Meyer, L.I. Wu, M. Emerman, and M.H. Malim.** 2001. HIV-1 infection requires a functional integrase NLS. *Mol. Cell* **7:**1025-1035.

18) **Brass, A.L., D.M. Dykxhoorn, Y. Benita, N. Yan, A. Engelman, R.J. Xavier, J. Lieberman and S.J. Elledge.** 2008. Identification of host proteins required for HIV infection through a functional genomic screen. *Science* **319:**921-926.

19) **Briggs, J.A., T. Wilk, R. Welker, H.G. Krausslich and S.D. Fuller**. 2003. Structural organization of authentic, mature HIV-1 virions and cores. *EMBO J*. **22:**1707-1715.

20) **Bryant, M., and L. Ratner**. 1990. Myristoylation-dependent replication and assembly of human immunodeficiency virus 1. *Proc. Natl. Acad. Sci. U.S.A.* **87**:523–527.

21) **Bukrinskaya, A., B. Brichacek, A. Mann, and M. Stevenson.** 1998. Establishment of a functional human immunodeficiency virus type 1 (HIV-1) reverse transcription complex involves the cytoskeleton. *J. Exp. Med.* **188:**2113-2125.

22) **Bukrinskaya, A.G., A. Ghorpade, N.K. Heinzinger, T.E. Smithgall, R.E.**

Lewis, and M. Stevenson. 1996. Phosphorylation-dependent human immunodeficiency virus type 1 infection and nuclear targeting of viral DNA. *Proc. Natl. Acad. Sci. U.S.A.* **93**:367–371.

23) **Bukrinsky, M.I., S. Haggerty, M.P. Dempsey, N. Sharova, A. Adzhubel, L. Spitz, P. Lewis, D. Goldfarb, M. Emerman, and M. Stevenson.** 1993. A nuclear localization signal within HIV-1 matrix protein that governs infection of non-dividing cells. *Nature* **365**:666-669.

24) **Bukrinsky, M.I., N. Sharova, M.P. Dempsey, T.L. Stanwick, A.G. Bukrinskaya, S. Haggerty, and M. Stevenson.** 1992. Active nuclear import of human immunodeficiency virus type 1 preintegration complexes. *Proc. Natl. Acad. Sci. U.S.A.* **89:**6580-6584.

25) **Bukrinsky, M.I., N. Sharova, T.L. McDonald, T. Pushkarskaya, W. G. Tarpley, and M. Stevenson.** 1993. Association of integrase, matrix, and reverse transcriptase antigens of human immunodeficiency virus type 1 with viral nucleic acids following acute infection. *Proc. Natl. Acad. Sci. U.S.A.* **90:**6125-6129.

26) **Burnette, B., G. Yu, and R.L. Felsted**. 1993. Phosphorylation of HIV-1 gag proteins by protein kinase C. *J. Biol. Chem***. 268**:8698–8703.

27) **Butler, S.L., E.P. Johnson, and F.D. Bushman.** 2002. Human immunodeficiency virus cDNA metabolism: notable stability of two-long terminal repeat circles. *J. Virol*. **76:**3739-3747.

28) **Camaur, D., P. Gallay, S. Swingler, and D. Trono.** 1997. Human immunodeficiency virus matrix tyrosine phosphorylation: characterization of the kinase and its substrate requirements. *J. Virol*. **71**:6834 - 6841.

29) **Campbell, S. M., S. M. Crowe, and J. Mak.** 2001. Lipid rafts and HIV-1: from viral entry to assembly of progeny virions. *J. Clin. Virol*. **22:**217-227.

30) **Cannon, P. M., S. Matthews, N. Clark, E. D. Byles, O. Iourin, D. J. Hockley, S. M. Kingsman, and A. J. Kingsman**. 1997. Structure-function studies of the human immunodeficiency virus type 1 matrix protein, p17. *J. Virol*. **71**:3474-3483.

31) **Casella, C. R., L. J. Raffini, and A. T. Panganiban**. 1997. Pleiotropic mutations in the HIV-1 matrix protein that affect diverse steps in replication. *J. Virol.* **228**:294–306.

32) **Cavrois, M., C. De Noronha, and W. C. Greene.** 2002. A sensitive and specific enzyme-based assay detecting HIV-1 virion fusion in primary T lymphocytes. *Nat. Biotechnol.* **20**:1151-1154.

33) **Centers for Disease Control**. 1981. Pneumocystis pneumonia — Los Angeles. *Morb. Mortal. Wkly. Rep*. **30**:250–252.

34) **Checkley, M.A., B.G. Luttge, F. Soheilian, K. Nagashima and E.O. Freed**, 2010. The capsid-spacer peptide 1 Gag processing intermediate is a dominant-negative inhibitor of HIV-1 maturation. *Virology* **400**(1):137–144.

35) **Christensen, A.M., M.A. Massiah, B.G. Turner, W.I. Sundquist, and M. Summers.** 1996. Three-dimensional structure of the HTLV-II matrix protein and comparative analysis of matrix proteins from the different classes of pathogenic human retroviruses. *J. Mol. Biol*. **264**(5)**:**1117-31.

36) **Clapham, P. R., and A. McKnight.** 2002. Cell surface receptors, virus entry and tropism of primate lentiviruses. *J. Gen. Virol*. **83:**1809-1829.

37) **Cohen, M.S., N. Hellmann, J.A. Levy, K. DeCock, and J. Lange**. 2008. The spread, treatment, and prevention of HIV-1: evolution of a global pandemic. *J. Clin. Invest.* **118**:1244.

38) **Conte, M. R., M. Klikova, E. Hunter, T. Ruml, and S. Matthews.** 1997. The three-dimensional solution structure of the matrix protein from the type D retrovirus, the Mason-Pfizer monkey virus, and implications for the morphology of retroviral assembly. *EMBO J.* **16:**5819-5826.

39) **Conte, M. R., and S. Matthews.** 1998. Retroviral matrix proteins: a structural perspective. *Virology* **246:**191-198.

40) **Cosson, P**. 1996. Direct interaction between the envelope and matrix proteins of HIV-1. *EMBO J.* **15**:5783-5788.

41) **Costin, J. M.** 2007. Cytopathic mechanisms of HIV-1. *Virology* **4:**100.

42) **Cutino-Moguel, T., and A. Fassati.** 2006. A phenotypic recessive, post-entry block in rabbit cells that results in aberrant trafficking of HIV-1. *Traffic* **7:**978-992.

43) **Davis, M., J. Jiang, J. Zhou, E. O. Freed, and C. Aiken**. 2006. A mutation in the human immunodeficiency virus type 1 Gag protein destabilizes the interaction of envelope protein subunits gp120 and gp41. *J. Virol.* **80**:2405–2417.

44) **De Francesco, M.A., M. Baronio, S. Fiorentini, C. Signorini, C. Bonfanti, *et al.*** 2002. HIV-1 matrix protein p17 increases the production of proinflammatory cytokines and counteracts IL-4 activity by binding to a cellular receptor. *Proc. Natl. Acad. Sci. U.S.A.* **99**:9972–9977.

45) **De Francesco, M.A., A. Caruso, F. Fallacara, A.D. Canaris, F. Dima, *et al*.** 1998. HIV p17 enhances lymphocyte proliferation and HIV-1 replication after binding to a human serum factor. *AIDS* **12**:245–252.

46) **DeLano W. L**. 2002. *The PYMOL User's Manual*, http:/www.pymol.org (Delano Scientific, San Carlos, CA).

47) **Dell'Angelica, E.C., H. Ohno, C.E. Ooi, E. Rabinovich, K.W. Roche, and J.S. Bonifacino.** 1997. AP-3: an adaptor-like protein complex with ubiquitous expression. *EMBO J.* **16**:917–928.

48) **Depienne, C., P. Roques, C. Creminon, L. Fritsch, R. Casseron, D. Dormont, *et al.*** 2000. Cellular distribution and karyophilic properties of matrix, integrase and Vpr proteins from the human and simian immunodeficiency viruses. *Exp. Cell Res.* **260**:387–395.

49) **Diaz, E., and S.R. Pfeffer.** 1998. TIP47, a cargo selection device for mannose 6-phosphate receptor trafficking. *Cell* **93**:433–443.

50) **Ding, L., A. Derdowski, J. J. Wang, and P. Spearman.** 2003. Independent segregation of human immunodeficiency virus type 1 Gag protein complexes and lipid rafts. *J. Virol*. **77:**1916-1926.

51) **Dong, X., H. Li, A. Derdowski, L. Ding, A. Burnett, X. Chen, T. R. Peters, T. S. Dermody, E. Woodruff, J. J. Wang, and P. Spearman.** 2005. AP-3 directs the intracellular trafficking of HIV-1 Gag and plays a key role in particle assembly. *Cell* **120:**663-674.

52) **Dorfman, T., F. Mammano, W. A. Haseltine, and H. G. Göttlinger**. 1994. Role of the matrix protein in the virion association of the human immunodeficiency virus type 1 envelope glycoprotein. *J. Virol*. **68**:1689-1696.

53) **Dubay, J. W., S. J. Roberts, B. H. Hahn, and E. Hunter.** 1992. Truncation of the human immunodeficiency virus type 1 transmembrane glycoprotein cytoplasmic domain blocks virus infectivity. *J. Virol*. **66:**6616-6625.

54) **Dube, M., M.G. Bego, C. Paquay, and E.A. Cohen**. 2010. Modulation of HIV-1-host interaction: role of the Vpu accessory protein. *Retrovirology* **7**:114.

55) **Dupont, S., N. Sharova, C. DeHoratius, C. Virbasius, X. Zhu, A.G. Bukrinskaya, M. R. Green, and M. Stevenson**. 1999. A novel nuclear export activity in HIV-1 matrix protein required for viral replication. *Nature* **402**:681–685.

56) **Dyer, R.B., and N.K. Herzog**. 1995. Isolation of intact nuclei for nuclear extract preparation from a fragile B-lymphocyte cell line. *Biotechniques* **19**:192–195

57) **Esposito, D., and R. Craigie**. 1999. HIV integrase structure and function. *Adv. Virus Res.* **52**:319-333.

58) **Fäcke, M., A. Janetzko, R. L. Shoeman, and H. G. Kräusslich**. 1993. A large deletion in the matrix domain of the human immunodeficiency virus *gag* gene redirects virus particle assembly from the plasma membrane to the endoplasmic reticulum. *J. Virol*. **67**:4972-4980.

59) **Fassati, A., and S. P. Goff**. 2001. Characterization of Intracellular Reverse Transcription Complexes of Human Immunodeficiency Virus Type 1. *J. Virol.* **75**:3626 - 3635.

60) **Feng, X., N. V. Heyden, and L. Ratner.** 2003. Alpha interferon inhibits human T-cell leukemia virus type 1 assembly by preventing Gag interaction with rafts. *J. Virol.* **77:**13389-13395.

61) **Ferrantelli, F., A. Cafaro, and B. Ensoli.** 2004. Nonstructural HIV proteins as targets for prophylactic or therapeutic vaccines. *Curr. Opin. Biotechnol.* **15**(6): 543–56.

62) **Fiorentini, S., E. Marini, S. Caracciolo and A. Caruso.** 2006. Functions of the HIV-1 matrix protein p17. *New Microbiol.* **29**: 1–10.

63) **Fouchier, R. A., B. E. Meyer, J. H. Simon, U. Fischer, and M. H. Malim.** 1997. HIV-1 infection of non-dividing cells: evidence that the amino-terminal basic region of the viral matrix protein is important for Gag processing but not for post-entry nuclear import. *EMBO J.* **16:**4531-4539.

64) **Freed, E. O**. 1998. HIV-1 gag proteins: diverse functions in the virus life cycle. *Virology* **251**:1–15.

65) **Freed, E. O.** 2003. The HIV-TSG101 interface: recent advances in a budding field. *Trends Microbiol*. **11:**56-59.

66) **Freed, E. O.** 2002. Viral late domains. *J. Virol*. **76:**4679-4687.

67) **Freed, E. O., G. Englund, F. Maldarelli, and M. A. Martin.** 1997. Phosphorylation of residue 131 of HIV-1 matrix is not required for macrophage infection. *Cell* **88:**171-173.

68) **Freed, E. O., G. Englund, and M. A. Martin.** 1995. Role of the basic domain of

human immunodeficiency virus type 1 matrix in macrophage infection. *J. Virol.* **69**(6):3949–3954.

69) **Freed, E. O., and M. A. Martin**. 1996. Domains of the human immunodeficiency virus type 1 matrix and gp41 cytoplasmic tail required for envelope incorporation into virions *J. Virol.* **70**:341–351.

70) **Freed, E. O., and M. A. Martin.** 1995. The role of human immunodeficiency virus type 1 envelope glycoproteins in virus infection. *J. Biol. Chem*. **270:**23883-23886.

71) **Freed, E. O., and M. A. Martin**. 1995. Virion incorporation of envelope glycoproteins with long but not short cytoplasmic tails is blocked by specific, single amino acid substitutions in the human immunodeficiency virus type 1 matrix. *J. Virol.* **69**:1984–1989.

72) **Freed, E. O., J. M. Orenstein, A. J. Buckler-White, and M. A. Martin**. 1994. Single amino acid changes in the human immunodeficiency virus type 1 matrix protein block virus particle production. *J. Virol.* **68**(8):5311–5320.

73) **Gallay, P., T. Hope, D. Chin, and D. Trono.** 1997. HIV-1 infection of nondividing cells through the recognition of integrase by the importin/karyopherin pathway. *Proc. Natl. Acad. Sci. U. S. A.* **94:**9825-9830.

74) **Gallay, P., V. Stitt, C. Mundy, M. Oettinger, and D. Trono.** 1996. Role of the karyopherin pathway in human immunodeficiency virus type 1 nuclear import. *J. Virol*. **70:**1027-1032.

75) **Gallay, P., S. Swingler, C. Aiken, and D. Trono.** 1995. HIV-1 infection of nondividing cells: C-terminal tyrosine phosphorylation of the viral matrix protein is a key

regulator. *Cell* **80:**379-388.

76) **Gallay, P., S. Swingler, J. Song, F. Bushman, and D. Trono**. 1995. HIV nuclear import is governed by the phosphotyrosine-mediated binding of matrix to the core domain of integrase. *Cell* **83** (4):569–576.

77) **Gallina, A., G. Mantoan, G. Rindi, and G. Milanesi.** 1994. Influence of MA internal sequences, but not of the myristoylated N-terminus sequence, on the budding site of HIV-1 Gag protein. *Biochem. Biophys. Res. Commun*. **204:**1031-1038.

78) **Gallo, R.C., P.S. Sarin, E.P. Gelmann, M. Robert-Guroff, E. Richardson, V.S. Kalyanaraman, D. Mann, G.D. Sidhu, R.E. Stahl, S. Zolla-Pazner, J. Leibowitch, and M. Popovic.** 1983. Isolation of human T-cell leukemia virus in acquired immune deficiency syndrome (AIDS). *Science* **220** (4599): 865–867.

79) **Gerondelis, P., R. H. Archer, C. Palaniappan, R. C. Reichman, P. J. Fay, R. A. Bambara, and L. M. Demeter.** 1999. The P236L delavirdine-resistant human immunodeficiency virus type 1 mutant is replication defective and demonstrates alterations in both RNA 5'-end- and DNA 3'-end-directed RNase H activities. *J. Virol*. **73:**5803-5813.

80) **Goff, S.P.** 2003. Death by deamination: a novel host restriction system for HIV-1. *Cell* **114:**281-283.

81) **Goff, S.P.** 2007. Host factors exploited by retroviruses. *Nat. Rev. Microbiol*. **5:**253-263.

82) **Gotte, M., X. Li, and M. A. Wainberg.** 1999. HIV-1 reverse transcription: a brief overview focused on structure-function relationships among molecules involved in

initiation of the reaction. *Arch. Biochem. Biophys*. **365:**199-210.

83) **Gottlieb, M.S., R. Schroff, H.M. Schanker, *et al*.** 1981. Pneumocystis carinii pneumonia and mucosal candidiasis in previously healthy homosexual men: evidence of a new acquired cellular immunodeficiency". *N. Engl. J. Med.* **305** (24): 1425–31.

84) **Göttlinger, H. G., J. G. Sodroski, and W. A. Haseltine**. 1989. Role of capsid precursor processing and myristoylation in morphogenesis and infectivity of human immunodeficiency virus type 1. *Proc. Natl. Acad. Sci. U.S.A.* **86**:5781-5785.

85) **Grossman, Z., M. Meier-Schellersheim, W.E. Paul, and L.J. Picker.** 2006. Pathogenesis of HIV infection: what the virus spares is as important as what it destroys. *Nat. Med.* **12**:289–295.

86) **Guyader, M., E. Kiyokawa, L. Abrami, P. Turelli, and D. Trono.** 2002. Role for human immunodeficiency virus type 1 membrane cholesterol in viral internalization. *J. Virol.* **76**:10356–10364.

87) **Haffar O., L. Dubrovsky, R. Lowe, R. Berro, F. Kashanchi, J. Godden, C. Vanpouille, J. Bajorath, and M. Bukrinsky.** 2005. Oxadiazols: a new class of rationally designed anti-human immunodeficiency virus compounds targeting the nuclear localization signal of the viral matrix protein. *J. Virol.* **79**(20):13028–13036.

88) **Haffar, O. K., S. Popov, L. Dubrovsky, I. Agostini, H. Tang, T. Pushkarsky, S. G. Nadler, and M. Bukrinsky.** 2000. Two nuclear localization signals in the HIV-1 matrix protein regulate nuclear import of the HIV-1 pre-integration complex. *J. Mol. Biol*. **299:**359-368.

89) **Halwani, R., A. Khorchid, S. Cen, and L. Kleiman.** 2003. Rapid localization of

Gag/GagPol complexes to detergent-resistant membrane during the assembly of human immunodeficiency virus type 1. *J. Virol.* **77**(7)**:**3973-84.

90) **Hamard-Peron, E., and D. Muriaux.** 2011. Retroviral matrix and lipids, the intimate interaction. *Retrovirology* **8**:15.

91) **Hannah, R., I. Stroke, and N. Betz**. 2003. Beta-Glo® Assay System: A luminescent β-galactosidase assay for multiple cell types and media. *Cell Notes* **6**:16–18.

92) **Heinzinger, N. K., M. I. Bukrinsky, S. A. Haggerty, A. M. Ragland, V. Kewalramani, M. A. Lee, H. E. Gendelman, L. Ratner, M. Stevenson, and M. Emerman.** 1994. The Vpr protein of human immunodeficiency virus type 1 influences nuclear localization of viral nucleic acids in nondividing host cells. *Proc. Natl. Acad. Sci. U.S.A.* **91:**7311-7315.

93) **Hill, C. P., D. Worthylake, D. P. Bancroft, A. M. Christensen, and W. I. Sundquist**. 1996. Crystal structures of the trimeric human immunodeficiency virus type 1 matrix protein: Implications for membrane association and assembly. *Proc. Natl. Acad. Sci. U.S.A.* **93**:3099–3104.

94) **Hill, M., G. Tachedjian, and J. Mak.** 2005. The packaging and maturation of the HIV-1 Pol proteins. *Curr. HIV Res*. **3:**73-85.

95) **Holm, K., K. Weclewicz, R. Hewson, and M. Suomalainen**. 2003. Human immunodeficiency virus type 1 assembly and lipid rafts: Pr55(gag) associates with membrane domains that are largely resistant to Brij98 but sensitive to Triton X-100. *J. Virol.* **77:**4805-4817.

96) **Hutter, G., D. Nowak, M. Mossner, S. Ganepola, A. Mussig, K. Allers, T.**

Schneider, J. Hofmann, C. Kucherer, O. Blau, I.W. Blau, W.K. Hofmann and E. Thiel. 2009. Long-term control of HIV by CCR5 Delta32/Delta32 stem-cell transplantation. *N. Engl. J. Med.* **360:**692-698.

97) **Joshi A., H. Garg, S. Ablan, E.O. Freed, K. Nagashima, N. Manjunath, and P. Shankar.** 2011. Targeting the HIV entry, assembly and release pathways for anti-HIV gene therapy. *Virology* **415**(2):95-106.

98) **Jouve, M., N. Sol-Foulon, S. Watson, O. Schwartz, and P. Benaroch.** 2007. HIV-1 Buds and Accumulates in "Nonacidic" Endosomes of Macrophages. *Cell Host Microbe* **2**:85-95.

99) **Jouvenet, N., M. Zhadina M, Bieniasz PD, and Simon SM.** 2011. Dynamics of ESCRT protein recruitment during retroviral assembly. *Nat. Cell Biol.* **3**(4):394-401.

100) **Kaplan, A. H., and R. Swanstrom.** 1991. HIV-1 gag proteins are processed in two cellular compartments. *Proc. Natl. Acad. Sci. U.S.A.* **88**:4528-4532.

101) **Kaushik, R., and L. Ratner**. 2004. Role of human immunodeficiency virus type 1 matrix phosphorylation in an early postentry step of virus replication. *J. Virol.* **78**:2319–2326.

102) **Kawada, S., T. Goto, H. Haraguchi, A. Ono, and Y. Morikawa.** 2008. Dominant negative inhibition of human immunodeficiency virus particle production by the nonmyristoylated form of *gag*. *J. Virol*. **82:**4384-4399.

103) **Khorchid, A., R. Halwani, M.A. Wainberg, and L. Kleiman**. 2002. Role of RNA in facilitating Gag/Gag-Pol Interaction. *J. Virol.* **76:**4131-4137.

104) **Kiernan, R. E., A. Ono, G. Englund, and E. O. Freed**. 1998. Role of matrix in an early postentry step in the human immunodeficiency virus type 1 life cycle. *J. Virol.* **72**:4116-4126.

105) **Kimpton. J., and M. Emerman.** 1992. Detection of replication-competent and pseudotyped human immunodeficiency virus with a sensitive cell line on the basis of activation of an integrated beta-galactosidase gene. *J. Virol.* **66**(4):2232–2239.

106) **Kirchhausen, T., E. Macia, and H. E. Pelish.** 2008. Use of dynasore, the small molecule inhibitor of dynamin, in the regulation of endocytosis. *Methods Enzymol*. **438:**77-93.

107) **Komano, J., K. Miyauchi, Z. Matsuda, and N. Yamamoto.** 2004. Inhibiting the Arp2/3 complex limits infection of both intracellular mature vaccinia virus and primate lentiviruses. *Mol. Biol. Cell* **15:**5197–5207.

108) **König, R., Y. Zhou, D. Elleder, T. L. Diamond, G. M. Bonamy, J. T. Irelan, C. Y. Chiang, B. P. Tu, P. D. De Jesus, C. E. Lilley, S. Seidel, A. M. Opaluch, J. S. Caldwell, M. D. Weitzman, K. L. Kuhen, S. Bandyopadhyay, T. Ideker, A. P. Orth, L. J. Miraglia, F. D. Bushman, J. A. Young, and S. K. Chanda.** 2008. Global analysis of host-pathogen interactions that regulate early-stage HIV-1 replication. *Cell* **135:**49-60.

109) **Kotwal, G.J.** 1999. Virokines: mediators of virus-host interaction and future immunomodulators in medicine. *Arch. Immunol. Ther. Exp. (Warsz)* **47**:135–8.

110) **Kunkel, T. A., J. D. Roberts, and R. A. Zakour**. 1987. Rapid and efficient site-specific mutagenesis without phenotypic selection. *Methods Enzymol.* **155**:16.

111) **Lee, Y. M., X. B. Tang, L. M. Cimakasky, J. E. Hildreth, and X. F. Yu**. 1997.

Mutations in the matrix protein of human immunodeficiency virus type 1 inhibit surface expression and virion incorporation of viral envelope glycoproteins in $CD4^+$ T lymphocytes. *J. Virol*. **71**:1443-1452.

112) **Letvin, N.** 2009. Moving Forward in HIV Vaccine Development. *Science* **326** (5957):1196-1198.

113) **Lewis, P. F., and M. Emerman.** 1994. Passage through mitosis is required for oncoretroviruses but not for the human immunodeficiency virus. *J. Virol*. **68:**510-516.

114) **Lingwood D, and K. Simons.** 2010. Lipid rafts as a membrane-organizing principle. *Science* **327**:46–50.

115) **Lodge, R., H. G. Göttlinger, D. Gabuzda, E. A. Cohen, and G. Lemay**. 1994. The intracytoplasmic domain of gp41 mediates polarized budding of human immunodeficiency virus type 1 in MDCK cells. *J. Virol*. **68**:4857-4861.

116) **Lopez-Verges, S., G. Camus, G. Blot, R. Beauvoir, and R. Benearous**. 2006. Tail-interacting protein TIP47 is a connector between Gag and Env and is required for Env incorporation into HIV-1 virions. *Proc. Natl. Acad. Sci. U.S.A.* **103**:14947-14952.

117) **Malim, M. H., and M. Emerman.** 2008. HIV-1 accessory proteins—ensuring viral survival in a hostile environment. *Cell Host Microbe* **3:**388-398.

118) **Mammano, F., E. Kondo, J. Sodroski, A. Bukovsky, and H. G. Göttlinger.** 1995. Rescue of human immunodeficiency virus type 1 matrix protein mutants by envelope glycoproteins with short cytoplasmic domains. *J. Virol*. **69**:3824-3830.

119) **Mammano, F., F. Salvatori, S. Indraccolo, A. De Rossi, L. Chieco-Bianchi,**

and H. G. Göttlinger. 1997. Truncation of the human immunodeficiency virus type 1 envelope glycoprotein allows efficient pseudotyping of Moloney murine leukemia virus particles and gene transfer into CD4+ cells. *J. Virol*. **71**:3341 - 3345.

120) **Mannioui, A., E. Nelson, C. Schiffer, N. Felix, E. Le Rouzic, S. Benichou, J. C. Gluckman, and B. Canque.** 2005. Human immunodeficiency virus type 1 KK26-27 matrix mutants display impaired infectivity, circularization and integration but not nuclear import. *Virology* **339:**21-30.

121) **Marchione, M.** 2011. 30 Years After First AIDS Cases, Hope For A Cure (www.npr.org/templates/story/story).

122) **Marsh, M., and A. Helenius.** 2006. Virus entry: open sesame. *Cell* **124:**729-740.

123) **Martin-Serrano, J., and P. D. Bieniasz.** 2003. A bipartite late-budding domain in human immunodeficiency virus type 1. *J. Virol*. **77:**12373-12377.

124) **Massiah, M. A., D. Worthylake, A. M. Christensen, W. I. Sundquist, C. P. Hill, and M. F. Summers.** 1996. Comparison of the NMR and X-ray structures of the HIV-1 matrix protein: evidence for conformational changes during viral assembly. *Protein Sci.* **5**:2391–2398.

125) **Masur, H., M.A. Michelis, J.B. Greene, *et al.*** 1981. An outbreak of community-acquired Pneumocystis carinii pneumonia: initial manifestation of cellular immune dysfunction. *N. Engl. J. Med.* **305** (24): 1431–8.

126) **Matthews, S., P. Barlow, J. Boyd, G. Barton, R. Russell, H. Mills, M. Cunningham, N. Meyers, N. Burns, N. Clark, *et al*.** 1994. Structural similarity between the p17 matrix protein of HIV-1 and interferon-gamma. *Nature* **370**(6491):666-8.

127) **Matthews, S., P. Barlow, N. Clark, S. Kingsman, A. Kingsman, and I. Campbell.** 1995. Refined solution structure of p17, the HIV matrix protein. *Biochem. Soc. Trans*. **23:**725-729.

128) **McClure, M. O., M. A. Sommerfelt, M. Marsh, and R. A. Weiss.** 1990. The pH independence of mammalian retrovirus infection. *J. Gen. Virol.* **71:**767-773.

129) **McDonald, D., M. A. Vodicka, G. Lucero, T. M. Svitkina, G. G. Borisy, M. Emerman, and T. J. Hope.** 2002. Visualization of the intracellular behavior of HIV in living cells. *J. Cell Biol*. **159:**441-452.

130) **Mehandru, S., M. A. Poles, K. Tenner-Racz, A. Horowitz, A. Hurley, C. Hogan, D. Boden, P. Racz, and M. Markowitz.** 2004. Primary HIV-1 infection is associated with preferential depletion of CD4+ T lymphocytes from effector sites in the gastrointestinal tract. *J. Exp. Med*. **200:**761-770.

131) **Miller, M. D., C. M. Farnet, and F. D. Bushman**. 1997. Human immunodeficiency virus type 1 preintegration complexes: studies of organization and composition. *J. Virol.* **71**:5382 - 5390.

132) **Mitsuya, H., K. J. Weinhold, P. A. Furman, M. H. St Clair, S. N. Lehrman, R. C. Gallo, D. Bolognesi, D. W. Barry, and S. Broder.** 1985. 3'-Azido-3'-deoxythymidine (BW A509U): an antiviral agent that inhibits the infectivity and cytopathic effect of human T-lymphotropic virus type III /lymphadenopathy-associated virus in vitro. *Proc. Natl. Acad. Sci. U.S.A.* **82:**7096-7100.

133) **Miyauchi, K., Y. Kim, O. Latinovic, V. Morozov, and G. B. Melikyan**. 2009. HIV enters cells via endocytosis and dynamin-dependent fusion with endosomes. *Cell*

137:433-444.

134) **Moore, M. S., and G. Blobel.** 1992. The two steps of nuclear import, targeting to the nuclear envelope and translocation through the nuclear pore, require different cytosolic factors. *Cell* **69:**939-950.

135) **Morgan, D., C. Mahe, B. Mayanja, J.M. Okongo, R. Lubega, and J.A. Whitworth.** 2002. HIV-1 infection in rural Africa: is there a difference in median time to AIDS and survival compared with that in industrialized countries? *AIDS* **16** (4): 597–632.

136) **Morikawa, Y., S. Hinata, H. Tomoda, T. Goto, M. Nakai, C. Aizawa, H. Tanaka, and S. Omura**. 1996. Complete inhibition of human immunodeficiency virus Gag myristoylation is necessary for inhibition of particle budding. *J. Biol. Chem*. **271**:2868-2873.

137) **Morikawa, Y., T. Kishi, W. H. Zhang, M. V. Nermut, D. J. Hockley, and I. M. Jones.** 1995. A molecular determinant of human immunodeficiency virus particle assembly located in matrix antigen p17. *J. Virol*. **69:**4519-4523.

138) **Morikawa, Y., W. Zhang, D. Hockley, M. Nermut, and I. Jones**. 1998. Detection of a trimeric human immunodeficiency virus type 1 Gag intermediate is dependent on sequences in the matrix domain, p17. *J. Virol.* **72**:7659–7663.

139) **Müller, B., M. Anders, H. Akiyama, S. Welsch, B. Glass, K. Nikovics, F. Clavel, H.M. Tervo, O.T. Keppler and H.-G. Kraüsslich.** 2009. HIV-1 Gag processing intermediates trans-dominantly interfere with HIV-1 infectivity. *J. Biol. Chem.* **284** (43): 29692–29703.

140) **Murakami, T.** 2008. Roles of the interactions between Env and Gag proteins in

the HIV-1 replication cycle. *Microbiol. Immunol*. **52:**287-295.

141) **Murakami, T., and E. O. Freed**. 2000. Genetic evidence for an interaction between human immunodeficiency virus type 1 matrix and helix 2 of the gp41 cytoplasmic tail. *J. Virol*. **74**:3548-3554.

142) **Murakami, T., and E. O. Freed**. 2000. The long cytoplasmic tail of gp41 is required in a cell type-dependent manner for HIV-1 envelope glycoprotein incorporation into virions. *Proc. Natl. Acad. Sci. U.S.A.* **97**:343-348.

143) **Navia, M. A., P. M. Fitzgerald, B. M. McKeever, C. T. Leu, J. C. Heimbach, W. K. Herber, I. S. Sigal, P. L. Darke, and J. P. Springer.** 1989. Three-dimensional structure of aspartyl protease from human immunodeficiency virus HIV-1. *Nature* **337:**615-620.

144) **Nekhai, S., and K.T. Jeang**. 2006. Transcriptional and post-transcriptional regulation of HIV-1 gene expression: role of cellular factors for Tat and Rev. *Future Microbiol.* **1**:417–426.

145) **Nermut, M., D. Hockley, J. Jowett, I. Jones, M. Garreau, and D. Thomas.** 1994. Fullerene-like organization of HIV Gag protein shell in virus-like particles produced by recombinant baculovirus. *Virology* **198**:288–296.

146) **Nguyen, D.H., and J.E. Hildreth**. 2000. Evidence for budding of human immunodeficiency virus type 1 selectively from glycolipid-enriched membrane lipid rafts. *J. Virol*. **74**(7)**:**3264-72.

147) **Ono, A., S. D. Ablan, S. J. Lockett, K. Nagashima, and E. O. Freed**. 2004. Phosphatidylinositol (4,5) bisphosphate regulates HIV-1 Gag targeting to the plasma

membrane. *Proc. Natl. Acad. Sci. U.S.A.* **101**:14889–14894.

148) **Ono, A., and E. O. Freed.** 1999. Binding of human immunodeficiency virus type 1 Gag to membrane: role of the matrix amino terminus. *J. Virol.* **73:**4136-4144.

149) **Ono, A., and E. O. Freed.** 2001. Plasma membrane rafts play a critical role in HIV-1 assembly and release. *Proc. Natl. Acad. Sci. U. S. A.* **98:**13925-13930.

150) **Ono, A., M. Huang, and E. O. Freed**. 1997. Characterization of human immunodeficiency virus type 1 matrix revertants: effects on virus assembly, Gag processing, and Env incorporation into virions. *J. Virol.* **71**:4409-4418.

151) **Ono, A., J. M. Orenstein, and E. O. Freed.** 2000. Role of the Gag Matrix domain in targeting human immunodeficiency virus type 1 assembly. *J. Virol.* **74**:2855–2866.

152) **Ono, A., A. A. Waheed, and E.O. Freed.** 2007. Depletion of cellular cholesterol inhibits membrane binding and higher-order multimerization of human immunodeficiency virus type 1 Gag**.** *Virology* **360:**27-35.

153) **Owens, R. J., J. W. Dubay, E. Hunter, and R. W. Compans.** 1991. Human immunodeficiency virus envelope protein determines the site of virus release in polarized epithelial cells. *Proc. Natl. Acad. Sci. U.S.A.* **88:**3987-3991.

154) **Page, K. A., N. R. Landau, and D. R. Littman.** 1990. Construction and use of a human immunodeficiency virus vector for analysis of virus infectivity. *J. Virol.* **64:**5270-5276.

155) **Paillart, J., and H. G. Göttlinger**. 1999. Opposing effects of human

immunodeficiency virus type 1 Gag to membrane: role of the matrix amino terminus. *J. Virol.* **73**:2604–2612.

156) **Palella, F. J., K.M. Delaney, A.C. Moorman, M.O. Loveless, J. Fuhrer, G.A. Satten, D.J. Aschman, and S.D. Holmberg.** 1998. Declining morbidity and mortality among patients with advanced human immunodeficiency virus infection. *N. Engl. J. Med.* **338** (13): 853–860.

157) **Papsidero, L. D., M. Sheu, and F. W. Ruscetti**. 1989. Human immunodeficiency virus type 1-neutralizing monoclonal antibodies which react with p17 core protein: characterization and epitope mapping. *J. Virol.* **63**:267–272.

158) **Peden, K., M. Emerman, and L. Montagnier.** 1991. Changes in growth properties on passage in tissue culture of viruses derived from infectious molecular clones of HIV-1LAI, HIV-1MAL, and HIV-1ELI. *Virology* **185**:661-672.

159) **Pelchen-Matthews, A., P. Clapham, and M. Marsh.** 1995. Role of CD4 endocytosis in human immunodeficiency virus infection. *J. Virol*. **69:**8164-8168.

160) **Pelchen-Matthews, A., B. Kramer, and M. Marsh.** 2003. Infectious HIV-1 assembles in late endosomes in primary macrophages. *J. Cell Biol*. **162:**443-455.

161) **Peytavi, R., S.S. Hong, B. Gay, A. Dupuy d'Angeac, L. Selig, S. Bénichou, R. Benarous, and P Boulanger**. 1999. H-EED, the product of the human homolog of the murine *eed* gene, binds to the matrix protein of HIV-1. *J Biol Chem.* **274**:1635–1645.

162) **Piller, S. C., J. W. Dubay, C. A. Derdeyn, and E. Hunter.** 2000. Mutational analysis of conserved domains within the cytoplasmic tail of gp41 from human immunodeficiency virus type 1: effects on glycoprotein incorporation and infectivity. *J.*

Virol. **74:**11717-11723.

163) **Poiesz, B. J., F. W. Ruscetti, A. F. Gazdar, P. A. Bunn, J. D. Minna, and R. C. Gallo**. 1980. Detection and isolation of type C retrovirus particles from fresh and cultured lymphocytes of a patient with cutaneous T-cell lymphoma. *Proc. Natl. Acad. Sci. U.S.A.* **77**(12):7415–7419.

164) **Popovic, M., K. Tenner-Racz, C. Pelser, H. J. Stellbrink, J. van Lunzen, G. Lewis, V. S. Kalyanaraman, R. C. Gallo, and P. Racz.** 2005. Persistence of HIV-1 structural proteins and glycoproteins in lymph nodes of patients under highly active antiretroviral therapy. *Proc. Natl. Acad. Sci. U.S.A.* **102**:14807-14812.

165) **Rao, Z., A. S. Belyaev, E. Fry, P. Roy, I. M. Jones, and D. I. Stuart.** 1995. Crystal structure of SIV matrix antigen and implications for virus assembly. *Nature* **378**(6558):743-747.

166) **Reicin, A., A. Ohagen, L. Yin, S. Hoglund, and S. Goff.** 1996. The role of Gag in human immunodeficiency virus type 1 virion morphogenesis and early steps of the viral life cycle. *J. Virol.* **70**:8645-8652.

167) **Reicin, A., S. Paik, R. D. Berkowitz, J. Luban, I. Lowy, and S. P. Goff.** 1995. Linker insertion mutations in the human immunodeficiency virus type 1 *gag* gene: effects on virion particle assembly, release, and infectivity. *J. Virol.* **69:**642-650.

168) **Reil, H., A. A. Bukovsky, H. R. Gelderblom, and H. G. Göttlinger.** 1998. Efficient HIV-1 replication can occur in the absence of the viral matrix protein. *EMBO J.* **17**:2699-2708.

169) **Rerks-Ngarm, S., P. Pitisuttithum, S. Nitayaphan, J. Kaewkungwal, J. Chiu,**

R. Paris, N. Premsri, C. Namwat, S.M. de, E. Adams, M. Benenson, S. Gurunathan, J. Tartaglia, J.G. McNeil, D.P. Francis, D. Stablein, D.L. Birx, S. Chunsuttiwat, C. Khamboonruang, P. Thongcharoen, M.L. Robb, N.L. Michael, P. Kunasol, and J.H. Kim. 2009. Vaccination with ALVAC and AIDSVAX to prevent HIV-1 infection in Thailand. *N. Engl. J. Med*. **361**:2209-2220.

170) **Resh, M.D.** 2004. A myristoyl switch regulates membrane binding of HIV-1 Gag. *Proc. Natl. Acad. Sci. U.S.A.* **101**(2)**:**417-8.

171) **Rhee, S. S., and E. Hunter.** 1990. A single amino acid substitution within the matrix protein of a type D retrovirus converts its morphogenesis to that of a type C retrovirus. *Cell* **63:**77-86.

172) **Riviere, L., J. L. Darlix, and A. Cimarelli.** 2010. Analysis of the viral elements required in the nuclear import of HIV-1 DNA. *J. Virol*. **84:**729-739.

173) **Rowell, J.F., A.L. Ruff, F.G. Guarnieri, K. Staveley-O'Carroll, X. Lin, J. Tang, *et al.*** 1995. Lysosome-associated membrane protein-1-mediated targeting of the HIV-1 envelope protein to an endosomal/lysosomal compartment enhances its presentation to MHC class II-restricted T cells. *J. Immunol.* **155**(4):1818–28.

174) **Saad, J. S., E. Loeliger, P. Luncsford, M. Liriano, J. Tai, A. Kim, J. Miller, A. Joshi, E. O. Freed, and M. F. Summers.** 2007. Point mutations in the HIV-1 matrix protein turn off the myristoyl switch. *J. Mol. Biol.* **366**(2):574-585.

175) **Saad, J. S., J. Miller, J. Tai, A. Kim, R. H. Ghanam, and M. F. Summers**. 2006. Structural basis for targeting HIV-1 Gag proteins to the plasma membrane for virus assembly. *Proc. Natl. Acad. Sci. U.S.A.* **103**:11364–11369.

176) **Sandefur, S., R. M. Smith, V. Varthakavi, and P. Spearman.** 2000. Mapping and characterization of the N-terminal I domain of human immunodeficiency virus type 1 Pr55(Gag). *J. Virol*. **74:**7238-7249.

177) **Scarlata, S., L. Ehrlich, and C. Carter**. 1998. Membrane-induced alterations in HIV-1 Gag and matrix protein-protein interactions. *J. Mol. Biol.* **277**:161–167.

178) **Sheehy, A. M., N. C. Gaddis, J. D. Choi, and M. H. Malim.** 2002. Isolation of a human gene that inhibits HIV-1 infection and is suppressed by the viral Vif protein. *Nature* **418:**646-650.

179) **Shimano, R., R. Inubushi, Y. Oshima, and A. Adachi.** 1999. Inhibition of HIV/SIV replication by dominant negative Gag mutants. *Virus Genes* **18:**197-201.

180) **Shimizu, H., F. Hasebe, H. Tsuchie, S. Morikawa, H. Ushijima, and T. Kitamura.** 1992. Analysis of a human immunodeficiency virus type 1 isolate carrying a truncated transmembrane glycoprotein. *Virology* **189:**534-546.

181) **Shkriabai, N., S.A.K. Datta, Z. Zhao, S. Hess, A. Rein, and M. Kvaratskhelia**. 2006. Interactions of HIV-1 Gag with assembly cofactors. *Biochemistry* **45**(13):4077-83.

182) **Shun, M.C., N.K. Raghavendra, N. Vandegraaff, J.E. Daigle, S. Hughes, P. Kellam, P. Cherepanov, and A. Engelman.** 2007. LEDGF/p75 functions downstream from preintegration complex formation to effect gene-specific HIV-1 integration. *Genes Dev.* **21**:1767–1778.

183) **Spearman, P., R. Horton, L. Ratner, and I. Kuli-Zade**. 1997. Membrane binding of human immunodeficiency virus type 1 matrix protein in vivo supports a conformational myristoyl switch mechanism. *J. Virol.* **71:**6582-6592.

184) **Spearman, P., J. Wang, N. Vander Heyden, and L. Ratner.** 1994. Identification of human immunodeficiency virus type 1 Gag protein domains essential to membrane binding and particle assembly. *J. Virol*. **68:**3232-3242.

185) **Steinbrook, R.** 2007. One step forward, two steps back: will there ever be an AIDS vaccine? *N. Engl. J. Med*. **357:**2653-2655.

186) **Strack B., A. Calistri, S. Craig, E. Popova, and H.G. Göttlinger**. 2003. AIP1/ALIX is a binding partner for HIV-1 p6 and EIAV p9 functioning in virus budding. *Cell* **114**:689–699.

187) **Stremlau, M., M. Perron, M. Lee, Y. Li, B. Song, H. Javanbakht, F. Diaz-Griffero, D. J. Anderson, W. I. Sundquist, and J. Sodroski.** 2006. Specific recognition and accelerated uncoating of retroviral capsids by the TRIM5alpha restriction factor. *Proc. Natl. Acad. Sci. U.S.A.* **103:**5514-5519.

188) **Suzuki, Y., N. Misawa, C. Sato, H. Ebina, T. Masuda, N. Yamamoto, and Y. Koyanagi.** 2003. Quantitative analysis of human immunodeficiency virus type 1 DNA dynamics by real-time PCR: integration efficiency in stimulated and unstimulated peripheral blood mononuclear cells. *Virus Genes* **27:**177-188.

189) **Swingler, S., P. Gallay, D. Camaur, J. Song, A. Abo, and D. Trono**. 1997. The Nef protein of human immunodeficiency virus type 1 enhances serine phosphorylation of the viral matrix. *J. Virol*. **71**:4372-4377.

190) **Takeuchi, Y., M. O. McClure, and M. Pizzato**. 2008. Identification of gammaretroviruses constitutively released from cell lines used for human immunodeficiency virus research. *J. Virol*. **82**:12585-12588.

191) **Tang, C., E. Loeliger, P. Luncsford, I. Kinde, D. Beckett, and M. F. Summers**. 2004. Entropic switch regulates myristate exposure in the HIV-1 matrix protein. *Proc. Natl. Acad. Sci. U.S.A.* **101**:517–522.

192) **Tang, C., Y. Ndassa, and M. F. Summers**. 2002. Structure of the N-terminal 283-residue fragment of the immature HIV-1 Gag polyprotein. *Nat. Struct. Biol.* **9**:537–543.

193) **Taniguchi, H., and S. Manenti.** 1993. Interaction of myristoylated alanine-rich protein kinase C substrate (MARCKS) with membrane phospholipids. *J. Biol. Chem.* **268:**9960-9963.

194) **Trono, D.** 1995. HIV accessory proteins: leading roles for the supporting cast. *Cell* **82:**189-192.

195) **Trono, D., M. B. Feinberg, and D. Baltimore.** 1989. HIV-1 Gag mutants can dominantly interfere with the replication of the wild-type virus. *Cell* **59:**113-120.

196) **United Nation AIDS (UNAIDS).** 2010. (www.unaids.org).

197) **Violot, S., S.S. Hong, D. Rakotobe, C. Petit, B. Gay, K. Moreau, G. Billaud, S. Priet, J. Sire, O. Schwartz, J.F. Mouscadet, and P. Boulanger.** 2003. The Human Polycomb Group EED Protein Interacts with the Integrase of Human Immunodeficiency Virus Type 1. *J. Virol.* **77**:12507–12522.

198) **Von Schwedler, U., R. S. Kornbluth, and D. Trono**. 1994. The nuclear localization signal of the matrix protein of human immunodeficiency virus type 1 allows the establishment of infection in macrophages and quiescent T lymphocytes. *Proc. Natl.*

Acad. Sci. U.S.A. **91**:6992-6996.

199) **Walker, B. D., and D. R. Burton.** 2008. Toward an AIDS vaccine. *Science* **320:**760-764.

200) **Wang, C.-T., Y. Zhang, J. McDermott, and E. Barklis.** 1993. Conditional infectivity of a human immunodeficiency virus matrix domain deletion mutant. *J. Virol*. **67:**7067-7076.

201) **Warrilow, D., G. Tachedjian, and D. Harrich**. 2009. Maturation of the HIV reverse transcription complex: putting the jigsaw together. *Rev. Med. Virol*. **19**:324-337.

202) **Wei, X., J. M. Decker, H. Liu, Z. Zhang, R. B. Arani, J. M. Kilby, M. S. Saag, X. Wu, G. M. Shaw, and J. C. Kappes**. 2002. Emergence of resistant human immunodeficiency virus type 1 in patients receiving fusion inhibitor (T-20) monotherapy. *Antimicrobial Agents and Chemotherapy* **46**:1896–1905.

203) **Welker, R., H. Hohenberg, U. Tessmer, C. Huckhagel, and H. G. Krausslich**. 2000. Biochemical and structural analysis of isolated mature cores of human immunodeficiency virus type 1. *J. Virol.* **74**(3):1168–1177.

204) **West, J. T., S. K. Weldon, S. Wyss, X. Lin, Q. Yu, M. Thali, and E. Hunter**. 2002. Mutation of the dominant endocytosis motif in human immunodeficiency virus type 1 gp41 can complement matrix mutations without increasing Env incorporation. *J. Virol*. **76**:3338-3349.

205) **Wilk, T., T. Pfeiffer, and V. Bosch.** 1992. Retained in vitro infectivity and cytopathogenicity of HIV-1 despite truncation of the C-terminal tail of the env gene product. *Virology* **189:**167-177.

206) **Wu, Z., J. Alexandratos, B. Ericksen, J. Lubkowski, R. C. Gallo, and W. Lu.** 2004. Total chemical synthesis of N-myristoylated HIV-1 matrix protein p17: structural and mechanistic implications of p17 myristoylation. *Proc. Natl. Acad. Sci. U.S.A.* **101:**11587-11592.

207) **Wyma, D. J., A. Kotov, and C. Aiken.** 2000. Evidence for a stable interaction of gp41 with $Pr55^{Gag}$ in immature human immunodeficiency virus type 1 particles. *J. Virol.* **74**:9381-9387.

208) **Wyma, D. J., J. Jiang, J. Shi, J. Zhou, J. E. Lineberger, M. D. Miller, and C. Aiken**. 2004. Coupling of human immunodeficiency virus type 1 fusion to virion maturation: a novel role of the gp41 cytoplasmic tail. *J. Virol.* **78**:3429–3435.

209) **Yamashita, M., and M. Emerman.** 2005. The cell cycle independence of HIV infections is not determined by known karyophilic viral elements. *PLoS Path.* **1:**18.

210) **Yee, J. K., T. Friedmann, and J. C. Burns.** 1994. Generation of high-titer pseudotyped retroviral vectors with very broad host range. *Methods Cell Biol.* **43**(Pt. A)**:**99-112.

211) **Yu, Z., N. Sanchez-Velar, I. E. Catrina, E. L. Kittler, E. B. Udofia, and M.L. Zapp.** 2005. The cellular HIV-1 Rev cofactor hRIP is required for viral replication. *Proc. Natl. Acad. Sci. U. S. A.* **102**(11):4027–4032.

212) **Yu, G., F. S. Shen, S. Sturch, A. Aquino, R. I. Glazer, and R. L. Felsted.** 1995. Regulation of HIV-1 gag protein subcellular targeting by protein kinase C. *J. Biol. Chem*. **270**:4792–4796.

213) **Yu, X., Q. C. Yu, T. H. Lee, and M. Essex.** 1992. The C terminus of human immunodeficiency virus type 1 matrix protein is involved in early steps of the virus life cycle. *J. Virol.* **66**:5667–5670.

214) **Yu, X., X. Yuan, Z. Matsuda, T. H. Lee, and M. Essex**. 1992. The matrix protein of human immunodeficiency virus type 1 is required for incorporation of viral envelope protein into mature virions. *J. Virol*. **66**:4966-4971.

215) **Zennou, V., C. Petit, D. Guetard, U. Nerhbass, L. Montagnier, and P. Charneau.** 2000. HIV-1 genome nuclear import is mediated by a central DNA flap. *Cell* **101:**173-185.

216) **Zhou, W., L. J. Parent, J. W. Wills, and M. D. Resh.** 1994. Identification of a membrane-binding domain within the amino-terminal region of human immunodeficiency virus type 1 Gag protein which interacts with acidic phospholipids. *J. Virol*. **68**:2556–2569.

217) **Zhou, W., and M. Resh**. 1996. Differential membrane binding of the human immunodeficiency virus type 1 matrix protein. *J. Virol.* **70**:8540–8548.

APPENDIX A: a-MLV Pseudotyping Studies

In addition to the VSV-G pseudotyping studies (presented in Chapter 5 section 5.2.2), the effects of pseudotyping mutant particles with the envelope from amphotropic Murine Leukemia Virus (a-MLV env) were also evaluated. Similar to VSV-G, the transmembrane protein of a-MLV env has a short cytoplasmic domain, and thus it is easily incorporated into HIV particles (119). Also, a-MLV env utilizes a common receptor for entry into cells, which confers broad tropism to particles that acquire it (128). In contrast to VSV-G, a-MLV env facilitates virus-cell fusion at the PM through a pH independent mechanism (128). This mode of virus entry deposits the viral core into the cytoplasm at the periphery of the cell. Thus a-MLV pseudotyped HIV-1 particles remain vulnerable to restrictions in the cytoplasm that may have been bypassed by endosomal fusion.

To produce a-MLV pseudotyped virus, the pLAI-ΔEnv, pE99V-ΔEnv, pE99K-ΔEnv, pK32E-ΔEnv and pL13E-ΔEnv proviral clones were co-transfected into 293T cells with an expression vector encoding the amphotropic Murine Leukemia Virus strain 4070 A glycoprotein (a-MLV). Virus was harvested 24 and 48 hours post-transfection, and then normalized by RT content. To determine whether the a-MLV-pseudotyped viruses were competent for a single round of infection, 2-fold serial dilutions of virus were incubated with TZM-bl cells and analyzed 24 hours post-infection with the Beta-Glo® assay system. In parallel, similar infections were also performed using viruses with wild-type HIV-1 Env. Non-pseudotyped LAI-ΔEnv particles were used as a negative control.

I found that the a-MLV-pseudotyped particles with wild-type MA (a-MLV-LAI-ΔEnv) were markedly less infectious than equivalent RT units of LAI-WT. However, considerable infection levels in TZM-bl cells by a-MLV-LAI-ΔEnv virus were observed in comparison to the non-pseudotyped LAI-ΔEnv control. The raw data from these infections, presented in Table B.4, indicate that a-MLV-LAI-ΔEnv particles were generated and infectious. The RLU values from each infection were normalized using the a-MLV-LAI-ΔEnv values at the corresponding titer to represent 100% infectivity. These normalized values are presented in Table A.1. This data demonstrates that pseudotyping with a-MLV env augmented the infections of virus with each MA mutation. However, the degree of enhancement varied depending on the MA mutation. Overall, a-MLV env was able to rescue infectivities of viruses bearing the L13E and K32E MA mutations. In contrast, this heterologous envelope could not substantially rescue infectivities of viruses containing either E99V or E99K MA mutations. The raw data suggests that a-MLV-LAI-ΔEnv was saturating at higher titers, as the values at 80K and 40K were very similar. Therefore, I suspect that the infectivity data observed for a-MLV-E99V-ΔEnv or a-MLV-E99K-ΔEnv at these viral inputs may not represent accurate improvements. Even at these high titers, a-MLV pseudotyping only improved the infectivity defects imposed by the E99V or E99K MA substitutions from less than 2%, to 18% or 11% of particles containing wild-type MA, respectively.

Because a-MLV-WT-ΔEnv was markedly less infectious than equal RT units of WT-LAI, I decided to compare infections between viral titers that generated similar raw values, as was done earlier. Shown in Figure A.1, normalized values of virus with WT

HIV-1 Env at 5K RTU per well were compared to infections with a-MLV pseudotyped particles at 40K RTU per well. Again, I found that the infectivity defects imposed by the L13E or K32E MA mutations were rescued by a-MLV pseudotyping, while the a-MLV-E99V-ΔEnv and a-MLV-E99K-ΔEnv viruses were markedly impaired for single-cycle infection. This data suggested that a-MLV pseudotyping was not able to significantly rescue the infectivity defects imposed by MA substitutions E99V or E99K.

Table A.1 Relative infectivities of LAI-derived MA mutants pseudotyped with a-MLV Env.

Virus	Titer (RT units per well)			
	80K	40K	20K	10K
WT-ΔEnv + a-MLV	100	100	100	100
E99V-ΔEnv + a-MLV	17.8	10.0	4.5	2.8
E99K-ΔEnv + a-MLV	11.0	4.0	7.8	3.3
L13E-ΔEnv + a-MLV	117.8	123.0	143.3	152.8
K32E-ΔEnv + a-MLV	91.8	86.3	98.3	102.5
LAI-ΔEnv	0.3	0.0	0.3	0

The data shown are normalized values from the raw RLU values from Table 8-5, which presented averages from four independent Beta-Glo® infectivity assays analyzed 24 hours after TZM-bl cells were infected with individual LAI-derived viruses (as indicated in the left column) at four serial dilutions (indicated in the top row as RT units of virus per well). The normalized values are based on the level of a-MLV-LAI-ΔEnv, which represents 100% infectivity at each dilution.

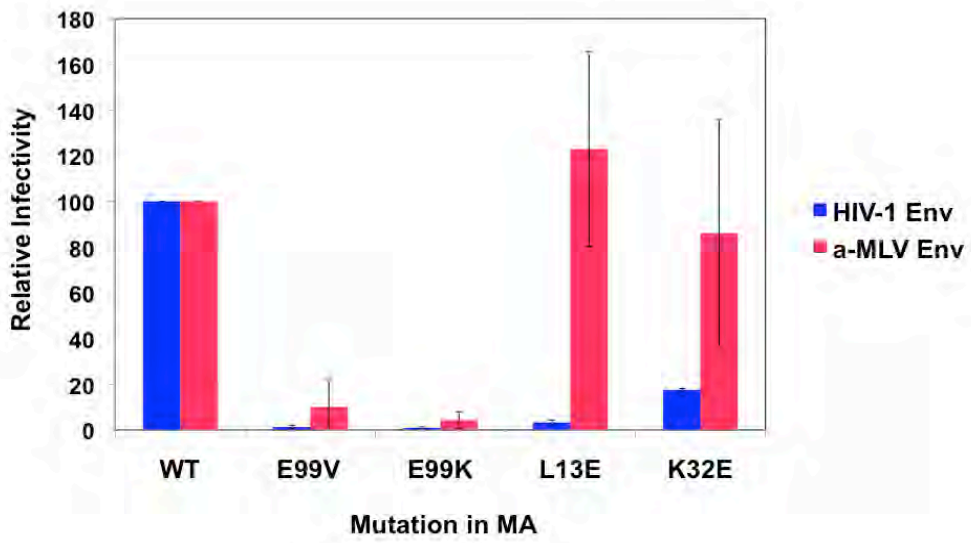

Figure A.1 Single-cycle infectivities of LAI-derived MA mutants containing WT HIV-1 Env or pseudotyped with a-MLV Env. Infectivity was monitored 24 hours post-infection using the Beta-Glo® reporter assay, as described in Figure 3.4. The assessment of infectivity for each mutant virus is based on the level of LAI-WT (**blue bars**, inoculated at 5 RTU/well) or a-MLV-LAI-ΔEnv (**red bars**, inoculated at 40 RTU/well), which represents 100% infectivity. Pseudotyped virus was generated by co-transfection of a pLAI-based Env deficient proviral clone and an expression plasmid encoding the a-MLV heterologous envelopes. Data is the average of four independent experiments performed in duplicate.

Next, I sought to determine whether a-MLV-env pseudotyped particles with the position 99 substitutions could fuse with TZM-bl cells. Proviral clones pLAI-ΔEnv, pE99V-ΔEnv, pE99K-ΔEnv, pK32E-ΔEnv or pL13E-ΔEnv were cotransfected into 293T cells with the BLaM-Vpr expression construct and the a-MLV env vector, as described in Materials and Methods (Chapter 2, section 2.4). At 24 hours and 48 hours after the transfection, virus-containing supernatants were harvested and normalized by RT content. Unfortunately, the production of a-MLV pseudotyped particles in the presence of the BLaM-Vpr chimeric proteins was inefficient. This was evidenced by the RT contents of a-MLV-LAI-ΔEnv transfected cell supernatants, which were consistently lower than those generated in parallel transfections by LAI-WT or VSV-G pseudotyped particles (data not shown).

Equal RT units of each virus were used to infect TZM-bl cells, and virus-cell fusion was monitored as described previously for Figure 3.7. Since high titers of virus were required to detect BLaM activity in cells challenged with virus, BLaM activity in cells challenged with a-MLV-LAI-ΔEnv could only be observed at levels above background when the virus was concentrated by centrifugation through a sucrose cushion. Interestingly, the Beta-Glo® assay was able to detect significant infectivity with equivalent titers of the a-MLV-LAI-ΔEnv (BLaM) virus, demonstrating the differences in sensitivity between the two assay systems. Figure A.2 shows results from the fusion assay, using the concentrated a-MLV pseudotyped particles. I was able to detect BLaM activity in cells challenged with a-MLV-LAI-ΔEnv, a-MLV-L13E-ΔEnv and a-MLV-K32E-ΔEnv, confirming the infectivity results suggesting a rescue. However, the fusion

capacities of a-MLV-E99V-ΔEnv or a-MLV-E99K-ΔEnv particles were only slightly better than LAI-ΔEnv particles, my negative control.

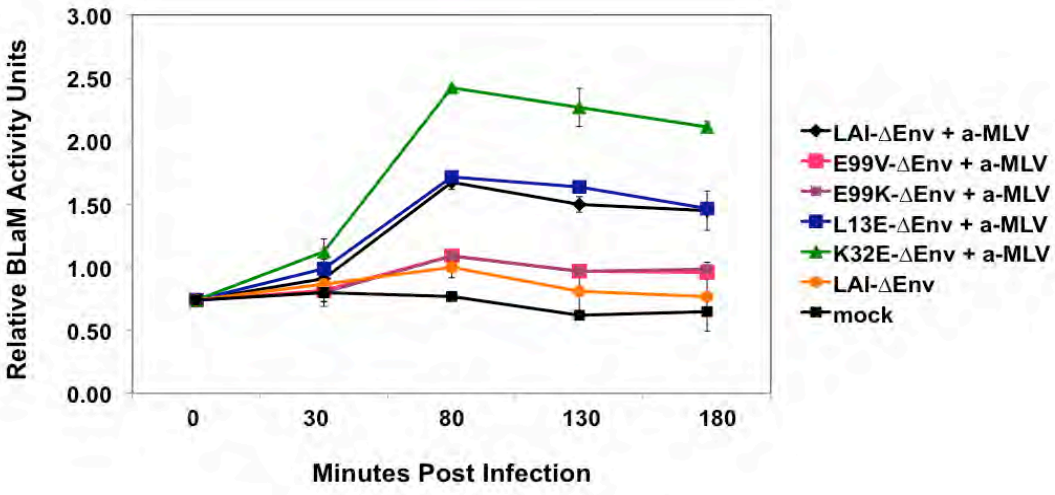

Figure A.2 Effects of a-MLV pseudotyping on virus-cell membrane fusion capacity in LAI-derived viruses bearing MA substitutions. Fusion events of a-MLV Env-pseudotyped particles were assayed in TZM-bl cells as described in Figure 3.7. The data shown is representative of three independent experiments performed in duplicate.

Next I wanted to determine whether the E99V and E99K MA mutations disrupted a-MLV Env expression in producer cells, or incorporation into particles. Virus particles were generated in HeLa cells through co-transfecting the a-MLV expression vector and the pLAI-ΔEnv, pE99V-ΔEnv, pE99K-ΔEnv, pK32E-ΔEnv or pL13E-ΔEnv proviral clones. As before, virus was harvested 24 and 48 hours post-transfection, and then normalized by RT content. Transfected HeLa cells were also harvested. I attempted to performed immunoblot analysis on particles made from transfected HeLa cells, as well as the cell lysates, using the 83A25 monoclonal antibody, kindly provided by Leonard Evans. However, I was unable to detect a-MLV env in any particles or cells, even in particles that demonstrated significant infectivity. These results suggest that the antibody did not efficiently recognize the protein. Therefore, I was unable to determine whether low fusion and infectivities of the a-MLV-env pseudotyped virus bearing the E99V or E99K MA mutations was a result of inefficient incorporation of a-MLV env into these particles or a specific fusion defect imposed by the E99V or E99K MA mutations.

Although I could not determine the efficiency of a-MLV-env incorporation into particles, I did examine reverse transcription products in cells challenged with a-MLV-E99V-ΔEnv. Proviral clones pLAI-ΔEnv and pE99V-ΔEnv were individually transfected into 293T cells with expression vectors encoding a-MLV. In parallel, the pLAI-WT, pLAI-E99V and pLAI-ΔEnv proviral clones were also transfected. Virus-containing supernatants were harvested 24 and 48 hours post-transfection, and normalized by RT content. Equal amounts of each virus were treated with DNase to eliminate possible contamination from transfected DNA. The DNase treated a-MLV pseudotyped virus was

used to infect MAGI cells. At the indicated time points, cells were harvested, and total DNA was extracted. Specific primers were used to quantify EPs and then the data was normalized by CCR5 copy number. The data was analyzed to determine the copies of EP per million cells, and is shown in Figures A.3.

Significant levels of EPs in MAGI cells infected with LAI-WT or a-MLV-LAI-ΔEnv were detected, and these quantities increased over time. By contrast, only minimal quantities of EPs were detectable in cells challenged with LAI-ΔEnv. Similarly, EPs detected in the MAGI cultures challenged with LAI-E99V or a-MLV-E99V-ΔEnv were only at levels just above background. With this data, I remain unable to conclude whether the E99V-ΔEnv particles were generated, or whether they could successfully fuse with target cells.

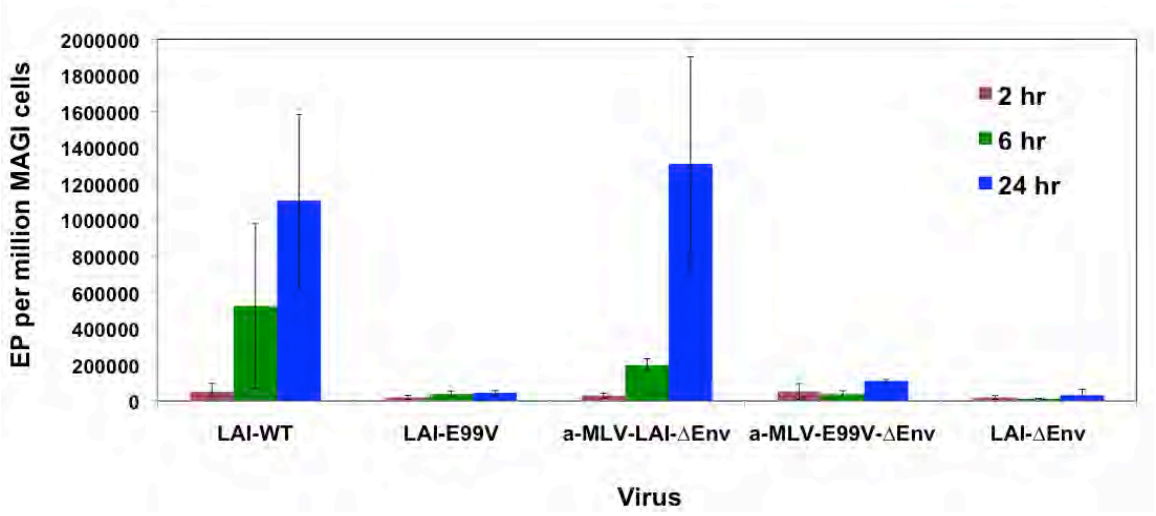

Figure A.3 Analysis of early products in cells infected with pseudotyped HIV-1 MA mutants. MAGI cells were infected with equal RT units of LAI-derived MA mutants containing WT HIV-1 Env, or pseudotyped with a-MLV. At the specified times post-infection, cells were lysed and EPs were directly quantified by real-time PCR, using primers specific for strong-stop viral DNA. Data was normalized by quantification of the cellular CCR5 gene in each sample. Data shown are the mean of two separate experiments performed in duplicate.

APPENDIX B: Single-Cycle Infectivity Data

Table B.1 Relative Luciferase Units from TZM-bl cell infections with LAI-derived viruses bearing single amino substitutions in MA

Virus	Titer (RT units per well)			
	20K	10K	5K	2.5K
LAI- WT	258590	122714	54020	28461
LAI- E99V	2095	1687	660	416
LAI- E99K	1190	663	488	379
LAI- L13E	6025	4070	1711	1362
LAI- K32E	52385	25667	9459	6040
LAI-ΔEnv	156	180	85	141

TZM-bl cells were infected with the indicated LAI-derived virus at four serial dilutions. Data shown are the average relative luciferase units (RLU) of four independent Beta-Glo® infectivity assays performed in duplicate and analyzed with a luminometer 24 hours post-infection.

Table B.2 Relative Luciferase Units from TZM-bl cell infections with LAI-derived double mutants bearing gp41 cytoplasmic domain truncation and individual substitutions in MA

Virus	Titer (RT units per well)			
	20K	10K	5K	2.5K
WT-Δ144	344477	190502	91117	51319
E99V-Δ144	33743	18303	8213	3492
E99K-Δ144	43498	23680	11796	7587
L13E-Δ144	383457	198160	102837	49174
K32E-Δ144	287248	143188	76855	37777
LAI-ΔEnv	992	584	335	187

TZM-bl cells were infected with the indicated LAI-derived viruses at four serial dilutions. Data shown are the average relative luciferase units (RLU) of four independent Beta-Glo® infectivity assays performed in duplicate and analyzed with a luminometer 24 hours post-infection.

Table B.3 Relative Luciferase Units from TZM-bl cell infections with LAI-derived MA mutants pseudotyped with VSV-G

Virus	Titer (RT units per well)							
	20K	10K	5K	2.5K	1.25K	625	312.5	156
VSV-G-LAI-ΔEnv	1085425	927276	724429	161899	79075	46531	19389	10778
VSV-G-E99V-ΔEnv	803147	567252	368611	59515	28179	14584	6048	4399
VSV-G-E99K-ΔEnv	569488	353591	217840	29926	16461	7616	2955	2457
VSV-G-L13E-ΔEnv	899225	675875	464166	68826	33763	18212	12314	5956
VSV-G-K32E-ΔEnv	994947	802706	590734	89087	54494	23372	17667	6592
LAI-ΔEnv	4189	3948	4478	211	165	98	0	0

TZM-bl cells were infected with the indicated LAI-derived viruses at eight serial dilutions. Data shown are the average relative luciferase units (RLU) of four independent Beta-Glo® infectivity assays performed in duplicate and analyzed with a luminometer 24 hours post-infection.

Table B.4 Relative Luciferase Units from TZM-bl cell infections with LAI-derived MA mutants pseudotyped with a-MLV env

Virus	Titer (RT units per well)			
	80K	40K	20K	10K
a-MLV-LAI-ΔEnv	38634	44352	26903	14475
a-MLV-E99V-ΔEnv	6596	5067	1511	457
a-MLV-E99K-ΔEnv	5227	1937	2162	519
a-MLV-L13E-ΔEnv	47163	56659	42788	21207
a-MLV-K32E-ΔEnv	37431	40474	28250	14981
LAI-ΔEnv	163	157	117	28

TZM-bl cells were infected with the indicated LAI-derived viruses at four serial dilutions. Data shown are the average relative luciferase units (RLU) of four independent Beta-Glo® infectivity assays performed in duplicate and analyzed with a luminometer 24 hours post-infection.